STOCHASTIC CHARACTERIZATION, SIMULATION, AND ANALYSIS OF ENVIRONMENTAL (PRECIPITATION AND TEMPERATURE) INPUTS INTO THE M-E DESIGN FRAMEWORK

A Thesis
Submitted to the Graduate Faculty
of the
North Dakota State University
of Agriculture and Applied Science

By

Joseph Membah

In Partial Fulfillment of the Requirements
for the Degree of
MASTER OF SCIENCE

Major Department:
Construction Management and Engineering

December 2010

Fargo, North Dakota

North Dakota State University
Graduate School

Title

Characterization, Simulation, and Analysis of Environmental

(Precipitation and Temperature) Inputs into the M-E Design Framework

By

Joseph Membah

The Supervisory Committee certifies that this ***disquisition*** complies with North Dakota State University's regulations and meets the accepted standards for the degree of

MASTER OF SCIENCE

ABSTRACT

Membah, Joseph, M.S., Department of Construction Management and Engineering, College of Engineering and Architecture, North Dakota State University, December 2010. Stochastic Characterization, Simulation, and Analysis of Environmental (Precipitation and Temperature) Inputs into the M-E Design Framework. Major Professor: Dr. Eric Asa.

The engineering design of pavements is a complex process requiring regular updating and calibration to produce durable and resilient road surfaces. To achieve this goal, research is conducted continuously to obtain input parameters which are used to produce advanced tools. Recently, an advanced pavement structural design tool termed the *Mechanistic Empirical (M-E) Pavement Design* approach was introduced to the engineering community. The M-E process employs issues about engineering, traffic, environmental factors, construction, and economics in the design and selection of appropriate types of road surfaces. Although the new M-E approach can result in improved designs, the approach does not address a design methodology for selecting the best pavement for a particular application. Currently, State Highway Agencies employ different procedures to design pavements based on empirical data collected in 1960s. The trials used data collected during two climatic seasons. Since then, a number of research initiatives have been conducted investigating issues such as soil characterization, traffic, and construction. However, none have focused on environmental issues which also provide inputs for the M-E design framework. This research focuses on temperature and precipitation: two main environmental factors of concern. The M-E design approach uses traditional statistical analysis to compute the input parameters of sampling points which are often spread over a large geographic region and do not provide a representative sample. Because temperature and precipitation are composed of continuous data, geostatistics were employed to compute statistical parameters through stochastic characterization, simulation, and analysis.

ACKNOWLEDGEMENTS

I wish to express my sincere appreciation to my academic adviser, Dr. Eric Asa, for his guidance and encouragement throughout my research. Dr. Asa's suggestions and patience right from the start of this research are appreciated. Working with Dr. Asa has given me energy and moral support to focus on the research; I am grateful.

It is an honor to have been part of the Department of Construction Management and Engineering at NDSU. I am indebted for its continuous support, both financially as well as technically, during my graduate studies. Special thanks to Dr. Charles McIntyre, Dr. Darshi De Saram, and Dr. Peter Oduor for their contributions to the success of this thesis topic. I sincerely thank Dr. Oduor for his time and patience on data organization.

It has been a blessing to have support from Ingrid Scarski which made me feel very comfortable in the Department of Construction Management and Engineering. My special thanks to Ann Denny who was there when I needed help.

I would like to acknowledge my appreciation and love to my parents; my brothers; my sisters; my wife, Hellen; and my children, Annette, Abigael, and Chris. I love you! It was their prayers and best wishes that gave me the courage and confidence to fulfill my lifelong dream.

DEDICATION

To my dad, and memory of my mum

My wife, Hellen, and children

Annette, Abigael, and Chris

TABLE OF CONTENTS

ABSTRACT iii

ACKNOWLEDGEMENTS iv

DEDICATION v

LIST OF TABLES x

LIST OF FIGURES xii

LIST OF ABBREVIATIONS xiv

CHAPTER 1. INTRODUCTION 1

1.1. Background 1

1.2. Research Objective 4

1.3. Research Methodology 4

1.4. Research Organization 6

CHAPTER 2. LITERATURE REVIEW 7

2.1. Introduction 7

2.2. Historical Overview of Pavement Design in the United States 10

2.3. Pavement Design Approaches 12

2.3.1. AASHO Road Test 12

2.3.2. AASHO Interim Design Guide 1972 13

2.3.3. AASHTO 1986/1993 Design Guides 14

2.4. M-E Design Approach 16

2.4.1. Traffic Loading 18

2.4.2. Pavement Materials Characterization 20

2.4.3. Climate/Environment 20

2.5. Environmental Factors 20
2.5.1 Temperature 22
2.5.2 Precipitation 22
2.6. Geostatistical Characterization 22
2.7. Kriging Methods 23
2.7.1. Simple Kriging 24
2.7.2. Ordinary Kriging 24
2.7.3. Universal Kriging 25
2.8. Cross Validation 25
2.9. Statistical Analysis 26
2.10. GIS Software 28
CHAPTER 3. EXPLORATORY/STATISTICAL DATA ANALYSIS 29
3.1. Introduction 29
3.2. Data Preparation 30
3.3. Exploratory Data Analysis 33
3.3.1. Temperature 33
3.3.2. Precipitation 35
3.4 Statistical Data Analysis 36
3.4.1. Temperature 37
3.4.2. Precipitation 37
3.5. Comparisons Between Temperature and Precipitation 38
CHAPTER 4. UNIVARIATE STOCHASTIC CHARACTERIZATION 41
4.1. Introduction 41

4.2. Experimental Design 41

4.3. Univariate Stochastic Characterization of Environmental Data 41

4.3.1. Variograms 42

4.3.2 Kriging 42

4.4. Stochastic Characterization of Environmental Data 43

CHAPTER 5. MULTIVARIATE STOCHASTIC CHARACTERIZATION 44

5.1. Introduction 44

5.2. Experimental Design 44

5.3. Stochastic Co-Simulation of Temperature and Precipitation 44

5.3.1. Variograms 45

5.3.2 Co-Kriging 45

5.4. Stochastic Characterization of Environmental Data 46

CHAPTER 6. ANALYSIS, DISCUSSIONS, AND CONTRIBUTIONS TO SCIENCE... 47

6.1. Analysis of Results 47

6.2. Temperature Dataset 47

6.2.1. Mean 48

6.2.2. Root-Mean-Square Error 49

6.2.3. Average Standard Error 50

6.2.4. Mean Standardized Error 51

6.2.5. Root-Mean-Square Error 52

6.3. Decision Matrix 54

6.4. Precipitation Dataset 56

6.4.1. Mean 56

6.4.2. Root-Mean-Square Error 57

6.4.3. Average Standard Error 58

6.4.4. Mean Standard Error 59

6.4.5. Root-Mean-Square Standardized Error 59

6.5. Co-Kriging 63

6.5.1. Mean 63

6.5.2. Root-Mean-Square Error 65

6.5.3. Average Standard Error 66

6.5.4. Mean Standardized Error 67

6.5.5. Root-Mean-Square Standardized 68

6.6. Discussions 72

6.7. Contributions to Science 73

CHAPTER 7. CONCLUSIONS AND RECOMMENDATIONS 74

7.1. Conclusions 74

7.2. Recommendations 75

7.3. Summary and Further Research 75

REFERENCES 76

APPENDIX A. TEMPERATURE DATASET 82

APPENDIX B. PRECIPITATION DATASET 97

APPENDIX C. UNIVARIATE STOCHASTIC CHARACTERIZATION DIAGRAMS 103

APPENDIX D. CO-KRIGING SEMIVARIOGRAM AND CROSS VALIDATIONS DIAGRAMS 119

LIST OF TABLES

Table Page

2.1. Recommended drainage coefficient values (AASHTO, 1993) 9

3.1. Summary of exploratory data analysis for temperature and precipitation................ 36

3.2. Summary of descriptive statistics for temperature and precipitation 38

5.1. Mean results of kriged temperature data for the six kriging methods. 48

5.2. Root-mean-square results of kriged temperature data for the six kriging methods.. 50

5.3. Average standard error results of kriged temperature for six kriging methods. 51

5.4. Mean standard error results of kriged temperature data for kriging methods.. 52

5.5. Root-mean-square standardized error results of kriged temperature data. 53

5.6. Decision matrix summarizing circular variogram predictions. 54

5.7. Decision matrix summarizing spherical variogram predictions. 55

5.8. Decision matrix summarizing exponential variogram predictions.......................... 55

5.9. Decision matrix summarizing gaussian variogram predictions............................... 55

5.10. Results of the mean of kriged precipitation data of the six kriging methods. 56

5.11. Root-mean-square error of the kriged precipitation data.. 57

5.12. Average standard error results of kriged precipitation dataset. 58

5.13. Results of the mean standardized error of kriged precipitation dataset.................. 60

5.14. Root-mean-square standardized error results of kriged precipitation dataset.......... 61

5.15. Decision matrix for circular variogram predictions of six kriging methods............ 62

5.16. Decision matrix for spherical variogram predictions of six kriging methods. 62

5.17. Decision matrix for exponential variogram predictions for kriging methods.. 62

5.18. Decision matrix for gaussian variogram predictions of six kriging methods. 63

6.19. Results of the mean of co-kriged datasets.. 64

6.20. Results of the root-mean-square error of co-kriged datasets. 65

6.21. Average standard error of co-kriged datasets. 66

6.22. Mean standardized error of co-kriged datasets. 68

6.23. Root-mean-square error standardized of co-kriged datasets 68

6.24. Decision matrix summarizing circular variogram predictions. 69

6.25. Decision matrix summarizing spherical variogram predictions. 70

6.26. Decision matrix summarizing exponential variogram predictions. 70

6.27. Decision matrix summarizing gaussian variogram predictions. 70

LIST OF FIGURES

Figure Page

1.1. Research methodology 5

2.1. Design outline of M-E pavement design guide process (NCHRP, 2004). 17

3.1. Map of North Dakota showing the location of the weather stations. 29

3.2. Diagram showing maximum temperatures of the sampled weather stations........... 30

3.3. Chart showing precipitation of 118 the sampled weather stations. 31

3.4. Diagram of temperature for January to December. 32

3.5. Diagram of precipitation for January to December. 32

3.6. Histogram for maximum temperature... 34

3.7. QQ plot for maximum temperature. 34

3.8. Histogram for precipitation.. 35

3.9. QQ plot for precipitation.. 36

3.10. Minitab relative frequency histogram for maximum temperature.......................... 37

3.11. Minitab relative frequency of the histogram for precipitation................................ 38

3.12. Precipitation versus temperature from January to December................................ 39

3.13. Precipitation versus temperature for construction period to February.. 40

4.1. Univariate steps followed in analyzing precipitation and temperature datasets...... 42

5.1. Co-kriging steps used in the analysis of the datasets 45

6.1. Mean error of the kriged temperature data. 49

6.2. Root-mean-square error of the kriged temperature data. 50

6.3. Average standard error prediction of kriged temperature data. ....:..... 51

6.4. Mean standardized prediction error of the kriged temperature data. 52

6.5. Root-mean-square error standardized of the kriged temperature data 53

6.6. Mean error of the kriged precipitation data. 57

6.7. Root-mean-square error of the kriged precipitation data 58

6.8. Average standard error prediction of kriged precipitation dataset 59

6.9. Mean standardized prediction error of the kriged precipitation data 60

6.10. Root-mean-square error standardized of the kriged precipitation dataset. 61

6.11. Mean error of the co-kriged datasets. 64

6.12. Root-mean-square error of co-kriged datasets. 65

6.13. Average standard error co-kriged datasets 66

6.14. Mean standardized error of co-kriged datasets. 67

6.15. Root-mean-square error standardized of co-kriged datasets 69

6.16. RMSE – ASE plot for maximum temperature. 71

6.17. RMSE – ASE plot for precipitation. 71

6.18. RMSE – ASE plot for co-kriging. 72

LIST OF ABBREVIATIONS

AASHO	American Association of State Highways Officials
AASHTO	American Association of State Highways and Transportation Officials
ART	AASHO Road Test
ASCE	American Society of Civil Engineers
ASE	Average Standard Error
ASTM	American Society for Testing and Materials
NCDC	National Climate Data Center
DOT	Department of Transportation
EICM	Enhanced Integrated Climatic Model
ESAL	Equivalent Single Axle Load
ESDA	Exploratory Data Analysis
ESRI	Environmental Systems Research Institute
FHWA	Federal Highway Administration
GIS	Geographical Information System
HRB	Highway Research Board
IK	Indicator Kriging
ME	Mean Error
M-E	Mechanistic Empirical
MSE	Mean Square Error
MSSE	Mean Standardized Square Error
NCHRP	National Cooperative Highway Research Program
ND	North Dakota State
NDDOT	North Dakota Department of Transportation
NDSU	North Dakota State University

NOAA	National Oceanic and Atmospheric Administration
OD	Ordinary Kriging
PK	Probability Kriging
RMSE	Root Mean Square Error
RMSES	Standardized Root Mean Square Error
SHAs	State Highway Agencies
SK	Simple Kriging
UK	Universal Kriging
U.S.	United States of America
VMT	Vehicle Miles of Travel

CHAPTER 1. INTRODUCTION

1.1. Background

Currently, State Highway Agencies (SHAs) use the 1993 American Association of State Highways and Transportation Officials (AASHTO) Guide for Design of Pavement Structures to design highway pavements to withstand load-induced distresses. The 1993 AASHTO design guide was derived from pavement-performance empirical data collected from an experiment administered by the former American Association of State Highway Officials (AASHO) Road Test (ART). Data collected from the test were used to develop empirical equations, which have been further refined to incorporate minor changes and improvements to the original equations to reflect on changing factors not specific to the original site location, Ottawa, Illinois (HRB, 1961; AASHO, 1962; AASHTO, 1972, 1986, 1993; NCHRP, 2002, 2004; Schwartz and Carvalho, 2006).

Several issues have been raised about the road test (Baladi and Thomas, 1994; FHWA, 2001a; NCHRP, 2002, 2004; Schwartz and Carvalho, 2006; Garber and Hoel, 2009). Some of the issues relate to the two climatic seasons (Basma and Al-Suleiman, 1991) at the time of the road test compared with today's designs which span a period of anywhere between 20 and 40 years for roads, and up to 100 years for bridges (Tonias and Zhao, 2007). Others include the original location, often described as low plasticity clay, coupled with low traffic volumes as compared with today's traffic volumes (FHWA, 2001a, 2001b; NCHRP, 2002, 2004; Schwartz and Carvalho, 2006; Garber and Hoel, 2009). To address these concerns, the Federal Highway Administration (FHWA) mandated the National Cooperative Highway Research Program (NCHRP) under Project 1-37A to carry out research and develop a state-of-art design tool for highway pavements. At the conclusion of the research, NCHRP developed an advanced pavement structural design process called the Mechanistic Empirical (M-E) Pavement Design Guide to replace the *1993 AASHTO Guide for Design of Pavement Structures*. The FHWA introduced the new M-E design approach to the state departments of transportation and the engineering community in 2004.

The M-E design philosophy was developed to produce superior designs in tandem with changing environmental factors and to match today's traffic volumes (FHWA, 2001a; NCHRP, 2004; Haider and Harichandran, 2007; Schwartz and Carvalho, 2006). Today, environmental distress must be considered when designing pavements which was not the case in the 1960s (NCHRP, 2004; Khanum, et al, 2005; Schwartz and Carvalho, 2006). It is observed that environmental factors were not factored into the formulation of empirical equations when developing earlier guides as compared to the current design guide. The new M-E methodology considers climate and environment among the input parameters by incorporating them into the design using the Enhanced Integrated Climatic Model (EICM), which predicts changes in the pavement surface over its entire design life period (NCHRP, 2004; Schwartz and Carvalho, 2006).

Environmental factors in the M-E design are currently obtained from weather stations close to the project location. The M-E design software contains a weather data library with approximately 800 weather stations scattered across the nation (Schwartz and Carvalho, 2006). From the current data library, the locations are widely spaced across the United States making it hard to obtain a representative sample of data for a given project and becoming expensive if more weather stations are added. The issue is further compounded by the method used to analyze the data: the traditional statistical analysis. Traditional statistical analysis cannot be extended to an adjacent, new project location to provide data for a project if the location is far from an existing weather station.

In addition, the M-E approach offers benefits to governing authorities and departments of transportation (DOTs) in designing pavements while, at the same time, it can be used as a forensic tool to analyze a failed highway road (NCHRP, 2004; Khanum, et al., 2005; Schwartz and Carvalho, 2006). These benefits include, but are not limited, to

1. Use of mechanistic-empirical procedures in the design of pavements.
2. Reduce the degree of design-process uncertainty giving better designs for the performance expected to minimize predominant distress types.
3. Provide better performance predictions of distresses much closer to the actual occurrence at the designed pavement life period, leading to less maintenance and rehabilitation.
4. Based on actual material properties, once research has been undertaken on the material properties, the same data will be available for use in other design projects within the geographical area.
5. Use as an advanced forensic tool when analyzing the conditions of existing pavements and investigating deficiencies for failed designs using actual material properties, climate, traffic, and other factors to identify the component or factor for failure.

The Mechanistic Empirical Pavement Design approach is credited for producing superior designs, but it does not outline a specific methodology to address uncertainty in the parameters. At present, pavement surfaces are designed to last from 20 years to 40 years (Tonias and Zhao, 2007). Considering the erratic spatial variability of environmental factors, it becomes necessary to account for them due to such long periods that pavements have to last as compared to the 10 years used in early designs. The environmental factors exhibit certainty from region to region and also within a region itself. For the case of the M-E methodology, the environmental factors have been generalized for the entire country, yet cold regions such as North Dakota (ND) may require more information to enhance the accuracy of designs.

The new design approach using geostatistics will provide a better tool to analyze the parameters while, at the same time, extending enhanced analysis to bridge areas not close to a weather station. The parameters obtained from weather stations can be used to obtain environmental factors information for a station that has missing data.

1.2. Research Objective

The fundamental objective of this research is to develop a stochastic characterization process to address the issue of environmental (temperature and precipitation) inputs to suit the M-E design framework. In this regard a variogram model and a method for kriging will be created to be used in the framework.

1.3. Research Methodology

In order to achieve the fundamental objective of this study, data were collected from the National Oceanic and Atmospheric Administration (NOAA) and a literature survey. First, a comprehensive literature survey was undertaken. The procedure for this study is broadly depicted in Figure 1.1. The tasks required for this research include, but not are limited to, the following:

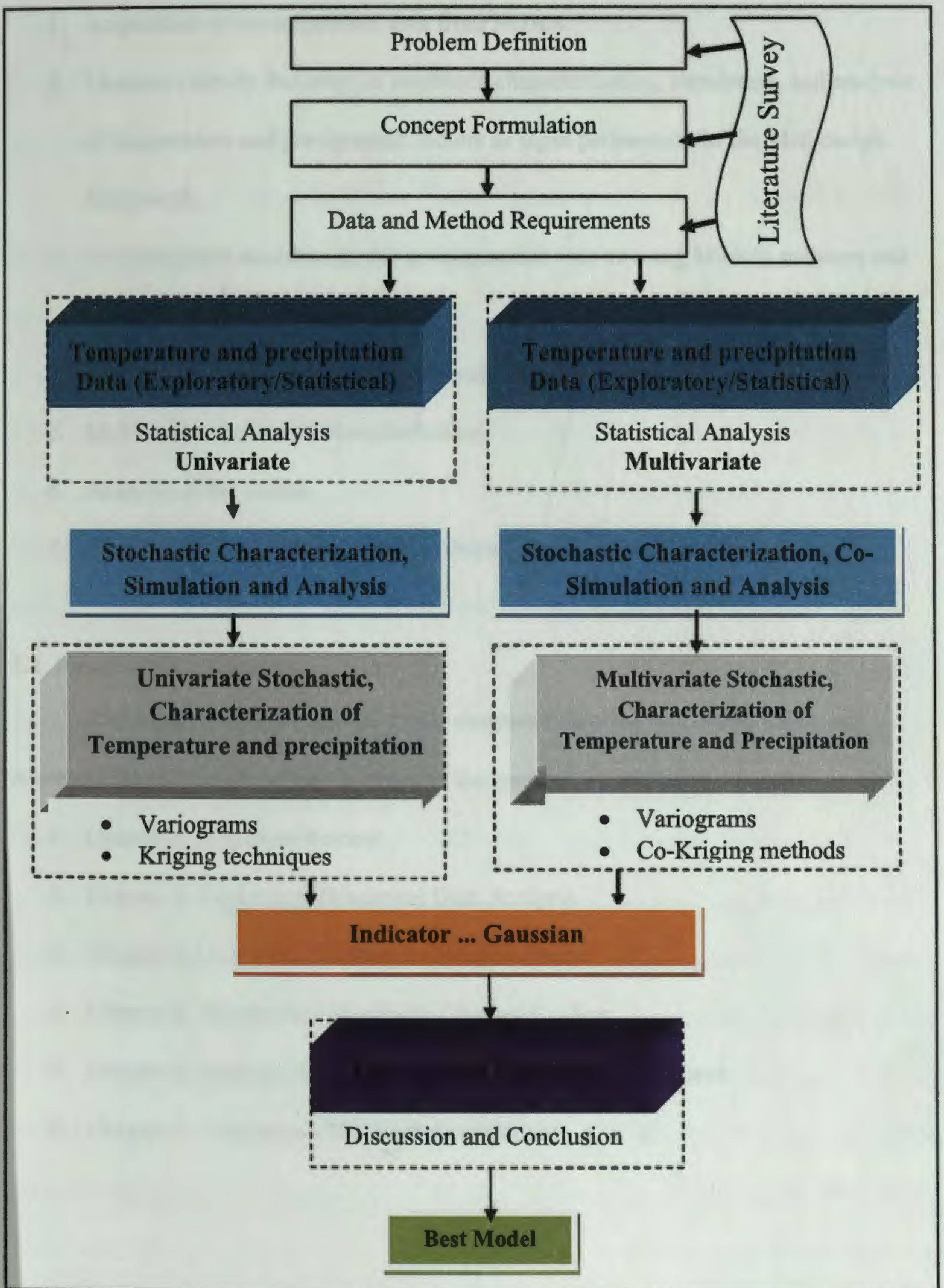

Figure 1.1. Research methodology.

1. Acquisition of environmental data from NOAA.
2. Literature survey focusing on stochastic characterization, simulation, and analysis of temperature and precipitation factors as input parameters for the M-E design framework.
3. Computational statistics on the environmental factors using Minitab software and GIS software.
4. Experimental design on univariate stochastic characterization.
5. Multivariate stochastic characterization.
6. Analysis of the results.
7. Conclusions and recommendations based on the analyzed results.

1.4. Research Organization

This thesis is divided into six major chapters following this Introduction and Abstract. The subsequent chapters describe the research methodology adopted:

1. Chapter 2. Literature Review
2. Chapter 3. Exploratory/Statistical Data Analysis
3. Chapter 4. Univariate Stochastic Characterization
4. Chapter 5. Multivariate Stochastic Characterization
5. Chapter 6. Analysis, Discussions, and Contributions to Science
6. Chapter 7. Conclusions and Recommendations.

CHAPTER 2. LITERATURE REVIEW

2.1. Introduction

Highway pavements constitute an important component of the U.S. transportation system, providing Americans with about 3 trillion vehicle miles of travel (VMT) in 2000; North Dakotans accounted for approximately 7.8 billion VMT during the same period (T.R.I.P., 2009). As of 2008, North Dakota had 7,384 miles of paved highways and 6,814 miles of paved county roads (NDDOT, 2008). North Dakotans depend on good roads in their communities to commute to work, to carry out everyday errands, and to enjoy recreational activities. Equally, businesses rely on a smooth, seamless, and efficient transportation system to move goods throughout the state and around the nation.

ASCE (2009) reports that North Dakota's highway VMT increased by 47 percent from 1990 to 2007. Furthermore, results from a 2007 study indicate that a quarter of North Dakota's major roads were rated poor or mediocre in condition, presenting considerable challenges to the motorists using them (ASCE, 2009; T.R.I.P., 2009). Although the NDDOT is determined to "continue to work cooperatively and collaboratively with local and tribal governmental entities, the legislature, congressional delegation, and the private sector to the best of their abilities to provide an integrated transportation system that safely moves people and goods," increased truck traffic volumes, has continued to exert considerable strain on the state's road system (NDDOT, 2008). If this trend of deterioration is not arrested, it is predicted that more than fifty percent of the state's highways would be under some type of distress in the next few years according the highlights of state biannual reports (NDDOT, 2008). With the current oil production boom in the western part of the state, the problem is further exacerbated by the increased activities (NDDOT, 2008; T.R.I.P., 2009).

A 2003 Federal Highway Administration (FWHA) survey found that the NDDOT uses the 1993 *AASHTO Guide for Design of Pavement Structures.* This design guide was developed using data collected from the ART site location (Ottawa, IL), consisting of a single performance criterion (PSI) and the concept of an equivalent single axle load (ESAL) (HRB, 1961; AASHTO, 1993; Brian and Zollinger, 1995; FHWA, 2003; NCHRP, 2004; Schwartz and Carvalho, 2006). Additionally, limitations such as 1) the two-year duration to conduct the experiment, 2) one climate with two climatic seasons, 3) one soil type, and 4) a small number of trucks with few axles were experienced when the experiment was conducted.

Most importantly, the environmental factors recommended for use in the 1993 AASHTO design guide were based on observations (Table 2.1). The drainage coefficient values were based on observations, experience, and rule of thumb within a specific region. The same data were then generalized for the entire country which has different climatic conditions, ranging from hot to very cold regions as is the case of North Dakota. On the other hand, there were inherent short-comings for this approach in terms of estimating environmental factors, because the factors are based on observations which do not address the issue of erratic spatial variability from region to region within the nation. Equally, environmental factors might fluctuate within a region which can led to an uneconomic design of pavements when taking into account that pavements are designed to last anywhere from 20 to 40 years (Tonias and Zhao, 2007).

Table 2.1. Recommended Drainage Coefficient Values (AASHTO, 1993).

	Percent of time Pavement Structure is Saturated			
Drainage Quality	**<1%**	**1-5%**	**5-25%**	**>25%**
Excellent (drainage within 2 hrs)	1.25 -1.20	1.20-1.15	1.15-1.10	1.10
Good (drainage within 1 day)	1.20-1.15	1.15-1.10	1.10-1.00	1.00
Fair (drainage within 1 week)	1.15-1.10	1.10-1.00	1.00-0.90	0.90
Poor (drainage within 1 month)	1.10-1.00	1.00-0.90	0.90-0.80	0.80
Very poor (no drainage)	1.00-0.90	0.90-0.80	0.80-0.70	0.70

To maintain the design quality of highway pavements and to address the issue of over- or under-design, too, it is recommended that a robust intervention be undertaken (NCHRP, 2004; Schwartz and Carvalho, 2006). Robust intervention which makes use of state-of-art-practice tools, new design tools as well as stochastic characterization of the environmental factors will have to be employed. The new M-E method, as used today, obtains environmental data from 800 weather stations scattered across the nation (Schwartz and Carvalho, 2006). The problem with this approach is that it analyzes data using the traditional statistical analysis which might not be extended to another location further away from the weather station. It thus makes it difficult to obtain representative sample data for the new project location.

In this research, the problem of non-representative data will be addressed by using geostatistics which will be utilized to develop a stochastic characterization, simulation, and analysis of environmental input factors methodology. This methodology will then be used to provide the necessary data required for environmental input parameters in the M-E design framework to avoid issues associated with over- or under-design of pavements. Geostatistics will be used to compute the necessary design data required for project locations further from the existing weather stations. Geostatistics has been successfully used in mapping extreme rainfall in mountainous regions (Prudhomme and Reed, 1999) and *Boophilus microplus* (Estrada-Peña, 1999). Other areas where geostatistics have been used include mapping ozone concentration levels in California and soil pollution in Belarus after the Chernobyl nuclear accident.

In this manner, most importantly, the method will provide the right data which will be used to aid in designing highway pavements which will be suited to a particular climatic area within a region; this information can be used to develop a framework for areas that have similar climatic conditions, thus avoiding over- or under-designs. The regions will be divided into areas with similar climatic conditions or divided into an area (for example 50 or 100 square miles) which will be manageable. The evaluation of temperature and precipitation distribution in North Dakota will be achieved by developing stochastic characterization, simulation, and analysis of the two environmental inputs using geostatistics. Developing such a model will provide a prediction map for the state compared to the current method which uses the Enhanced Integrated Climatic Model based on a few weather stations spread across the nation.

2.2. Historical Overview of Pavement Design in the United States

Although early highway pavements can be traced to ancient Babylon and Egypt, no concrete archeological information is available to attest to this in literature. The Romans were at the forefront in perfecting the art of road construction as exemplified from established networks of highways covering the entire empire; those roads were mainly used to transport military forces and materials to protect the empire (Wikipedia, 2010b). Later, the highways were used by the governing authority to govern the entire empire by improving its communication and trade within its large empire.

The Romans' pavement structures consisted of large, cut rocks which were placed on the natural formation, and the voids were filled in with coarse aggregates (fine stones and limestone dust) placed to cover them. Lastly, a final layer of carefully, cut dressed stone was then laid to form the wearing course. In most cases, this layer of the pavement was constructed to be strong, durable, and able to withstand any load without causing any serious distress on the pavement structure. Studies also showed that roads were raised above the adjacent areas to improve poor drainage to enhance pavements' life span.

Strictly speaking, the term "design" was not featured in any of the early pavement structures because pavements were built by the rule of thumb. This fact was illustrated by the abundance of available data to prove that earlier engineers exercised their innovativeness in the selection of materials as well appropriate ground support as shown by different cross-sections reported in a number of archaeological excavations and studies (Caesar, 1996; Vitruvius, 1960).

Before addressing pavement-design approaches, it is necessary to understand the different pavement surfaces used in highway design. Broadly, pavement surfaces can be categorized into three categories: flexible, rigid, and composite (Papagiannakis and Masad, 2008). A flexible pavement surface consists of layers of granular base and/or subbase layers with asphalt concrete (Papagiannakis and Masad, 2008). Rigid pavement surfaces consist of a Portland concrete layer over a subgrade or other suitable base (Papagiannakis and Masad, 2008). A composite pavement surface consists of Portland cement concrete which is used to cover a damaged asphalt concrete or Portland cement concrete pavement.

2.3. Pavement Design Approaches

Most earlier 19th-century highways in the United States were built almost at the same period as the invention of the automobile. Because the United States was a British colony, the pavements built during this era were a replica of the technology used in Europe, particularly in Great Britain. Many of the pavements built during this period were flexible pavements.

In 1824, Joseph Aspdin invented, and patented hydraulic cement, and termed it "Portland" cement (Wikipedia, 2010a). Although Portland cement has been around for some time, it was not used in pavements until 1889 when George Bartholomew proposed to use it in the first Portland cement concrete (PCC) pavement in Bellefontaine, Ohio. As with the flexible pavement, rigid pavements were designed on the basis of experience and engineering judgment.

2.3.1. AASHO Road Test

Between 1958 and 1960, a landmark test facility was constructed in Ottawa, Illinois; the objective was to collect data during the final phase. Basically, this experiment was based on performance and was administered by the American Association of State and Highway Officials, termed the AASHO Road Test (ART). ART roads consisted of four 2-lane loops covering a distance of two miles. Different specific traffic configurations of fixed axle loads were assigned to the loop-lanes. The loop-lane pavement surfaces consisted of both asphalt concrete and Portland cement concrete pavements composed of different layer thicknesses. During the test, more than one million loads were applied to the different pavement sections, and their performance data were collected bi-weekly during the entire two-year span before the pavement surfaces failed (AASHTO, 1993; FHWA, 2001a; HRB, 1961; NCHRP, 2004; Schwartz and Carvalho, 2006).

Data collected from the ART were then used to develop empirical equations. These equations were created through regression analysis to determine the relationship between the numbers of axle-load passes and the performance of different pavement surfaces. The empirical pavement design equations developed were for both asphalt and Portland concrete pavement structures. From the ART experiment, two important concepts were identified: serviceability and the relationship between change in serviceability and repetition load, Equivalent Single Axle Load (ESAL). Serviceability is defined by the Highway Research Board (HRB) report has, "the ability of a specific section of pavement to serve high speed, high volume, and mixed traffic in its existing condition" (Schwartz and Carvalho, 2006). For rigid pavements, Equation 2.1 is used (HRB, 1961):

$$PSI = 5.41 - 1.9\log(1 + SV) - 0.09\sqrt{C + P}, \tag{2.1}$$

where *PSI* is the present serviceability index, *SV* is slope variance, *C* is linear feet of major cracking per 1000 ft^2 of area, and *P* is patching per 1000 ft^2 of area.

2.3.2. AASHO Interim Design Guide 1972

The data collected from ART formed the basis of the 1972 design guide which was introduced to SHAs and the engineering community by the AASHO. The original empirical equations were based on a specific subgrade, pavement materials, and environmental conditions at the ART site location (NCHRP, 2004). The 1972 AASHO design guide introduced some of the most important concepts which have withstood for a long time. These landmark concepts included traffic damage loss, Equivalent Single Axle

Loads, present serviceability index, and the structural number. The original equation is shown in Equation 2.2 (AASHO, 1972):

$$\left(\log(W_{18}\right) = 7.5.\log(D+1) - 0.06 + \log\left(\frac{(4.5 - p_t)}{(4.2 - 1.5)}\right), \tag{2.2}$$

where W_{18} is the accumulated 18 kip equivalent single axle load for the design period, P_t is the terminal serviceability at the end of design life, and D is the thickness of the slab in inches.

Because the information used to develop the equation only related to the ART conditions, the equation was further refined to take into account other conditions which did not exist at the trial location (AASHTO, 1972). It is worthwhile to note that experience and theory were used to determine the strength of the subgrade using the Westergaard modulus of subgrade reaction equation to compute the strain and stress that developed in the pavements.

2.3.3. AASHTO 1986/1993 Design Guides

The 1986 AASHTO guide was a product of revisions to the 1972 design approach. The 1986 revision focused on 1) better characterization of the subgrade, 2) incorporation of pavement drainage, 3) better consideration of environmental effects, and 4) incorporation of reliability as a factor in the design equation (Schwartz and Carvalho, 2006). The 1986 guide also took into account the life-cycle cost analysis to determine the pavement surface to be used.

Emphasis for the 1986 AASHTO guide focused on the effects of environment on pavement serviceability, especially frost heave, thaw weakening, and the swelling of subgrade soils. The environmental effects were divided into two groups: separation of total serviceability loss into traffic load and environmental components, and estimation of effective subgrade resilient modulus that reflects the seasonal variation of the moisture in the subgrade (Papagiannakis and Masad, 2008). The total serviceability loss, *ΔPSI,* is related to three components in Equation 2.3 (Papagiannakis and Masad, 2008).

$$\Delta PSI = \Delta PSI_{TR} + \Delta PSI_{SW} + \Delta PSI_{FH} , \tag{2.3}$$

where ΔPSI_{TR}, ΔPSI_{SW}, and ΔPSI_{FH} the components attributed to traffic, swelling, and frost heave related to loss of ΔPSI, respectively.

Few changes were made between the current 1993 AASHTO version and the 1986 version except in the area of rehabilitation design for pavements using overlays and the use of non-destructive testing to evaluate existing pavements and backcalculate the layer moduli to determine layer coefficients (NCHRP, 2004; Schwartz and Carvalho, 2006). In both the 1986 and 1993 AASHTO design approaches, the traffic damage loss (serviceability) for rigid pavement was calculated from the following empirical equation which gives the result in imperial units (AASHTO, 1993):

$$\begin{aligned}\log(W_{18}) = Z_R S_0) + 7.5\log(D+1) - 0.06 + \frac{\log\left(\Delta PSI / (4.5-1.5)\right)}{1+\left(1.624*10^7/(D+1)^{8.46}\right)} + \\ + (4.22 - 0.32P_t)\log\left(\frac{S'_c C_d\left(D^{0.75}-1.132\right)}{215.63J\left[D^{0.75} - \dfrac{18.42}{(E_c/k)^{0.25}}\right]}\right)\end{aligned} \tag{2.4}$$

where W_{18} is the number of ESALs predicted to be carried by the pavement; D is the Portland concrete slab thickness, inches; P_t is the terminal serviceability of the section; S'_C

is the modulus in rupture of the Portland concrete (lbs/in^2); C_d is the drainage coefficient; J is a load transfer coefficient; E_C is the modulus of elasticity for the Portland concrete (lbs/in^2); k is the modulus of subgrade reaction (lbs/in^2); Z_R is the standard deviation corresponding to the selected level of reliability; and S_0 is the overall standard error in predicting the pavement serviceability.

The recommended drainage coefficient, *Cd*, values were based on drainage quality and levels at the time of exposure for a pavement near saturation (AASHTO, 1993). On the other hand, recommended values for the transfer coefficient, *J* were based on the type of pavement and the shoulder material/load transfer reinforcement used across joints or transverse cracks (AASHTO, 1993).

2.4. M-E Design Approach

The Mechanistic Empirical Design approach is the latest design guide which is currently being evaluated by several SHAs before its introduction as an AASHTO design guide. The latest guide provides methodologies for mechanistic-empirical pavement design that take into account the local materials, environmental conditions, and actual highway traffic load distribution by means of axle load spectra (NCHRP, 2004; Schwartz and Carvalho, 2006). The materials, traffic, environmental factors, and reliability are the input components in the M-E design approach as shown in Figure 2.1. The M-E design approach is defined as a design philosophy or approach wherein the classical mechanics of solids are used in conjunction with empirically derived relationships to accomplish the design objectives (NCHRP, 2004).

is the modulus in rupture of the Portland concrete (lbs/in^2); C_d is the drainage coefficient; J is a load transfer coefficient; E_C is the modulus of elasticity for the Portland concrete (lbs/in^2); k is the modulus of subgrade reaction (lbs/in^2); Z_R is the standard deviation corresponding to the selected level of reliability; and S_0 is the overall standard error in predicting the pavement serviceability.

The recommended drainage coefficient, *Cd*, values were based on drainage quality and levels at the time of exposure for a pavement near saturation (AASHTO, 1993). On the other hand, recommended values for the transfer coefficient, *J* were based on the type of pavement and the shoulder material/load transfer reinforcement used across joints or transverse cracks (AASHTO, 1993).

2.4. M-E Design Approach

The Mechanistic Empirical Design approach is the latest design guide which is currently being evaluated by several SHAs before its introduction as an AASHTO design guide. The latest guide provides methodologies for mechanistic-empirical pavement design that take into account the local materials, environmental conditions, and actual highway traffic load distribution by means of axle load spectra (NCHRP, 2004; Schwartz and Carvalho, 2006). The materials, traffic, environmental factors, and reliability are the input components in the M-E design approach as shown in Figure 2.1. The M-E design approach is defined as a design philosophy or approach wherein the classical mechanics of solids are used in conjunction with empirically derived relationships to accomplish the design objectives (NCHRP, 2004).

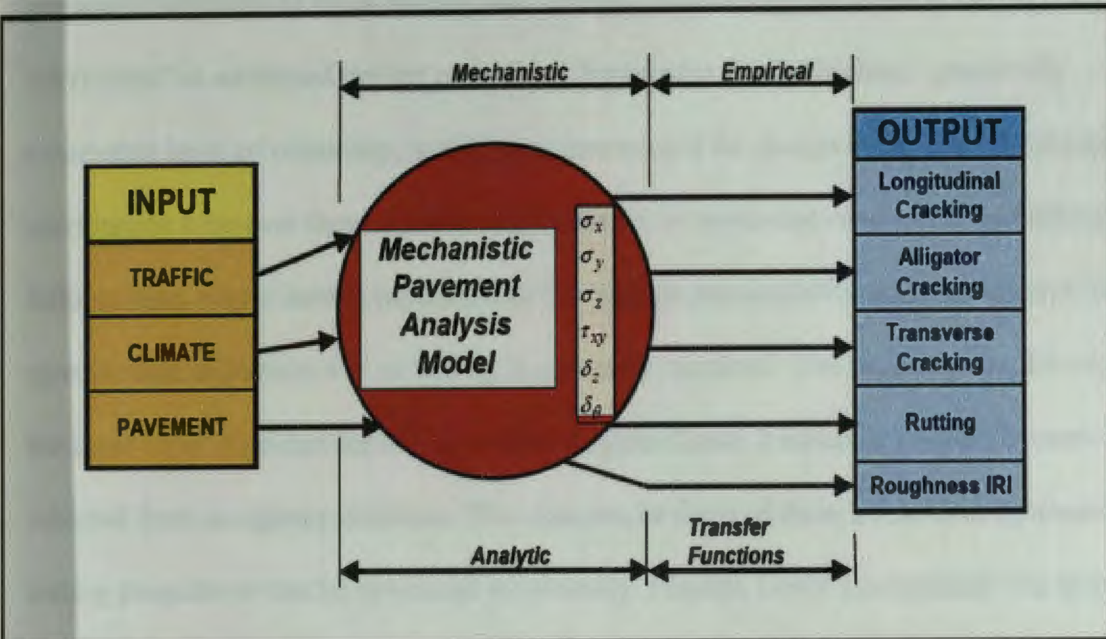

Figure 2.1. Design outline of M-E pavement design guide process (NCHRP, 2004).

The M-E design methodology uses the hierarchical process to select data for inputs when designing a pavement surface. This hierarchical process allows the designer flexibility to create a pavement surface by considering different levels to produce superior pavement designs for the specific class or level of reliability required. This process is achieved by using 1) mechanistic where the cumulative damage, stresses and strain, are computed over the life span of the pavement; and 2) empirical which predicts pavement distresses such as rutting, cracking, and roughness in the pavement during the selection of a trial design. The NCHRP (2004) software primarily employs a hierarchical approach to traffic, materials, and environmental inputs.

Three levels of input can be used, depending on several factors, such as type of project, sensitivity of pavement performance, resources available to the designer, and the availability of data at the time of the design (NCHRP, 2004). Khanum, et al. (2005)

proposed the levels of input for the M-E design methodology as follows: Level 1 which is a "first class" or advanced design procedure. It provides for the highest practically achievable level of reliability, and it is recommended for design in the heaviest design corridors or wherever there are dire safety issues, or economic consequences with early failure. Also, where design inputs are of the highest practicability achievable level, site-specific data collection and or testing is generally required. The second level, Level 2, is the input level expected for use in routine designs. Level 2 inputs are typically user-selected from an agency database. The data can be derived from a less-than-optimum testing program or can be estimated empirically. Finally, Level 3 is typically the lowest class of design and should be used where there are minimal consequences for early failure. Inputs are typically user-selected default values or the typical average for the region. A summary of the input components for the design approach follows in the next sections.

2.4.1. Traffic Loading

Traffic loading is an important input element in the M-E design approach; traffic loading is measured in terms of axle-load distributions by axle configuration. Anticipated truck traffic is classified according to axle type (tandem, triple, tridem, or quad) (Zhang, et al., 2000; FHWA, 2001a; NCHRP, 2004; Haider and Harichandran, 2007). The FHWA study on "Traffic Monitoring Guide" classifies axle configurations into 13 vehicle classes (FHWA, 2001a). Traffic data used for pavement loading are collected by: 1) automatic traffic recorders (ATR), 2) automated vehicle classifiers (AVC), and 3) weigh-in-motion devices (WIM) (Papagiannnakis and Masad, 2008; Papagiannnakis et al., 2006). These devices are installed on the driving lane, and record traffic data at normal driving speeds.

Traffic data input in the M-E design approach are categorized into four levels by specifying the method used for data collection from the weigh stations: Level I input requires traffic data from WIM that is project specific. Level II input requires traffic from WIM that is a regional representative weight or AVC that is project specific. Level III input is similar to Level II and also includes an estimated percentage of trucks or ATR data which is site specific. Level IV input requires traffic data from ATR which are site specific. The Federal Highway Administration has proposed a number of equations to use when computing traffic loading for pavement design (FHWA, 2001a; NCHRP, 2004; Papagiannnakis and Masad, 2007), which have also been adopted by AASHTO. The equation commonly used for traffic loading computation is shown:

$$AADTT_c = \frac{1}{7}\sum_{i=1}^{7}\left[\frac{1}{12}\sum_{j=1}^{12}\left(\frac{1}{n}\sum_{k=1}^{n} AADTT_{ijkl}\right)\right], \tag{2.5}$$

where *AADTTc* is the average daily traffic volume for vehicle class, *c*, for day, *k*, of week *(DOW)*, *i*, and month, *j*; *i* is the *DOW*, ranging from 1 to 7 for Monday to Sunday, respectively; *j* is the month of the year ranging from 1 to 12 for January to December, respectively; and *n* is the number of times data from a particular *DOW* are available for computing the average in a given month. The monthly traffic volume adjustment factor for month *j* (MAF_j) is computed from Equation 2.6:

$$MAF_j = \frac{AADTT_c}{VOL_{cj}}, \tag{2.6}$$

where $AADTT_c$ is the average annual daily truck traffic volume for vehicle class, c, and VOL_{cj} is the average annual daily truck traffic volume.

2.4.2. Pavement Materials Characterization

Material characterization is among the most important input parameters required in the design of pavements as shown in the literature (Olidis and Hein, 2004). Olidis and Hein (2004) provide tables that give the information required for material characterization of the pavement and subgrade materials of input into the M-E design procedure. Some State Highway Agencies that have developed material characterization for the M-E methodology include WSDOT, Mn/DOT, MoDOT, and NCDOT (Schwartz and Carvalho, 2006). The NCHRP (2002) 1-37 report provides details of material factors required to fully implement the recommendation contained in the M-E design guide. Data were obtained from the Long-Term Pavement Performance study sections around the nation.

2.4.3. Climate/Environment

Climate/environment parameters inputs in the M-E approach are simulated using the Enhanced Integrated Climatic Model (EICM) to predict changes in the pavement surface over its entire design life (Schwartz and Carvalho, 2006). The hourly air temperature, hourly precipitation, hourly wind speed, hourly percentage of sunshine, and hourly relative humidity used in the EICM are obtained from weather stations close to the project location. The M-E design software has a weather data library containing approximately 800 weather stations scattered across the nation (Schwartz and Carvalho, 2007). A full detail of the climate/environment is described next.

2.5. Environmental Factors

Environmental factors contribute greatly to the performance of the pavements. As stated earlier, the main environmental factors of concern are temperature and precipitation.

These two factors play a significant role when water freezes in the pores of pavement materials and during the spring-thaw period. The presence of water in the subgrade is a major factor of concern because it accelerates pavement deterioration which can lead to pavement failure due to heavy loads. This problem is referred to as pumping, which is generally common in concrete roads (FHWA, 2001a; NCHRP, 2004; Papagiannnakis and Masad, 2008).

In the M-E design, varying pavement properties and the subgrade materials due to environmental change is modeled using the Enhanced Integrated Climate Model (EICM) (NCHRP, 2004; Papagiannnakis and Masad, 2008; Schwartz and Carvalho, 2006). The EICM uses a master climate database to predict the impact of climate change on a specific material property. Also, temperature and precipitation data can be used to model material properties such as resilient modulus to determine the load carrying capacity during various seasons of the year. In the design of rigid pavements, environmental conditions have significant effects on their performance (Papagiannnakis and Masad, 2008; Garber and Hoel, 2009). Different specifications are used for other issues of concern, such as materials and traffic in different levels in the design, however, when it comes to weather specification, the same values are used for the three hierarchical design input levels in the M-E design approach (NCHRP, 2004)

Environmental data used to conduct this research was extracted from the National Climate Data Center (NCDC) titled Climatography of the United States No. 81 from NOAA (2009) web site. The extracted data contain monthly information for temperature and precipitation for a 30-year period, called normals, from 1971-2000. The extracted data were from 152 sampled weather stations across the state of North Dakota.

2.5.1 Temperature

The effect of temperature on flexible pavements is different from that of rigid pavements. With flexible pavements, temperature affects the resilient modulus of the asphalt layers while, for rigid pavements, it causes curling of the slab. Curling occurs because of the difference in temperatures between the top and the bottom of the concrete slab which causes temperature stresses in the slab.

For the case of flexible pavements, the dynamic modulus of asphalt concrete varies with temperature. The most common issue affecting flexible pavement is frost heaving which occurs during the spring and results in differential settlements and pavement roughness. In spring, this is the period when the ice melts and the subgrade is in a fully saturated condition.

2.5.2 Precipitation

Precipitation is defined as a form of water from rain and snow which affects the quantity of surface water infiltrating the subgrade and percolating into the ground water table. Cedergren (1974) studied drainage of ground-water seepage under pavements, and the results showed that this area is overlooked by engineers when designing pavements. Where pavements are poorly designed, drainage may produce a lack of shear strength, pumping, and even loss of support.

2.6. Geostatistical Characterization

Stochastic characterization is achieved using the kriging method, which was established by Danie Krige (1951) and Georges Matheron (1962). Kriging is described as an optimal spatial-prediction procedure based on regression analysis against observed data points at surrounding locations. These points are weighed against spatial covariance values optimized with respect to specific error criteria (Bohling, 2005). The method is used to interpolate a minimum linear error variance estimate at the location where an actual value is unknown. Because of this minimum linear error, kriging can be used for interpolation when analyzing environmental data, calculating the cumulative distribution function values and a mapping model (Goldberger, 1968; Matheron, 1971; Journel, 1989; Goovaerts, 1997; Deustch and Journel, 1998; Chilès and Delfiner, 1999; Journel and Huijbregts, 2003)

Kriging algorithms are utilized in different fields such as engineering, earth sciences, and environmental sciences (Zhou, et al., 2007). The algorithms make use of a variogram, which is the relationship between the geological distance and Euclidean distance, and then assigns weights to estimate the unsampled location data values. ASTM defines a variogram that has a measure of spatial variation that is one-half for the variance of the difference between two variables and then expressed as a function of the lag, usually referred to as the semi-variogram. The variogram is defined as a function of distance as shown in Equation 2.7 (Nalder and Wein, 1998):

$$\gamma(h) = \frac{1}{2N(h)} \sum_{k=1}^{N(h)} \left[(X_k + h) - Z(X_k) \right]^2 \tag{2.7}$$

where $\gamma(h)$ is the variogram of variable Z at the separation distance of h and $N(h)$ is the number of pair points separated by distance interval $h + \Delta h$.

2.7. Kriging Methods

Broadly speaking, the kriging methods can be classified into two groups: linear and non-linear. Linear methods include 1) simple kriging (SK), 2) ordinarily kriging (OD), 3) universal kriging (UK), 4) Bayesian kriging, and 5) factorial kriging. On the other hand, non-linear methods include 1) indicator kriging (IK), 2) probability kriging (PK), and 3) disjunctive kriging (DK). In this study, simple kriging, ordinary kriging, universal kriging, indicator kriging, probability kriging and disjunctive kriging methods are evaluated to recommend the best method to use when analyzing an environmental dataset.

2.7.1. Simple Kriging

In areas where simple kriging (SK) is used, it is assumed that the mean is known and constant throughout the area of study considered and is applied only to transformed, normal data. Equation 2.8 gives the basic linear estimator for simple kriging (Journel and Deustch, 1998):

$$Z^{*}_{SK}(x) = \sum_{i=1}^{n} \omega_i(x) Z(x_i) + \left[1 - \sum_{i=1}^{n} \omega_i(x)\right] m \qquad (2.8)$$

where $Z(x)$ is the random variable at location x, all x_i values are the n number locations to consider, $m(x)=E\{Z(x)\}$ is the location-dependent expected value of the $RV\ Z(x)$, $Z^{*}_{SK}(x)$ is the linear regression estimator, $\omega_i(x)$ is the weights, and m is the constant mean. The assumptions made while developing this method make it restrictive for kriging.

2.7.2. Ordinary Kriging

Ordinary kriging (OK) is the formulation of improved simple kriging to compute optimal weights to minimize the mean square estimation error (Goovaerts, 1997; Deustch and Journel, 1998). The OK estimator is given below and assumes that the mean is constant, but unknown (Goovaerts, 1997):

$$Z^{*}_{OK}(x)=\sum_{i=1}^{n}\omega_i(x)Z(x_i)+\left[1-\sum_{i=1}^{n}\omega_i(x)\right]m \quad (2.9)$$

2.7.3. Universal Kriging

Universal Kriging (UK) is also known as kriging with a trend. UK is used to deal with a non-stationary mean where the expected value of *Z(x)* is a deterministic function of the coordinates, but a thorough analysis should be done prior to its application as (Goovaerts, 1997; Deustch and Journel, 1998):

$$Z(x)=m(x)+R(x)\ and\ m(x)=E\{Z(x)\}=\sum_{k=0}^{n}\mu_k\lambda_k(x) \quad (2.10)$$

2.8. Cross Validation

Cross validation is used to check the correctness of developed variogram models which consist of estimated experimental values. The process consists of removing half the points from the dataset at a time and then using the remaining dataset with different variograms (Goovaerts, 1997). From this computation, the true error can be estimated as shown in Equation 2.11 (Pardo-Iguzquiza, 1998):

$$\varepsilon i=\hat{\rho}(xi)-\rho(xi) \quad (2.11)$$

where ε is the error, $\hat{\rho}(x)$ is the estimated value, and $\rho(x)$ is the true value. The estimated value is computed based on the experimental data, *n*. The following are the interpolation techniques used in cross validation:

Mean error (ME)

$$ME=\frac{1}{n}\sum_{i=1}^{n}\varepsilon i \quad (2.12)$$

Mean square error (MSE)

$$MSE = \frac{1}{n}\sum_{i=1}^{n}\varepsilon^{2}i \tag{2.13}$$

Mean standardized square error (MSSE)

$$MSSE = \frac{1}{n}\sum_{i=1}^{n}\frac{\varepsilon^{2}i}{\sigma^{2}i} \tag{2.14}$$

Root mean square Error (RMSE)

$$RMSE = \sqrt{\frac{1}{n}\sum_{i=1}^{n}\varepsilon^{2}i} \tag{2.15}$$

Standardized root mean square error (RMSES)

$$RMSES = \sqrt{\frac{1}{n}\sum_{i=1}^{n}\left(\frac{mean}{\sigma^{2}(xi)}\right)} \tag{2.16}$$

The ME, MSE, MSSE, RMSE, and RMSES will be used to compare and contrast the kriging techniques. Pardo-Iguzquiza (1998) proposed the following criteria to evaluate the kriging methods using a combination of kriging and variogram techniques. The best variogram to use should have the following characteristics: 1) ME value to be closest to zero, 2) MSE to have a small value, 3) MSSE to be closest to 1, 4) RMSE to be a small value, and 5) RMSES to be near 1.

2.9. Statistical Analysis

With statistical analysis, two methods were used to analyze the environmental data: numerical descriptive measure and exploratory data analysis (ESDA). The main difference between descriptive analysis and ESDA is that the later will give a prediction map of the data apart from numerical measures. Numerical descriptive statistics, which measure the central tendency (mean and median), and the variability (variance and standard deviation) were used to analyze the primary environmental data (temperature and precipitation). Mean is defined as the sum of the measurements, divided by the number of measurements contained in the set (McClave and Sincich, 2009). The following equation is used when computing the mean as shown in Equation 2.17.

$$\bar{x} = \frac{\sum_{i=1}^{n} x_i}{n}, \tag{2.17}$$

While, sample variance can be defined as the sum of the squared distances from the mean, divided by *(n-1)* (McClave and Sincich, 2009), and is shown in Equation 2.18.

$$s^2 = \frac{\sum_{i=1}^{n} \left(x_i - \bar{x}\right)^2}{n-1}, \tag{2.18}$$

where s^2 is the sample variance; n is the number of sample measurements; x_i is sample measurement, i to n; and $\bar{x}$ is the mean of the sample.

The sample standard deviation, s, is the positive square root of the sample variance, s^2. Minitab software was used to compute numerical descriptive measures such as the mean, standard deviation, skewness, and the median. The prepared and filtered data for temperature and precipitation were input into the Minitab software and analyzed to give a summary of the required statistics.

The second method, exploratory data analysis, is used to explore data for creating a surface. The exploratory spatial data analysis (ESDA) allows data to be fully analyzed to make better decisions about selecting a suitable method to use when analyzing the data. ESRI describes ESDA as an environment which is composed of a series of tools (histogram, voronoi map, normal and general QQ Plot, trend analysis, variograms/covariance cloud, and crosscovariance cloud), each allowing a view into the data. The ESDA environment is designed to graphically investigate the dataset to gain a better understanding of the data.

The program used in the Geostatistical Analyst requires the data to be normally distributed. In cases where the dataset is skewed, the dataset must be transformed to make it normal. The histogram and the normal QQ Plot are two methods that allow investigators to explore the outcome of the transformations made on the dataset.

2.10. GIS Software

GIS software was used to analyze the environmental data. A geographical information system (GIS) as commonly known can be defined differently depending on its area of application (Clarke, 2003). GIS basically consists of 1) the database, 2) the spatial or map information, and 3) some way to link the first two (Clarke, 2003). The definition used for this study is closely linked to the way GIS operates as proposed by Dueker (1979) (Clarke, 2003). Dueker defined GIS as "a special case of information systems where the database consists of observations on spatially distributed features, activities, or events, which are definable in space as such points, lines, or areas. A geographical system manipulates data about these points, lines, and areas to retrieve data for ad hoc queries and analyses" (Clarke, 2003). The development of GIS, as well as the introduction of computers in the 1960s, has revolutionized the management of geographical data; in particular, introduction of the user interface in the 1990s has further improved GIS' ease of use (Clarke, 2003).

CHAPTER 3. EXPLORATORY/STATISTICAL DATA ANALYSIS

3.1. Introduction

As stated earlier, the environmental data used for this research were extracted from the NCDC for the period of 1971-2000; the data contained 152 weather station points. Two datasets were used: monthly weather sample points for normal temperature and precipitation. Weather stations with a single dataset were filtered to produce 118 sample data points. These dataset points were converted into latitudes and longitudes, and plotted on a map. The dataset points used to conduct this experiment are shown in Figure 3.1.

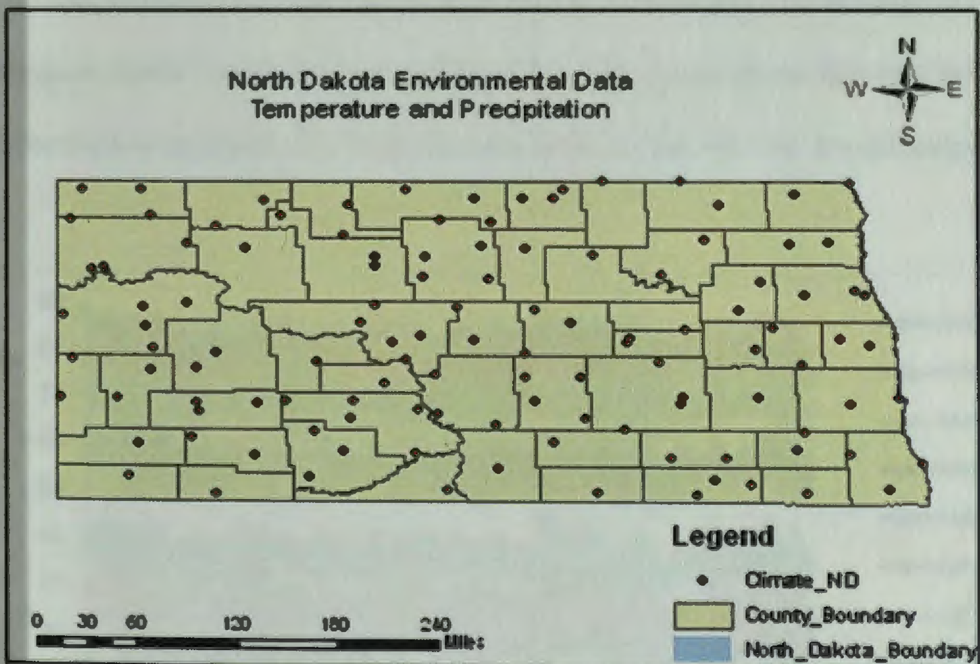

Figure 3.1. Map of North Dakota showing the location of the weather stations.

3.2. Data Preparation

The original NCDC data were in ASCII files format (NOAA, 2009), but they were converted into spreadsheet files for easy manipulation and conversion to text files used as input for the Geostatistical Analyst of ESRI's GIS software (Arcview, version 9.3). The data consisted of monthly maximum, average, and minimum temperatures as well as average monthly precipitation values for the 152 locations. Quantitative monthly temperature and precipitation data for the entire period under consideration were filtered based on the availability of data for each sampled location. After sorting the data, 118 weather stations had the required data used in this research; the data are given in Appendices A and B.

The monthly maximum and annual temperature for the 118 sampled weather station locations in North Dakota is given in Figure 3.2. This figure shows that July is the month with the highest temperatures, while January is the month with the lowest temperatures.

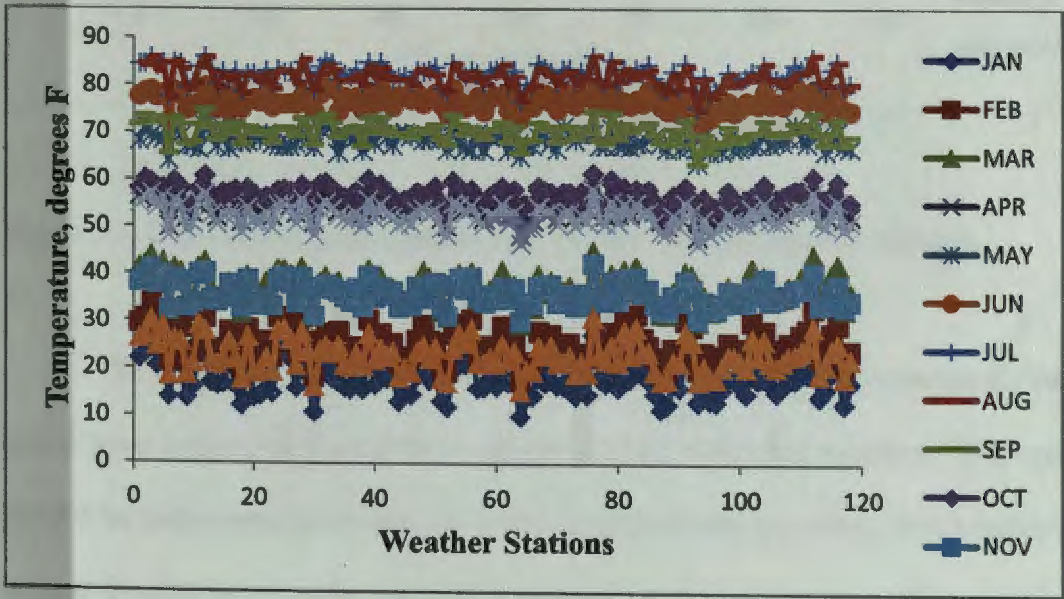

Figure 3.2. Diagram showing maximum temperatures of the sampled weather stations.

Figure 3.3 is a presentation of the precipitation dataset for 118 weather stations sampled for the months of January to December. January and July are the months that have the smallest and highest precipitation for the 30-year period, respectively. In general, when the two figures 3.2 and 3.3 for maximum temperature and precipitation are compared, it shows that as temperature increases, precipitation equally increases and vice versa in the case of a decrease.

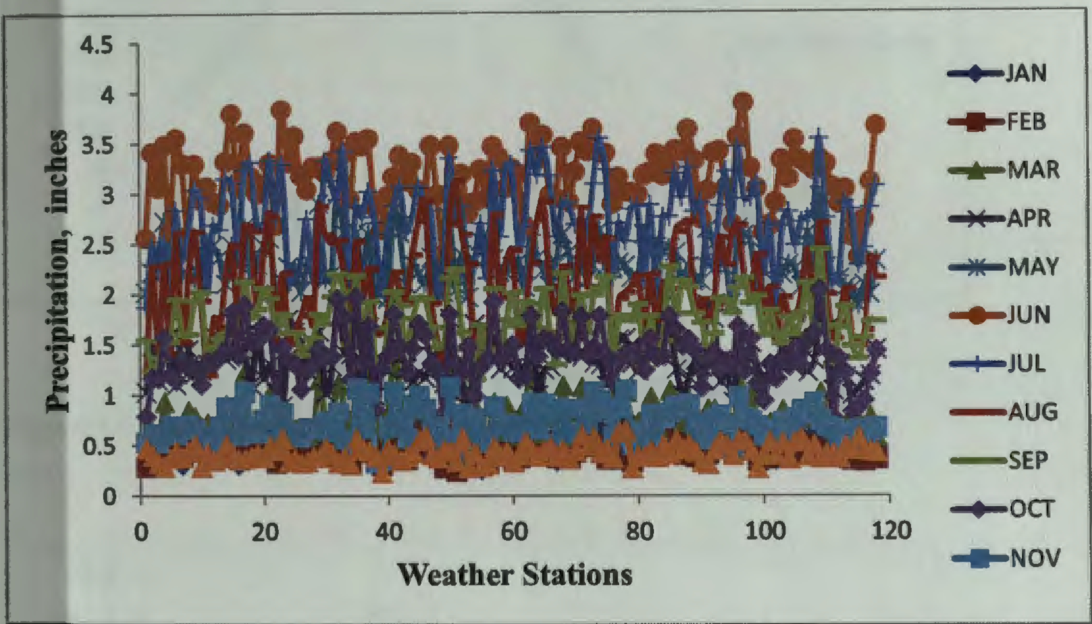

Figure 3.3. Chart showing precipitation of 118 the sampled weather stations.

The sampled weather stations' temperature and precipitation average for each month from January to December is compared in the following diagrams. When graphs are plotted for both temperature and precipitation against time (months), both roughly have a normal distribution (Figures 3.4 and 3.5). The data were further proofed by carrying out both exploratory data analysis and the traditional statistical analysis to show that the datasets had a normal distribution. The particular type of distribution is important because it will determine if a trend is to be removed before a method is selected for geostatistical analysis done on the two datasets.

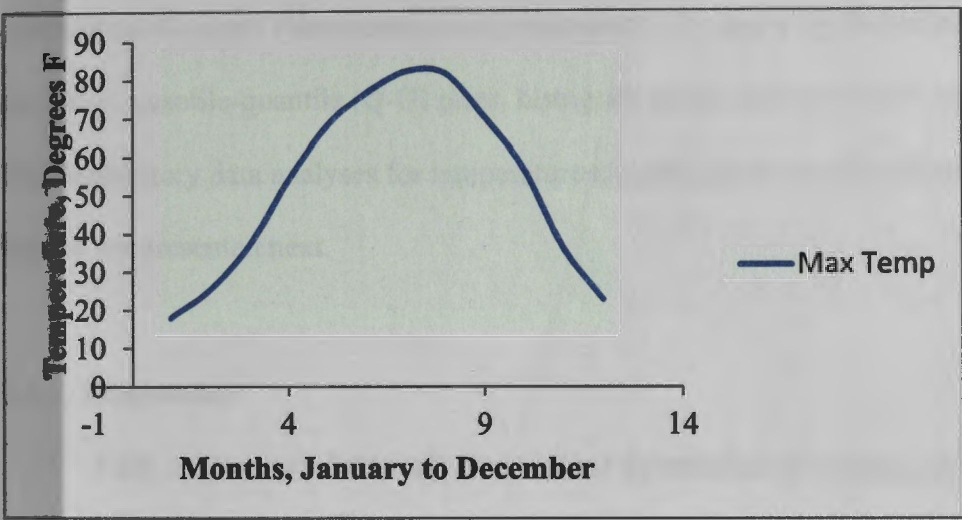

Figure 3.4. Diagram of temperature for January to December.

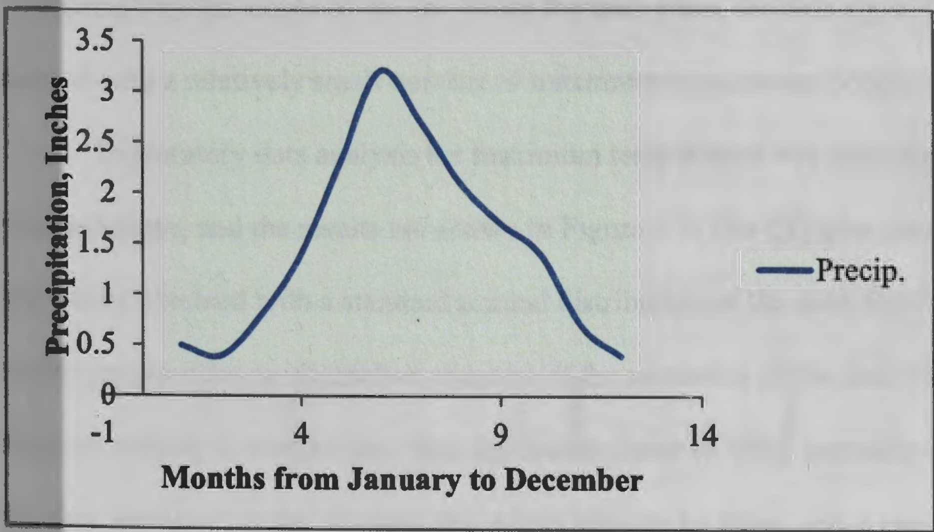

Figure 3.5. Diagram of precipitation for January to December.

3.3. Exploratory Data Analysis

After the prepared data were converted into text files, the files were then input into GIS software. The software further transformed text files into shape files for use in Arcview for exploratory data analysis. Exploratory data analysis was conducted on the two environmental inputs (temperature and precipitation) by applying the techniques of central tendency, quantile-quantile (Q-Q) plots, histogram plots, cross plots and probability plots. The exploratory data analyses for temperature and precipitation of the environmental factors are presented next.

3.3.1. Temperature

First, exploratory data analysis was done on maximum, average, and minimum annual temperature data. The unit of measurement for temperature used in this study was degrees Fahrenheit. The result from exploratory data analysis for maximum temperature is depicted by the histogram shown in Figure 3.6. The density within each class distribution is represented by the height of the bar. From the histogram, the data appear to be close to normal with a relatively small number of maximum temperature concentration values.

Exploratory data analysis for maximum temperature was done by applying the QQ plot technique, and the results are shown in Figure 3.7. The QQ plot compares well with the results obtained with a standard normal distribution of the data. Further, the QQ Plot technique provides an alternative measure of the normality of the data. If the points are close to creating a straight line, then the data is closer to being normally distributed. From the data presented in the diagram, the points seem to be close, and it can be assumed that the maximum temperature dataset is normally distributed.

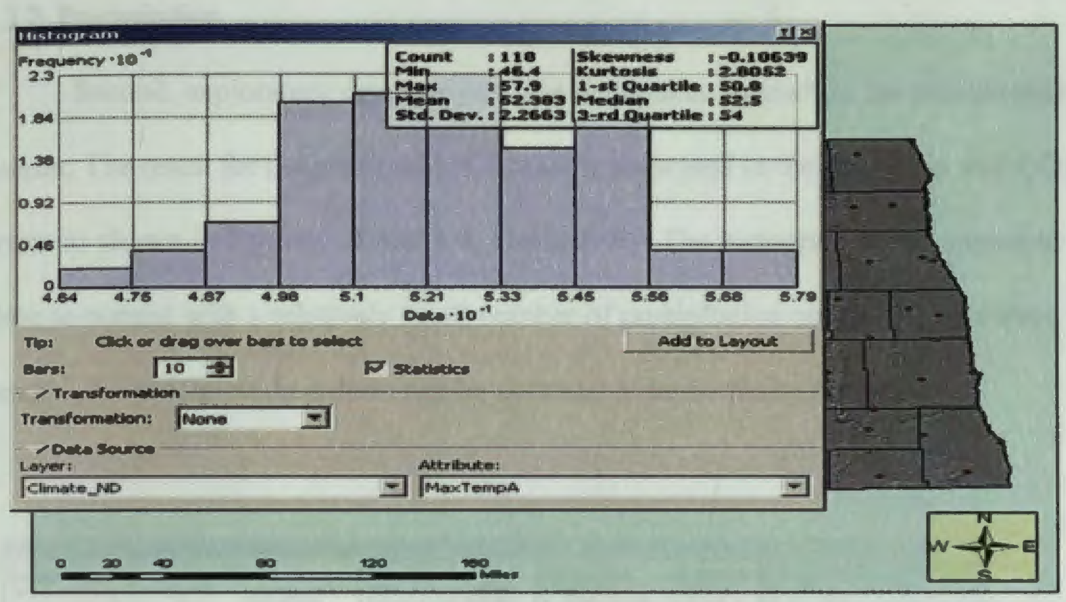

Figure 3.6. Histogram for maximum temperature.

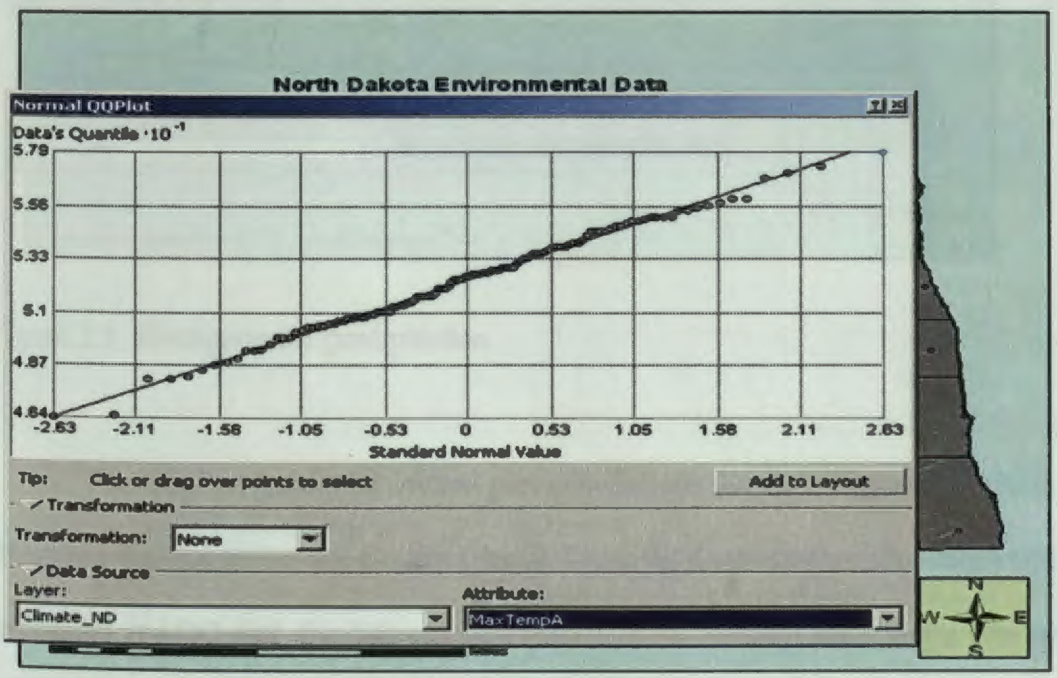

Figure 3.7. QQ plot for maximum temperature.

3.3.2. Precipitation

Second, exploratory data analysis was undertaken to analyze the precipitation dataset. The result for the precipitation dataset is presented in the histogram and QQ plot printouts shown in Figures 3.8 and 3.9, respectively. The histogram points appear to be close to normal with a relatively small number of precipitation concentration values. In general, the precipitation dataset can be assumed to be normally distributed.

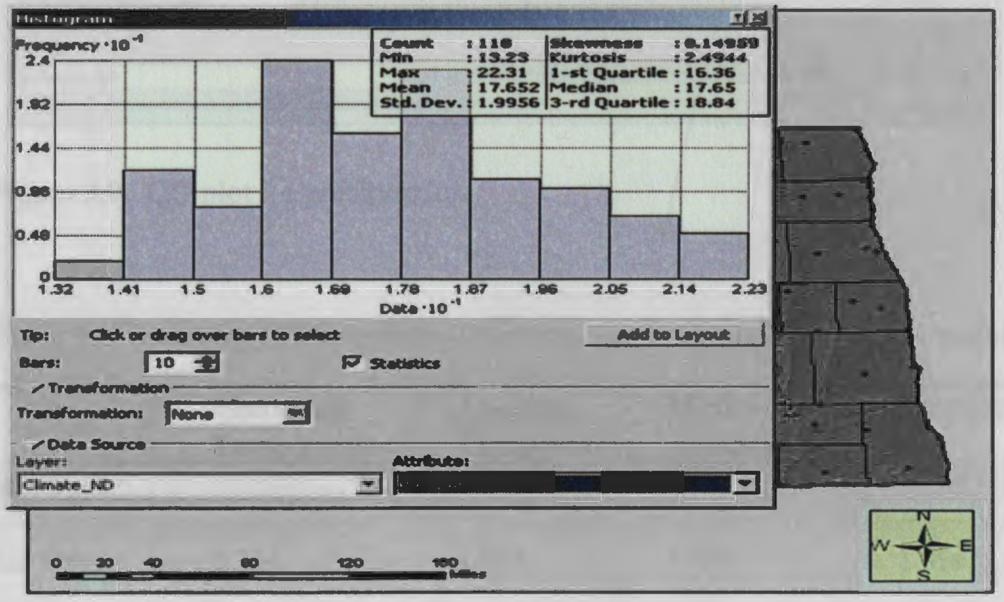

Figure 3.8. Histogram for precipitation.

The QQ Plot results for annual precipitation are shown in Figure 3.8 which illustrates that the points are closely spaced. From the distribution of the dataset on the histogram and QQ plot, the data can be assumed to be normally distributed. The summary of exploratory data analysis for temperature and precipitation is shown in Table 3.1.

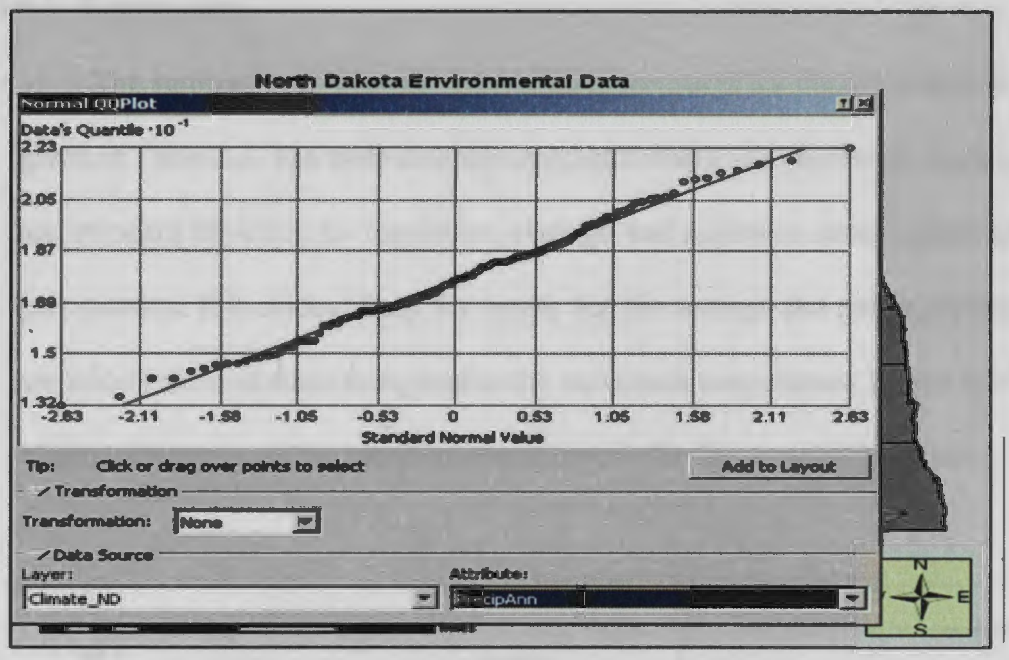

Figure 3.9. QQ plot for precipitation.

Table 3.1. Summary of Exploratory Data Analysis for Temperature and Precipitation.

	Maximum Temperature	Average Temperature	Minimum Temperature	Precipitation
Mean	52.383	40.668	28.902	17.652
Std Dev.	2.264	1.908	1.890	1.996
Skewness	-0.100	-0.45	-0.47	0.15
Median	52.504	40.850	29.258	17.650

3.4 Statistical Data Analysis

The methodology used for the traditional statistical computation of the primary data was numerical descriptive measures as described in the literature survey. The mathematical equations used to analyze the data were given in Equations 2.17 and 2.18

3.4.1. Temperature

The summaries of numerical descriptive measures for the sampled primary data are given in Table 3.1. The table contains computed results for the mean, median, skewness, and standard deviation for maximum, average, and minimum temperatures and precipitation. It is evident from the results that the average and minimum temperatures are widely skewed when compared to the maximum temperature. Figure 3.10 is a Minitab histogram of the maximum temperature for the sampled locations.

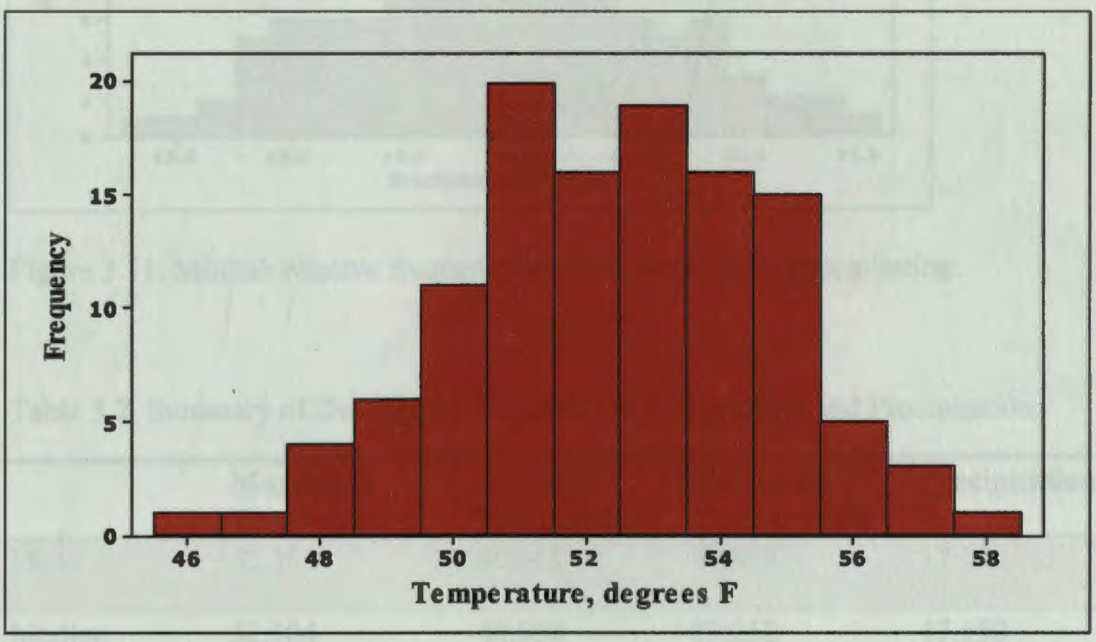

Figure 3.10. Minitab relative frequency printout of the histogram for maximum temperature.

3.4.2. Precipitation

The Minitab relative frequency histogram diagram for precipitation is shown in Figure 3.11. The mean, median, skewness, and standard deviation for precipitation are given in Table 3.2. From the descriptive statistics and histogram, precipitation is skewed by 0.15 inches to the right because the mean is higher. The summary of the traditional statistical analysis for temperature and precipitation is given in Table 3.2.

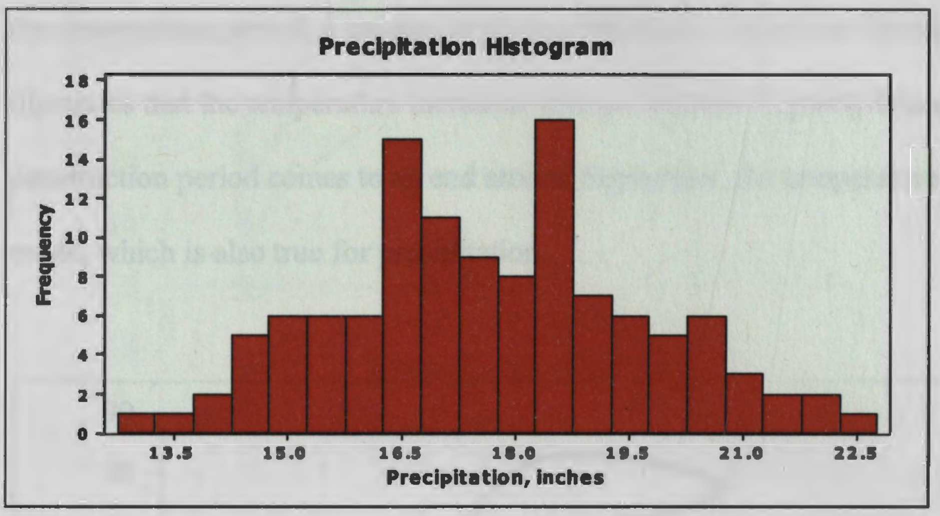

Figure 3.11. Minitab relative frequency of the histogram for precipitation.

Table 3.2. Summary of Descriptive Statistics for Temperature and Precipitation.

	Maximum Temperature	Average Temperature	Minimum Temperature	Precipitation
Mean	52.382	40.661	28.892	17.652
Median	52.504	40.850	29.258	17.650
Skewness	-0.100	-0.45	-0.47	0.15
Std Dev.	2.264	1.908	1.890	1.996

3.5. Comparisons Between Temperature and Precipitation

When the exploratory data analysis was compared to the traditional statistical analysis, almost similar statistical results were obtained. Graphical data analysis was done by graphing temperature and precipitation to explore the relationship that might exist between the two inputs. After the two environmental inputs were graphed, temperature versus precipitation for January to December, no distinct graph is obtained as shown in Figure 3.12. However, after shifting the start from January to March, which is the start of the construction period, a unique curve was obtained as shown in Figure 3.13. Figure 3.13 illustrates that the temperature increases with an increase in precipitation. As the construction period comes to an end around September, the temperatures take a reverse mode, which is also true for precipitation.

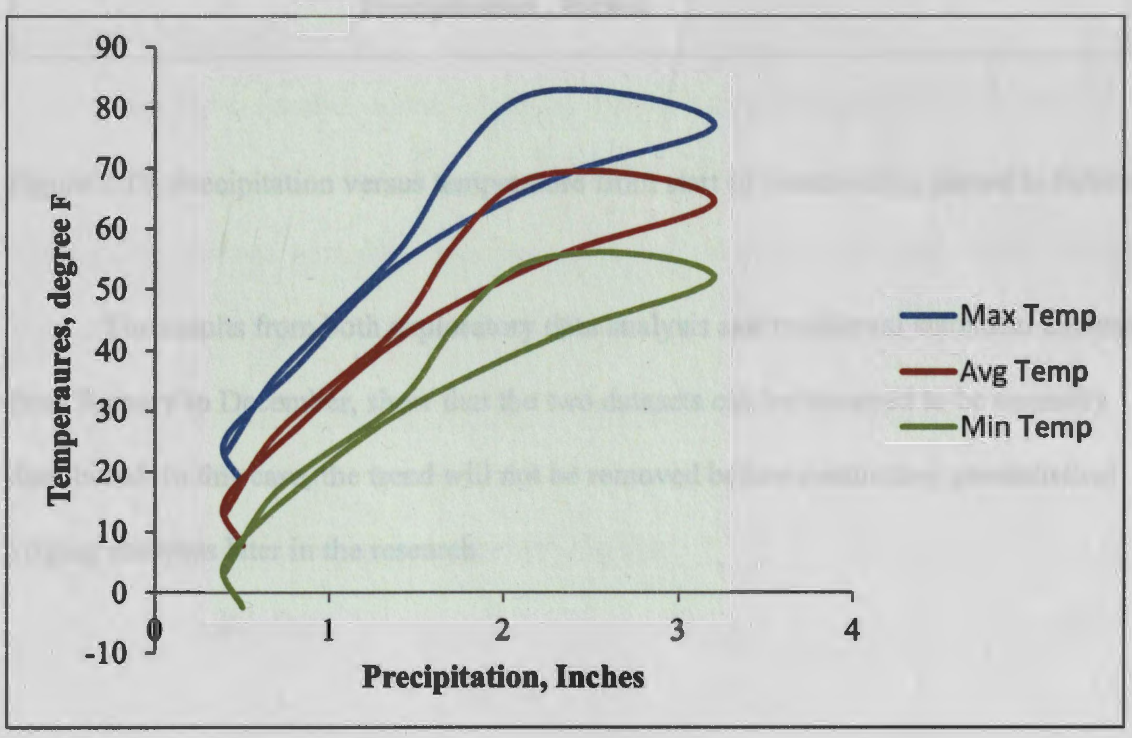

Figure 3.12. Precipitation versus temperature from January to December.

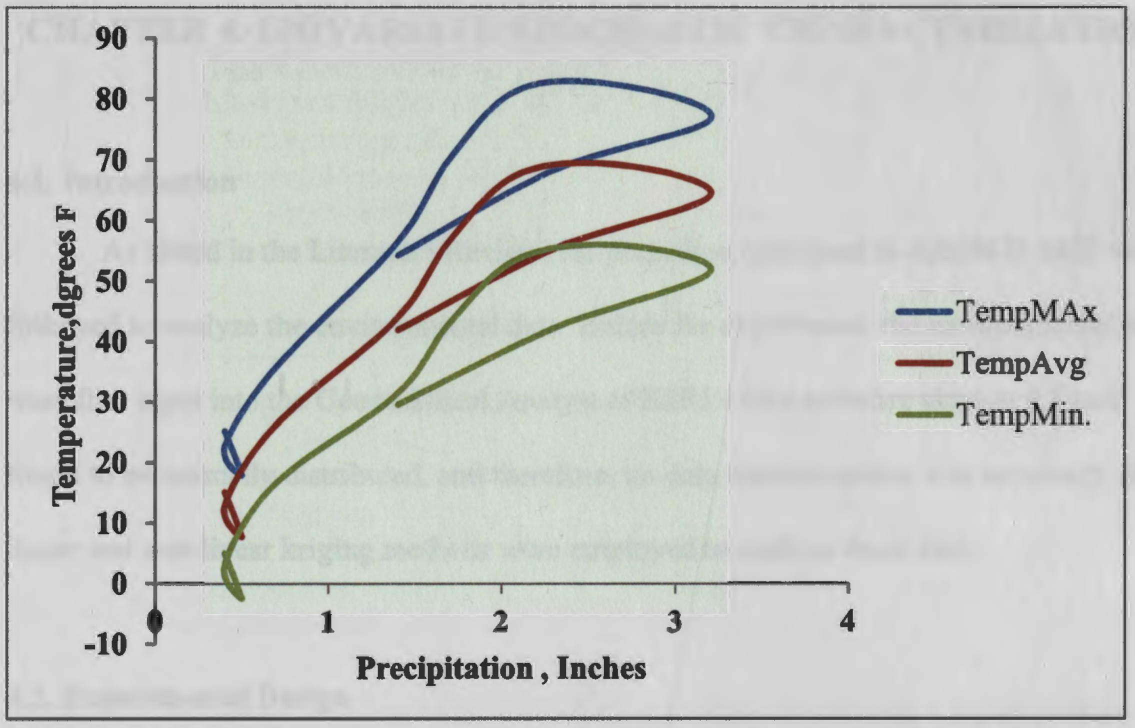

Figure 3.13. Precipitation versus temperature from start of construction period to February.

The results from both exploratory data analysis and traditional statistical analysis, from January to December, show that the two datasets can be assumed to be normally distributed. In this case, the trend will not be removed before conducting geostatistical kriging analyses later in the research.

CHAPTER 4. UNIVARIATE STOCHASTIC CHARACTERIZATION

4.1. Introduction

As stated in the Literature Review, the procedure contained in ASTM D 5922 was followed to analyze the environmental data. Before the experiment, the environmental data were first input into the Geostatistical Analyst of ESRI's GIS software version 9.5 and found to be normally distributed, and therefore, no data transformation was necessary. Both linear and non-linear kriging methods were employed to analyze these data.

4.2. Experimental Design

In order to conduct characterization of environmental data (precipitation and temperature), the data were first input into ESRI's GIS software. The precipitation and temperature datasets were then examined to understand their distribution before creating a prediction map (Chapter 3). The Geostatistical Wizard was used to characterize the two sets of data. The following steps were followed as shown in Figure 4.1.

1. Input data selection (precipitation or maximum temperature) and method.
2. Variogram modeling (selection of models).
3. Cross validation.

4.3. Univariate Stochastic Characterization of Environmental Data

This section will provide details about the various variogram models and kriging methods used in analyzing the environmental data. The results of linear and non-linear kriging processes for temperature and precipitation data will also be presented.

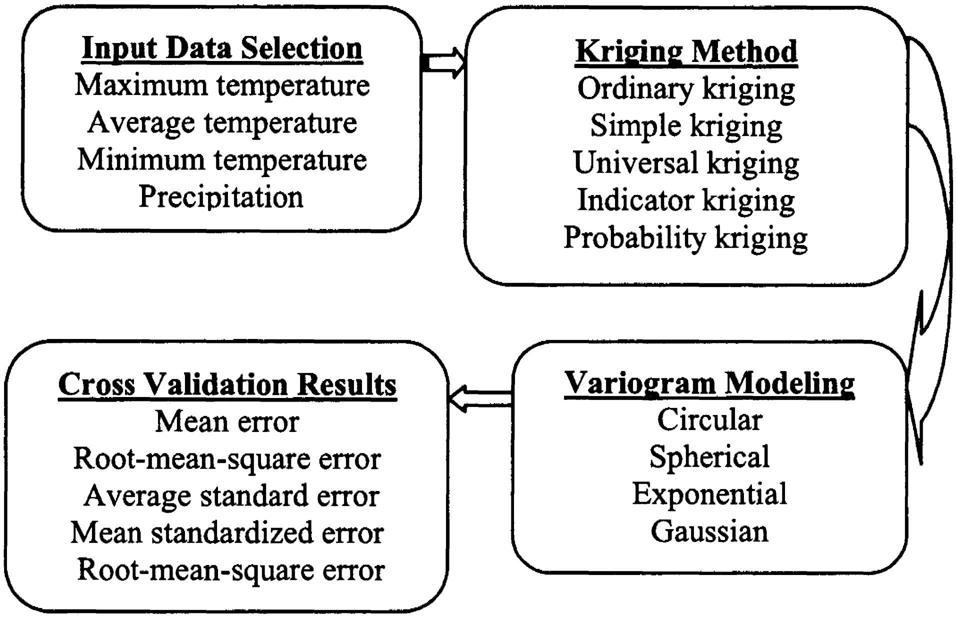

Figure 4.1. Univariate steps followed in analyzing precipitation and temperature datasets.

4.3.1. Variograms

Variograms are tools used in the initial steps of spatial prediction to provide insight about the spatial continuity and structure of a random process. In general, Goovaerts (1997) suggests that the main aim of a model is to capture most of the important features to obtain an accurate fit. Variogram modeling can also be applied as a prediction tool to estimate the value of a measure at a new location. Four variogram models were used to evaluate both linear and non-linear kriging processes: circular, spherical, exponential, and Gaussian.

4.3.2 Kriging

The Geostastical Wizard contains several methods which can be used for kriging. In this analysis, three methods each for linear and non-linear kriging were used to analyze the temperature and precipitation datasets. The linear kriging techniques were ordinary kriging, simple kriging, and universal kriging while, on the other hand, the non-linear techniques were indicator kriging, probability kriging, and universal kriging. Results from different variograms and cross validation were compared to select the best-fit kriging process for use during univariate characterization of the environmental input parameters.

4.4. Stochastic Characterization of Environmental Data

Diagrams of variograms and cross-validation results for the different kriging methods for univariate characterization of the environmental input parameters, temperature and precipitation, are presented in Appendix C. Results obtained using the linear kriging methods are presented first and then followed by results of the non-linear kriging methods for temperature and precipitation, respectively.

CHAPTER 5. MULTIVARIATE STOCHASTIC CHARACTERIZATION

5.1. Introduction

This chapter provides details about the various co-kriging methods used in multivariate stochastic characterization of temperature and precipitation datasets. The results of the co-kriging processes are presented.

5.2. Experimental Design

In order to conduct multivariate characterization of temperature and precipitation, the data had to be input into ESRI's GIS software. The Geostatistical Wizard was then used to characterize the two sets of data. The following steps were followed as depicted in Figure 5.1.

1. Input data selection (In this case, it was maximum temperature and precipitation.) and method (linear or non-linear kriging).
2. Variogram modeling (selection of model-circular: spherical, exponential or Guassian).
3. Cross validation.

5.3. Stochastic Co-Simulation of Temperature and Precipitation

Stochastic co-simulation of temperature and precipitation section provides details on variogram models and kriging techniques. The variogram models and kriging methods are used in analyzing temperature and precipitation. The models and kriging techniques are presented next.

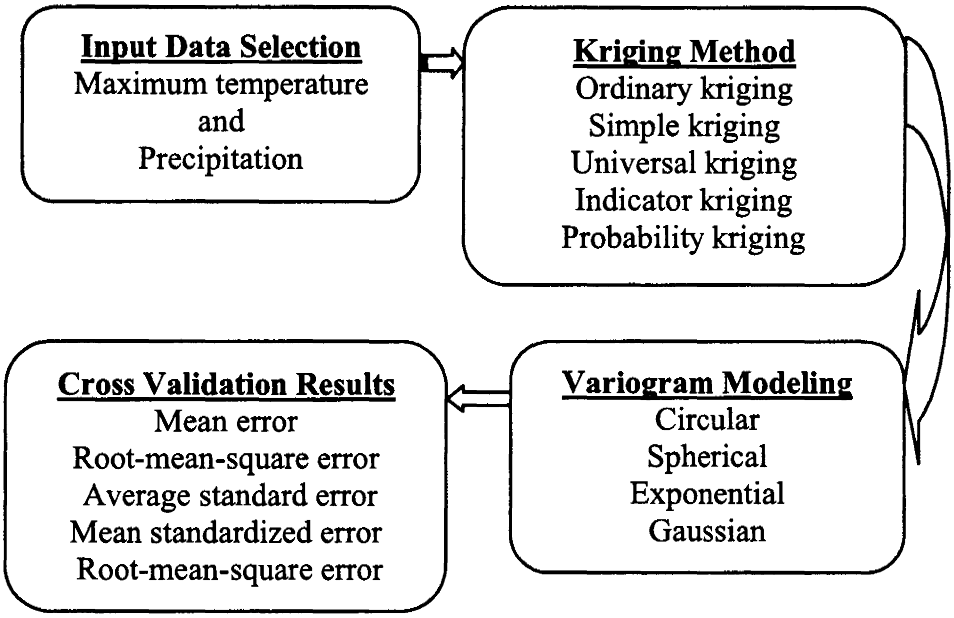

Figure 5.1. Co-kriging steps used in the analysis of the datasets.

5.3.1. Variograms

For the co-kriging process four variogram models were used: circular, spherical, exponential, and Gaussian. The variogram models were used to evaluate both linear and non-linear kriging techniques.

5.3.2 Co-Kriging

In total, six co-kriging techniques were used to analyze temperature and precipitation datasets. First, three linear techniques were utilized to study the environmental data. The linear techniques used in the analysis were ordinary kriging, simple kriging, and universal kriging together with the variogram models already selected. Similarly, the same procedure was done for the three non-linear co-kriging techniques: indicator kriging, probability kriging, and disjunctive kriging. The results obtained from cross-validation techniques were then used to plot graphs in the analysis section this thesis.

From the cross-validation graphs, the best-fit variogram model for the co-kriging process can be selected to characterize the temperature and precipitation input parameters.

5.4. Stochastic Characterization of Environmental Data

The results for the multivariate characterization of temperature and precipitation (co-kriging) input parameters in Appendix D. The figures are printouts of variograms and cross-validation results for the kriging methods used with the multivariate characterization. The left and right diagrams represent semivariograms and cross-validation kriging results respectively. The results are grouped corresponding to the specific model used to compute them.

CHAPTER 6. ANALYSIS, DISCUSSIONS, AND CONTRIBUTIONS TO SCIENCE

This chapter presents an analysis of cross-validation results obtained from univariate stochastic characterization of temperature and precipitation datasets as well as multivariate stochastic characterization. Based on results obtained from cross-validation analysis, a kriging model will then be proposed. For this study, three linear and three non-linear kriging techniques were considered. Linear models consisted of ordinary kriging, simple kriging, and universal kriging, and non-linear models were indicator kriging, probability kriging, and disjunction kriging. These models were used in conjunction with different variogram models: circular, spherical, exponential, and Gaussian.

6.1. Analysis of Results

The statistics obtained from cross validation consisted of the mean error, the root-mean-square error, the average standard error, mean standardized error, and the root-mean-square error standardized. The results are shown in Tables 6.1 to 6.10. The behavior of the mean, the root-mean-square error, the average standard error, mean standardized error, and the root-mean-square error standardized is plotted in Figures 6.1 to 6.10 for both temperature and precipitation. Figures 6.1 to 6.5 represent the results of temperature, and Figures 6.6 to 6.10 illustrate precipitation.

6.2. Temperature Dataset

The results also contain different variograms used to generate the cross validation for the temperature dataset, which provide different cross-validation results. The results from the statistics are then used to plot the behavior of the various statistics. The statistics obtained from cross validation and the variogram results are analyzed next.

6.2.1. Mean

Table 6.1 gives the mean error results from different variogram models used to plot Figure 6.1. From Figure 6.1, the spherical variogram had the lowest mean (close to zero) and was followed closely by circular variogram. Results from the plot of the four considered variogram models, show that the Gaussian variogram deviates the most from zero while the exponential variogram had the largest negative mean. When the mean error is considered, indicator kriging has the lowest value (nearest to zero) and followed is closely by probability kriging. Probability kriging is followed closely by ordinary kriging. Disjunctive kriging has the lowest negative and highest positive mean values for exponential and Gaussian variograms, respectively. The worst kriging algorithm for both Gaussian and probability variograms is the simple kriging.

Table 6.1. Mean Results of Kriged Temperature Data for the Six Kriging Methods.

	Circular	**Spherical**	**Exponential**	**Gaussian**
Ordinary	0.00233	0.00251	0.0000188	0.007858
Simple	-0.00193	0.0003494	0.01576	0.01576
Universal	0.00233	0.002521	0.0000188	0.007858
Indicator	-0.00147	-0.001521	-0.001369	-0.001341
Probability	-0.00281	-0.002921	-0.004418	0.000097
Disjunctive	-0.00157	0.0016666	-0.007601	0.01566

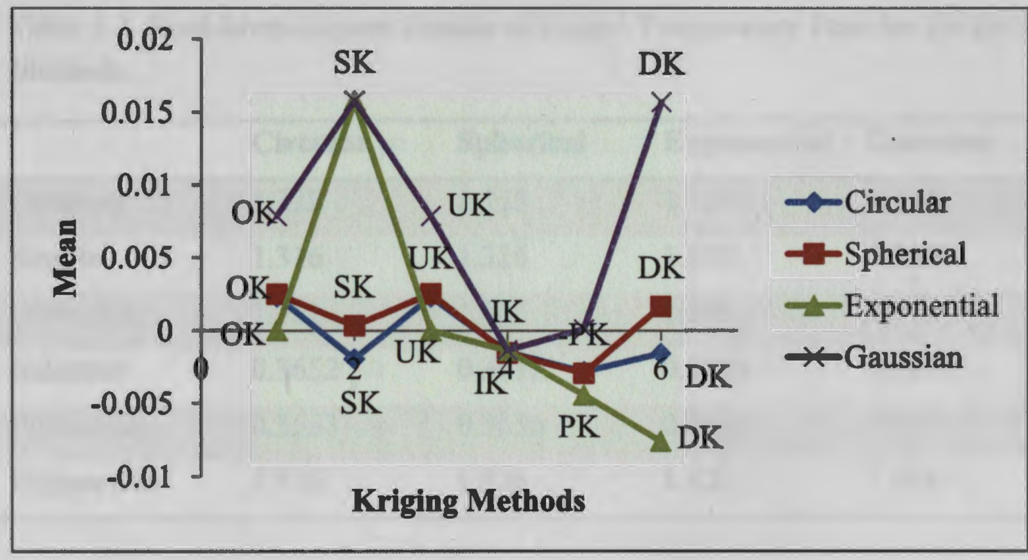

Figure 6.1. Mean error of the kriged temperature data.

The kriging algorithm, which has a mean near zero, is considered the best. In this case, indicator kriging is the best method if the mean prediction error is used as the decision criterion. For the other kriging methods, it is difficult to determine the next best model because the values of mean error are scattered from negative to positive all over the plot. In this case, a decision matrix will be used to rank the methods to identify the preference order of the methods.

6.2.2. Root-Mean-Square Error

Table 6.2 shows the results of the root-mean-square prediction error which were used to plot Figure 6.2. Indicator kriging and probability kriging are almost the same (Figure 6.2). Ordinary kriging, simple kriging, universal kriging, and disjunctive kriging are approximately the same as well (Figure 6.2). Indicator kriging and probability kriging have the smallest root-mean square error value.

Table 6.2. Root-Mean-Square Results of Kriged Temperature Data for the Six Kriging Methods.

	Circular	Spherical	Exponential	Gaussian
Ordinary	1.322	1.325	1.363	1.292
Simple	1.316	1.326	1.309	1.309
Universal	1.322	1.325	1.363	1.292
Indicator	0.3652	0.3652	0.3668	0.3672
Probability	0.3653	0.3656	0.3689	0.3766
Disjunctive	1.316	1.325	1.421	1.308

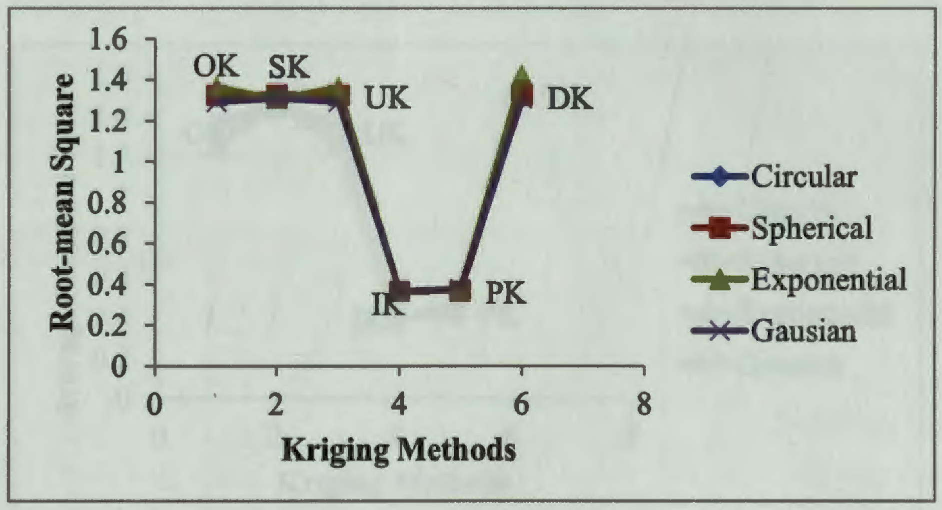

Figure 6.2. Root-mean-square error of the kriged temperature data.

6.2.3. Average Standard Error

The average mean standard prediction error results shown in Table 6.3 were used to plot Figure 6.3. In the ASE, indicator kriging is almost the same with probability kriging for all the variograms used as shown in Figure 6.3. Ordinary kriging and universal kriging, are approximately the same. Equally disjunctive kriging and simple kriging are also approximately the same (Figure 6.3). Indicator kriging has the smallest average mean standard error value.

Table 6.3. Average Standard Error Results of Kriged Temperature for Six Kriging Methods.

	Circular	Spherical	Exponential	Gaussian
Ordinary	1.321	1.317	1.256	1.375
Simple	1.481	1.435	1.454	1.454
Universal	1.321	1.317	1.256	1.375
Indicator	0.3919	0.3926	0.3875	0.3952
Probability	0.4208	0.4246	0.4625	0.4067
Disjunctive	1.502	1.458	1.483	1.475

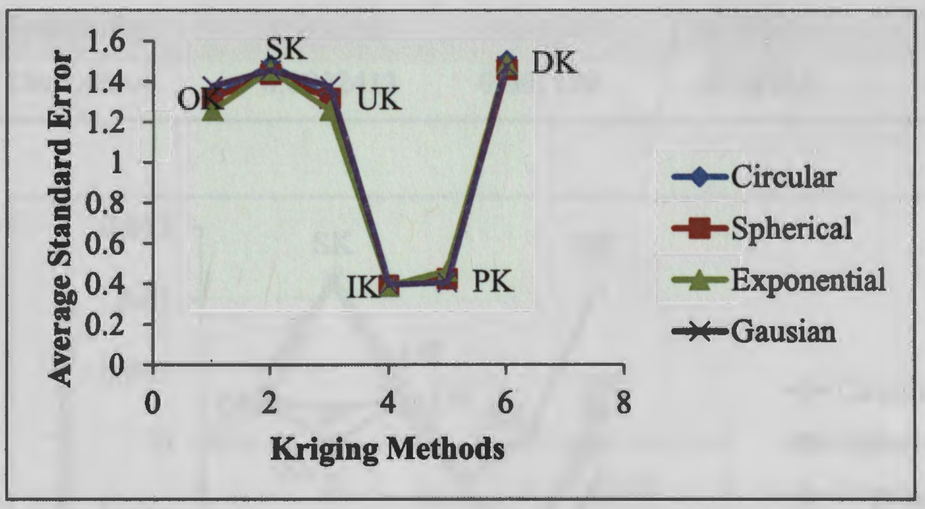

Figure 6.3. Average standard error prediction of kriged temperature data.

6.2.4. Mean Standardized Error

The mean standard error results given in Table 6.4 were used to plot Figure 6.4. Figure 6.4 shows that indicator kriging has the same negative value for all the variogram models, thus presents the best model. Ordinary kriging and universal kriging have approximately the same value (Figure 6.4). The others kriging methods (probability kriging and disjunctive kriging) have different values for the variogram models scattered all over the plot (Figure 6.4).

Table 6.4. Mean Standard Error Results of Kriged Temperature Data of the Six Kriging Methods.

	Circular	Spherical	Exponential	Gaussian
Ordinary	0.003098	0.003349	0.002847	0.005009
Simple	0.0001885	0.002257	0.01128	0.01128
Universal	0.003098	0.003349	0.002847	0.005009
Indicator	-0.003143	-0.003268	-0.00309	-0.002497
Probability	-0.006103	-0.006301	-0.00911	0.000875
Disjunctive	0.0002413	0.002189	-0.00264	0.01104

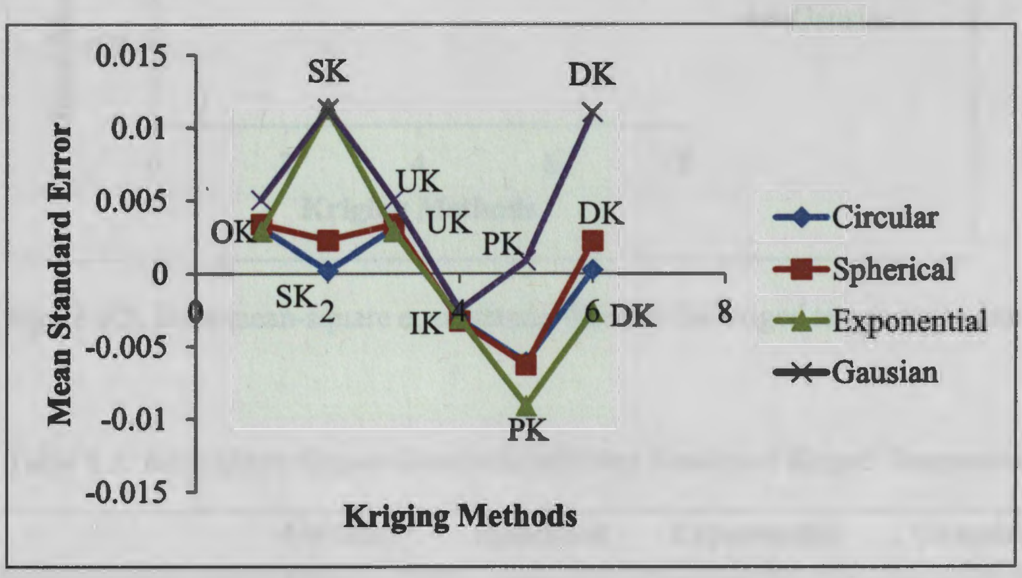

Figure 6.4. Mean standardized prediction error of the kriged temperature data.

6.2.5. Root-Mean-Square Error

Root-mean-square error values used to plot Figure 6.5 are given in Table 6.5. Usually, the best RMSES has to be approximately 1 (one) which, in this plot, is indicator kriging for all the variograms. The Indicator kriging technique is closely followed by simple kriging with a value of approximately 1 for all the variogram models. The remaining kriging methods (OK, UK, PK, and DK) have different values for the various variogram models used, ranging from slightly less than 1 to more than 1 (Figure 6.5).

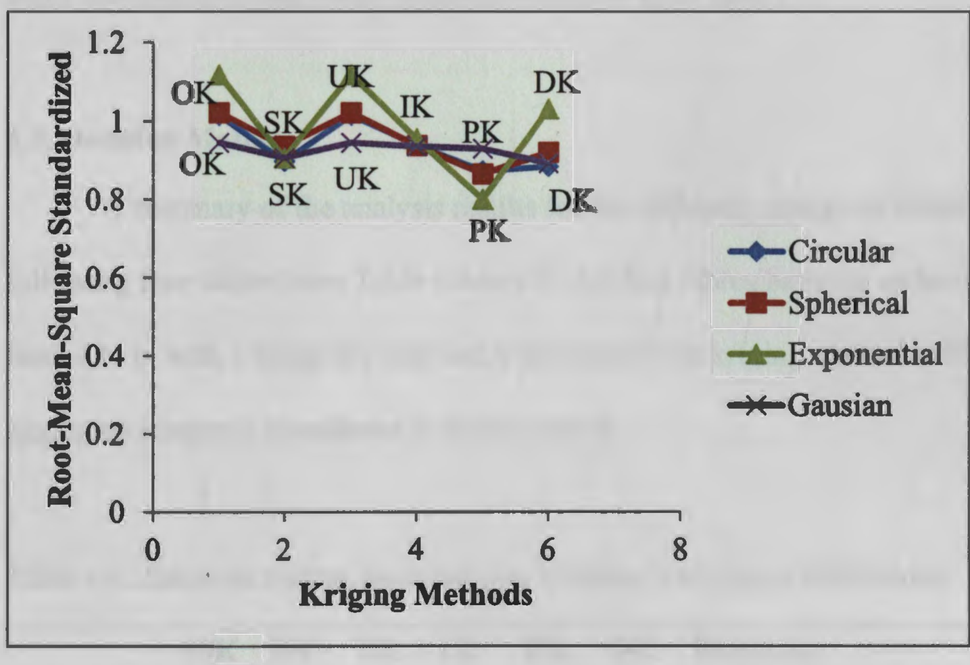

Figure 6.5. Root-mean-square error standardized of the kriged temperature data.

Table 6.5. Root-Mean-Square Standardized Error Results of Kriged Temperature Data.

	Circular	Spherical	Exponential	Gaussian
Ordinary	1.016	1.022	1.119	0.9455
Simple	0.8983	0.9365	0.9068	0.9068
Universal	1.016	1.022	1.119	0.9455
Indicator	0.9394	0.938	0.9556	0.9362
Probability	0.8736	0.8661	0.8009	0.9302
Disjunctive	0.8852	0.9205	1.032	0.8933

When analyzing the temperature dataset, a specific criterion should be used to evaluate the predictions of the kriging methods together with different variogram models. Overall, to select the best kriging method, it must have the following properties: a mean prediction error near zero, thus an unbiased dataset that honors the true mean; a standardized mean prediction error near zero; a small root-mean-square prediction error; and a standardized root-mean-squared prediction error near 1.

6.3. Decision Matrix

A summary of the analysis results for the different variogram models is given in the following four tables from Table 6.6 to 6.9. All four tables have the order of preference from 1 to 6, with 1 being the best and 6 the worst. The kriging method with the lowest aggregate integer is considered to be the best fit.

Table 6.6. Decision Matrix Summarizing Circular Variogram Predictions.

	OK	SK	UK	IK	PK	DK	Remarks
Mean	4	3	4	**1**	5	2	OK and UK, same values
RMSE	3	2	3	1	1	2	OK and UK; SK and DK; IK and PK
ASE	3	4	3	**1**	2	5	OK and UK – same values
MSE	3	1	3	4	5	2	OK and UK – same values
RMSES	2	3	2	**1**	5	4	OK and UK – same values
Aggregate	15	13	15	**8**	18	15	

Table 6.7. Decision Matrix Summarizing Spherical Variogram Predictions.

	OK	SK	UK	IK	PK	DK	Remarks
Mean	4	1	4	**2**	5	3	OK and UK – same values
RMSE	2	2	2	**1**	1	2	IK and PK; OK, SK UK, DK, same
ASE	3	4	3	**1**	2	5	OK and UK – same values
MSE	3	2	3	**4**	5	1	Ditto
RMSES	1	3	1	**2**	5	4	Ditto
Aggregate	13	12	13	**10**	18	15	

Table 6.8. Decision Matrix Summarizing Exponential Variogram Predictions.

	OK	SK	UK	IK	PK	DK	Remarks
Mean	1	5	1	**2**	3	4	OK and UK – same values
RMSE	4	3	4	**1**	2	5	OK and UK – same values
ASE	3	4	3	**1**	2	5	OK and UK – same values
MSE	1	5	1	**3**	4	2	OK and UK – same values
RMSES	4	3	4	**2**	5	1	OK and UK – same values
Aggregate	13	20	13	**9**	16	17	

Table 6.9. Decision Matrix Summarizing Gaussian Variogram Predictions.

	OK	SK	UK	IK	PK	DK	Remarks
Mean	3	5	3	2	**1**	4	OK and UK- same values
RMSE	3	4	3	2	**1**	4	OK and UK – same values
ASE	3	4	3	1	**2**	5	OK and UK – same values
MSE	3	5	3	2	**1**	4	OK and UK – same values
RMSES	1	4	1	2	**3**	5	OK and UK – same values
Aggregate	13	22	13	9	**8**	22	

6.4. Precipitation Dataset

The statistics obtained from the cross validation are analyzed and discussed. These statistics are mean error, the root-mean-square error, the average standard error, mean standardized error, and the root-mean-square error standardized. The cross-validation results used to plot the Figures 6.6 to 6.10 are given in the accompanying tables 6.10 to 6.14.

6.4.1. Mean

Table 6.10 gives cross-validation results used to plot Figure 6.6. From Figure 6.6, spherical and circular variograms had the lowest mean (closest to zero) and were followed closely by circular model. In all the four variograms considered, the Gaussian one deviated most from zero together with exponential variogram which also had the largest negative mean. Indicator kriging had the lowest mean near zero for all the variograms. It was followed by probability kriging which lies on both the positive and negative side with different variogram results. The results of other kriging methods ranged from small to larger and scattered (Figure 6.6).

Table 6.10. Results of the Mean of Kriged Precipitation Data of the Six Kriging Methods.

	Circular	Spherical	Exponential	Gaussian
Ordinary	0.016	0.01626	0.01948	-0.02701
Simple	0.004542	0.006137	0.02315	-0.007475
Universal	0.016	0.01626	0.01948	-0.02701
Indicator	0.0005212	0.0005899	0.002049	-0.001988
Probability	-0.0006708	-0.000576	0.001102	-0.007445
Disjunctive	0.002739	0.000423	0.02273	-0.008876

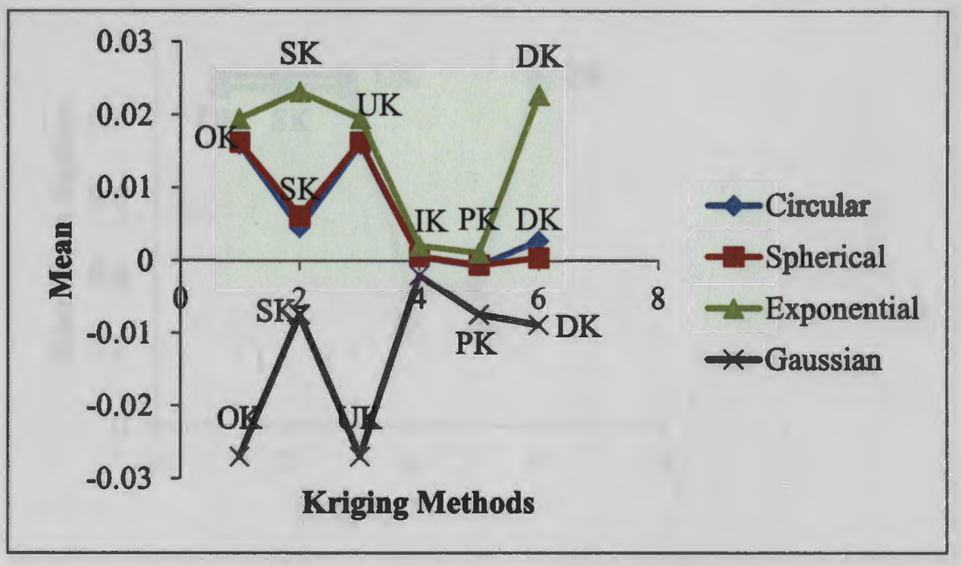

Figure 6.6. Mean error of the kriged precipitation data

6.4.2. Root-Mean-Square Error

Table 6.11 results were used to plot Figure 6.7. When the root-mean square prediction error is considered, indicator kriging is almost the same as probability kriging, as shown in Figure 6.7. The other kriging techniques, ordinary kriging, simple kriging, universal kriging, and disjunctive kriging have approximately the same value (Figure 6.7). Indicator kriging and probability kriging have the smallest root-mean-square error values.

Table 6.11. Root-Mean-Square Error of the Kriged Precipitation Data.

	Circular	Spherical	Exponential	Gaussian
Ordinary	0.8837	0.8839	0.8818	0.9158
Simple	0.8791	0.8772	0.8872	0.9141
Universal	0.8837	0.8839	0.8818	0.9158
Indicator	0.3495	0.3495	0.3493	0.354
Probability	0.3514	0.3513	0.3498	0.3637
Disjunctive	0.8871	0.8845	0.8926	0.9206

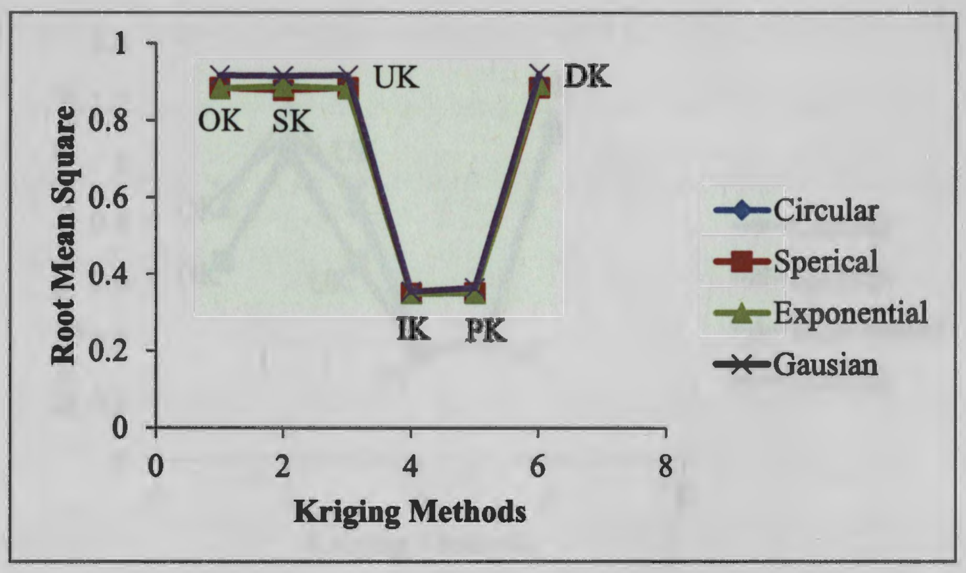

Figure 6.7. Root-mean-square error of the kriged precipitation data

6.4.3. Average Standard Error

In the average mean standard prediction error, Table 6.12 was used to plot Figure 6.8. Indicator kriging is almost the same as probability kriging for all the variograms as shown in Figure 6.8. Ordinary kriging and universal kriging are approximately the same. Equally disjunctive kriging and simple kriging are also approximately the same (Figure 6.8). Indicator kriging has the smallest average mean standard error value.

Table 6.12. Average Standard Error Results of Kriged Precipitation Dataset.

	Circular	Spherical	Exponential	Gaussian
Ordinary	0.6549	0.6693	0.8522	0.9032
Simple	1.067	1.027	1.185	1.096
Universal	0.6549	0.6693	0.8522	0.9032
Indicator	0.3544	0.3554	0.3521	0.3655
Probability	0.3984	0.3994	0.3943	0.4112
Disjunctive	1.128	1.095	1.154	1.15

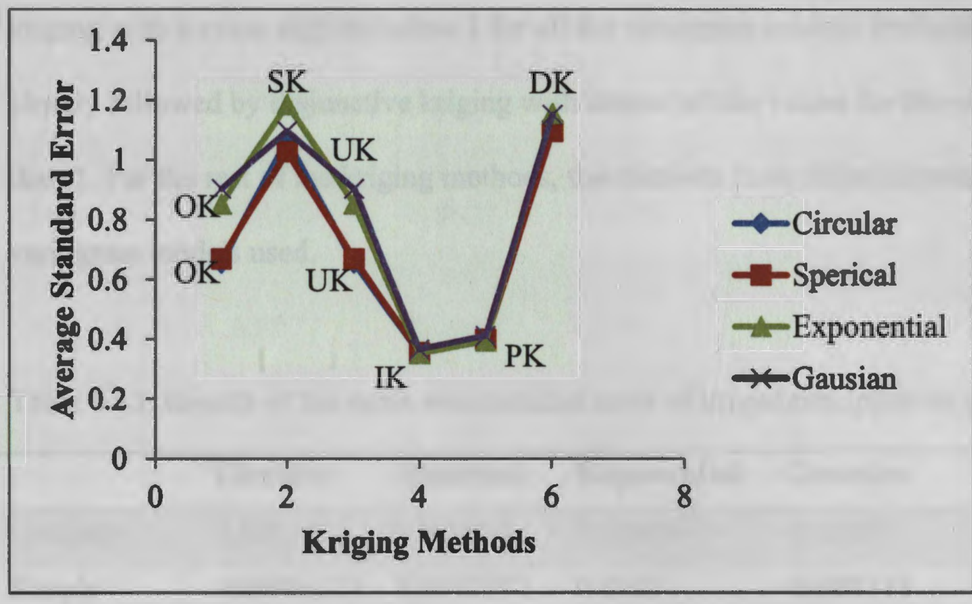

Figure 6.8. Average standard error prediction of kriged precipitation dataset.

6.4.4. Mean Standard Error

The results shown in Table 6.13 were used to plot Figure 6.9. When considering the mean standard error, indicator kriging and probability kriging have approximately the smallest value for all the variogram models. All other kriging techniques have different values for the variogram models used. The exponential variogram has the greatest positive value while, on the other hand, the Gaussian variogram has the least value but, on the negative. From Figure 6.9, it is difficult to rank the different kriging methods because their variogram values are scattered on the plot.

6.4.5. Root-Mean-Square Standardized Error

The results given in Table 6.14 were used to plot Figure 6.10. The behavior of the root-mean-square error standardized is shown in Figure 6.10. Indicator kriging has the best value of approximately 1 for all the variogram models. It is followed closely by probability kriging with a value slightly below 1 for all the variogram models. Probability kriging is closely followed by disjunctive kriging with almost all the values for the variograms less than 1. For the rest of the kriging methods, the methods have different results for the variogram models used.

Table 6.13. Results of the mean standardized error of kriged precipitation dataset.

	Circular	Spherical	Exponential	Gaussian
Ordinary	0.009742	0.009805	0.01044	-0.03083
Simple	-0.0006123	0.0002972	0.0101	-0.008518
Universal	0.009742	0.009805	0.01044	-0.03083
Indicator	-0.0007497	-0.0006193	0.002327	-0.006279
Probability	-0.003308	-0.003081	0.0003832	-0.01888
Disjunctive	-0.00188	-0.001055	0.01033	-0.009368

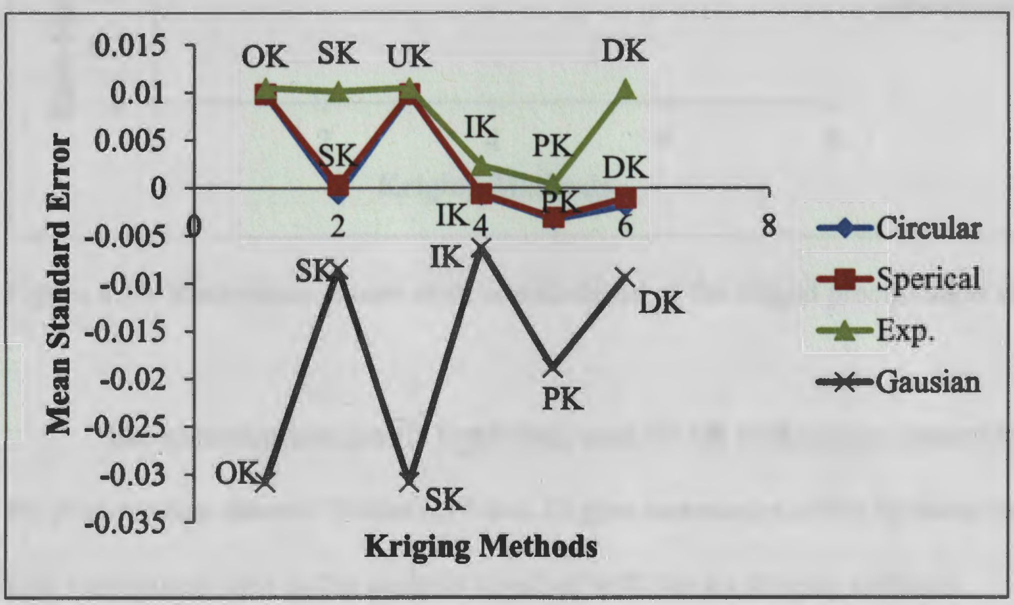

Figure 6.9. Mean standardized prediction error of the kriged precipitation data.

Table 6.14. Root-Mean-Square Standardized Error Results of Kriged Precipitation Dataset.

	Circular	Spherical	Exponential	Gaussian
Ordinary	1.376	1.347	1.052	1.019
Simple	0.8226	0.8522	0.7537	0.8362
Universal	1.376	1.347	1.052	1.019
Indicator	0.997	0.9944	1.005	0.9761
Probability	0.8892	0.8873	0.8965	0.887
Disjunctive	0.7857	0.8065	0.7773	0.8021

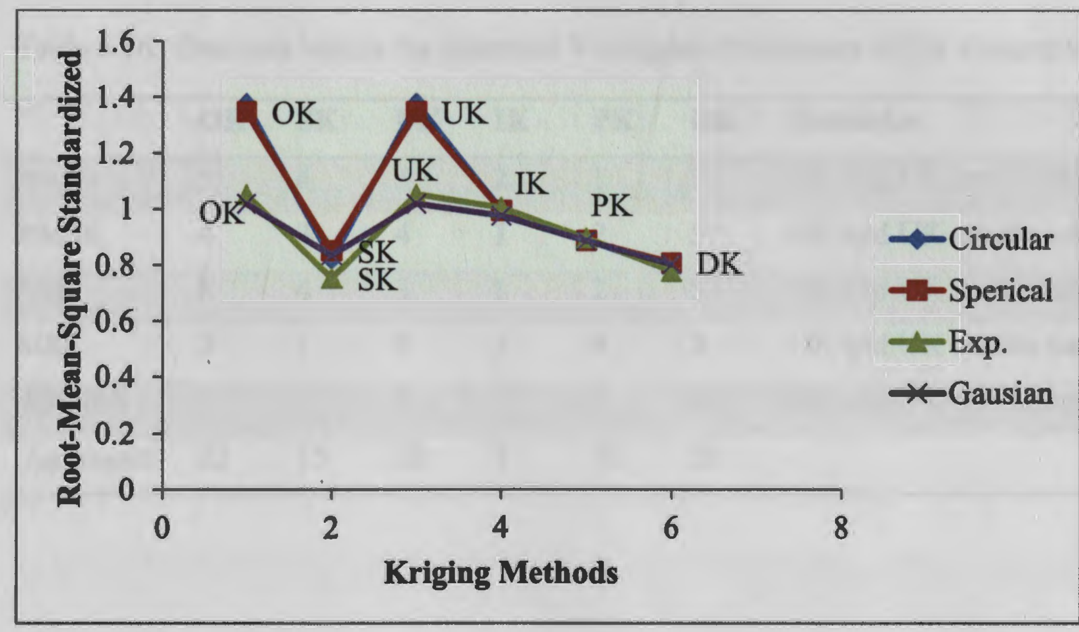

Figure 6.10. Root-mean-square error standardized of the kriged precipitation dataset.

The same decision matrix (criterion) used for the temperature dataset was used for the precipitation dataset. Tables 6.15 to 6.18 give summaries of the decision matrix for the four variograms used in the analysis together with the six kriging methods.

Table 6.15. Decision Matrix for Circular Variogram Predictions of Six Kriging Methods.

	OK	SK	UK	IK	PK	DK	Remarks
Mean	5	4	5	**1**	2	3	OK and UK are the same
RMSE	4	3	4	**1**	2	5	OK and UK are the same
ASE	3	4	3	**1**	2	5	OK and UK are the same
MSE	5	1	5	**2**	4	3	OK and UK are the same
RMSES	5	3	5	**1**	2	4	OK and UK are the same
Aggregate	22	15	22	**6**	12	20	

Table 6.16. Decision Matrix for Spherical Variogram Predictions of Six Kriging Methods.

	OK	SK	UK	IK	PK	DK	Remarks
Mean	5	4	5	**2**	1	3	OK and UK are the same
RMSE	4	3	4	**1**	2	5	OK and UK are the same
ASE	3	4	3	**1**	2	5	OK and UK are the same
MSE	5	1	5	**2**	4	3	OK and UK are the same
RMSES	5	3	5	**1**	2	4	OK and UK are the same
Aggregate	22	15	22	**7**	11	20	

Table 6.17. Decision Matrix for Exponential Variogram Predictions of Six Kriging Methods.

	OK	SK	UK	IK	PK	DK	Remarks
Mean	3	5	3	**2**	1	4	OK and UK- same values
RMSE	3	4	3	1	2	5	OK and UK- same values
ASE	3	5	3	1	2	4	OK and UK- same values
MSE	5	3	5	2	1	4	OK and UK- same values
RMSES	2	5	2	1	3	4	OK and UK- same values
Aggregate	16	22	16	7	9	21	

Table 6.18. Decision Matrix for Gaussian Variogram Predictions of Six Kriging Methods.

	OK	SK	UK	IK	PK	DK	Remarks
Mean	5	3	5	**1**	2	4	OK and UK – same values
RMSE	3	4	3	**1**	1	5	OK and UK – same values
ASE	3	4	3	**1**	2	5	OK and UK – same values
MSE	5	2	5	**1**	4	3	OK and UK – same values
RMSES	1	4	1	**2**	3	5	OK and UK – same values
Aggregate	17	17	17	**6**	12	22	

6.5. Co-Kriging

Cross-validation results obtained from multivariate stochastic characterization (co-kriging) for temperature and precipitation datasets were analyzed using different models. Three linear and three non-linear models were employed. The linear models were OK, SK, and UK and the non-linear models were IK, PK, and DK.

During the analysis, the following statistical results were obtained from the cross validation of the co-kriging models: mean error, root mean square error, average standard error, mean standard error, and root mean square standardized. These results are presented in the Tables 6.19 to 6.23, and the behavior of the statistical results for co-kriging is shown in Figures 6.11 to 6.15.

6.5.1. Mean

Table 6.19 gives the mean results of the different variogram values used to plot the behavior of the statistical results shown in Figure 6.11. Figure 6.11 shows that the circular variogram has the lowest mean followed closely by the spherical variogram. In all the four variogram models considered, the Gaussian model deviates most from zero followed by the exponential model. From Figure 6.11, it is difficult to pinpoint the linear method with the lowest mean because all the variograms have different values.

The kriging model which has a mean close to zero is considered the best model. In this case, it is difficult to deduce the best model because all the variograms have different values. A decision matrix will be employed to rank all the methods to identify the best method fit.

Table 6.19. Results of the Mean of Co-Kriged Datasets.

	Circular	Spherical	Exponential	Gaussian
Ordinary	0.000815	0.001144	0.002343	0.01044
Simple	-8.3E-05	0.000275	0.005237	0.007983
Universal	0.000815	0.001144	0.002343	0.01044
Indicator	-0.00336	-0.00301	-0.00148	-0.00489
Probability	0.000815	-0.00473	-0.00459	-0.00199
Disjunctive	1.21E-05	0.000451	0.005559	0.007709

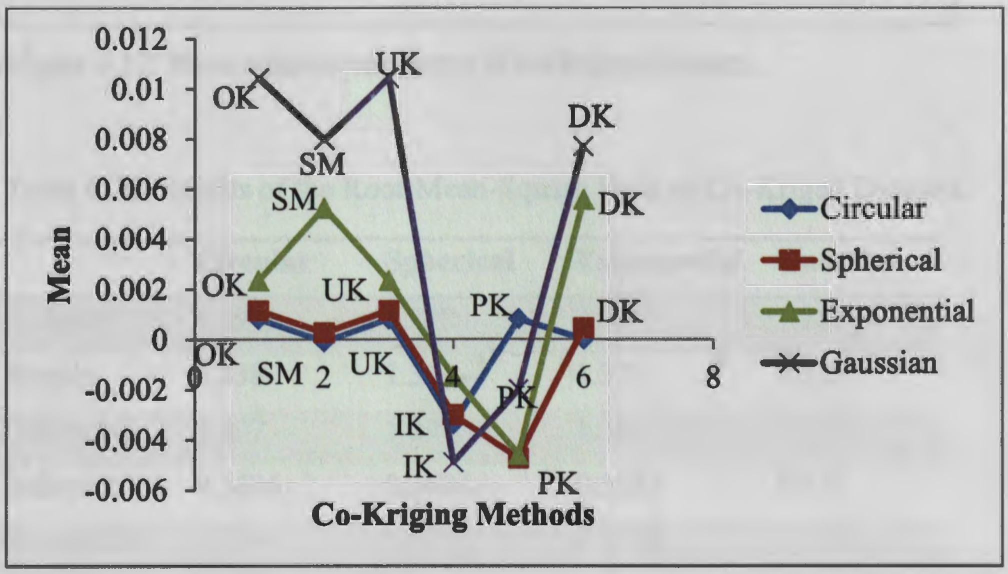

Figure 6.11. Mean error of the co-kriged datasets.

6.5.2. Root-Mean-Square Error

The root-mean square error values used to plot Figure 6.12 are given in Table 6.20. The best variogram model is one where the root-mean error is close to zero. In this case, all the variograms have approximately the same shape except the circular variogram when the PK technique is used. IK and PK have the smallest mean-root square error value, and the remaining OK, SK, UK, and DK are about the same.

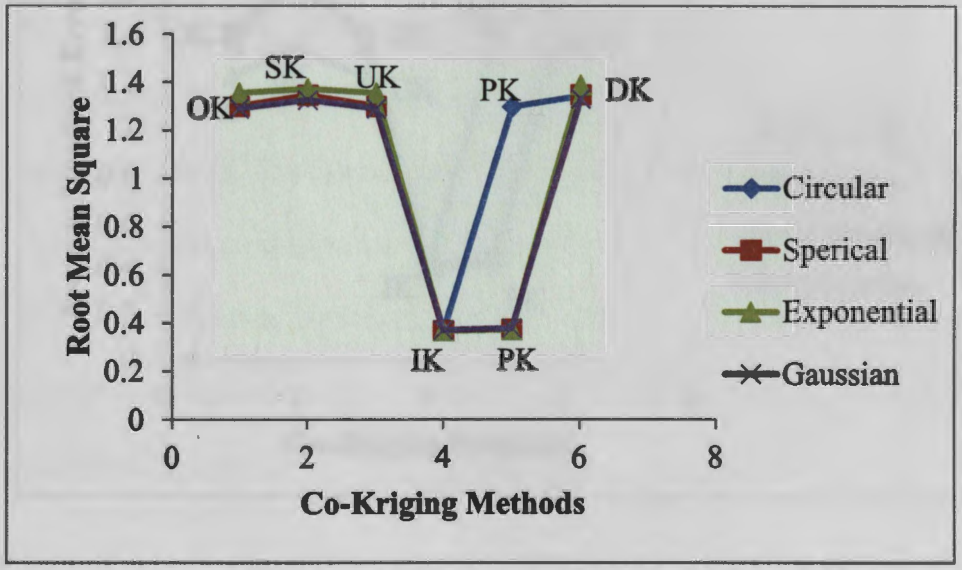

Figure 6.12. Root-mean-square error of co-kriged datasets.

Table 6.20. Results of the Root-Mean-Square Error of Co-Kriged Datasets.

	Circular	Spherical	Exponential	Gaussian
Ordinary	1.297	1.298	1.354	1.289
Simple	1.338	1.344	1.371	1.325
Universal	1.297	1.298	1.354	1.289
Indicator	0.3686	0.3684	0.3685	0.371
Probability	1.297	0.3746	0.3729	0.3792
Disjunctive	1.343	1.347	1.387	1.331

6.5.3. Average Standard Error

The average standard error cross-validation results used to plot Figure 6.13 are given in Table 6.21. From Figure 6.13, the exponential variogram model had the lowest average standard error close to zero. The remaining variogram models were approximately the same, apart from the circular variogram which deviates most with the PK technique.

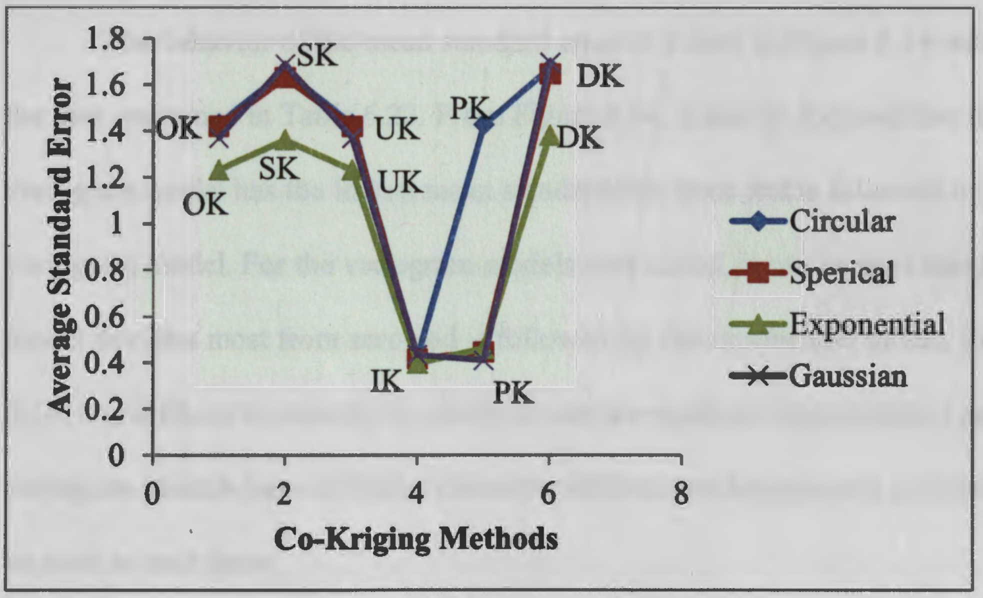

Figure 6.13. Average standard error co-kriged datasets.

Table 6.21. Average Standard Error of Co-Kriged Datasets.

	Circular	Spherical	Exponential	Gaussian
Ordinary	1.428	1.419	1.231	1.369
Simple	1.657	1.629	1.361	1.687
Universal	1.428	1.419	1.231	1.369
Indicator	0.4208	0.4167	0.397	0.4336
Probability	1.428	0.4461	0.4609	0.4108
Disjunctive	1.671	1.646	1.381	1.695

All the variograms have approximately the same ASE value for the IK method as shown in Figure 6.13 and a similar trend is observed for PK, except that for circular variogram model, it deviates substantially from zero. The best method is IK. For the remaining techniques a decision matrix will be used to rank them.

6.5.4. Mean Standardized Error

The behavior of the mean standard error is shown in Figure 6.14 was plotted from the data contained in Table 6.22. From Figure 6.14, it can be deduced that the circular variogram model has the lowest mean standardized error and is followed by the spherical variogram model. For the variogram models considered, it can be seen that the Gaussian model deviates most from zero and is followed by the exponential model. From Figure 6.14, it is difficult to identify the method with the smallest mean standard error. All the variogram models have different values for different techniques and a decision matrix will be used to rank them.

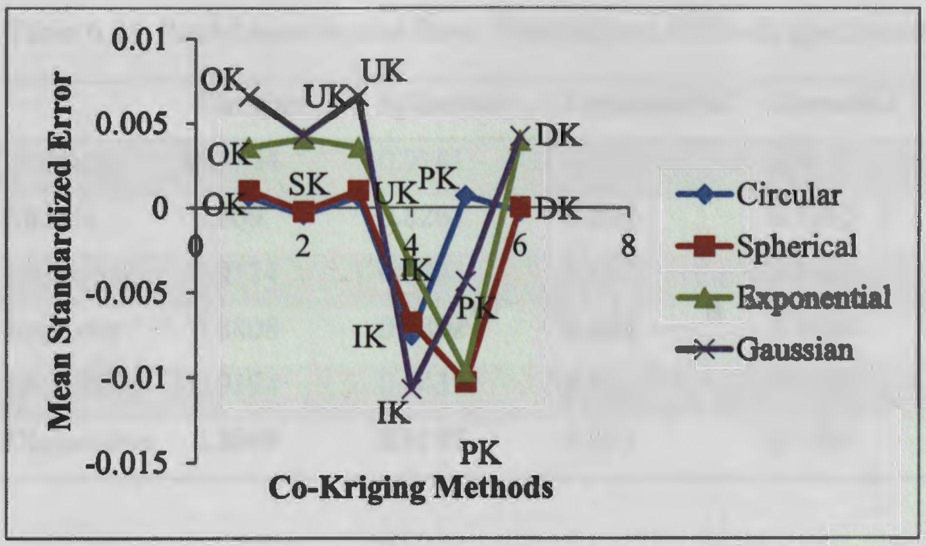

Figure 6.14. Mean standardized error of co-kriged datasets.

Table 6.22. Mean Standardized Error of Co-Kriged Datasets.

	Circular	Spherical	Exponential	Gaussian
Ordinary	0.000658	0.00102	0.003557	0.006593
Simple	-0.00039	-0.00021	0.004079	0.004298
Universal	0.000658	0.00102	0.003557	0.006593
Indicator	-0.00753	-0.00676	-0.00346	-0.01069
Probability	0.000684	-0.01027	-0.00967	-0.00436
Disjunctive	-0.00022	1.65E-05	0.003948	0.004187

6.5.5. Root-Mean-Square Standardized

The plot of the root-mean-square error from Table 6.23 is shown in Figure 6.15. The circular and Gaussian models are close together and close to 1. The spherical model differs from the rest when using the PK model. The exponential variogram deviates the most from 1. The best kriging model is IK as all the variograms have almost the same value. The other kriging models have different values for the variograms used.

Table 6.23. Root-Mean-Square Error Standardized of Co-Kriged Datasets.

	Circular	Spherical	Exponential	Gaussian
Ordinary	0.9174	0.9241	1.137	0.9462
Simple	0.809	0.8267	1.024	0.7865
Universal	0.9174	0.9241	1.137	0.9462
Indicator	0.8808	0.8892	0.936	0.8588
Probability	0.9194	0.8433	0.8125	0.9259
Disjunctive	0.8049	0.8197	1.017	0.7858

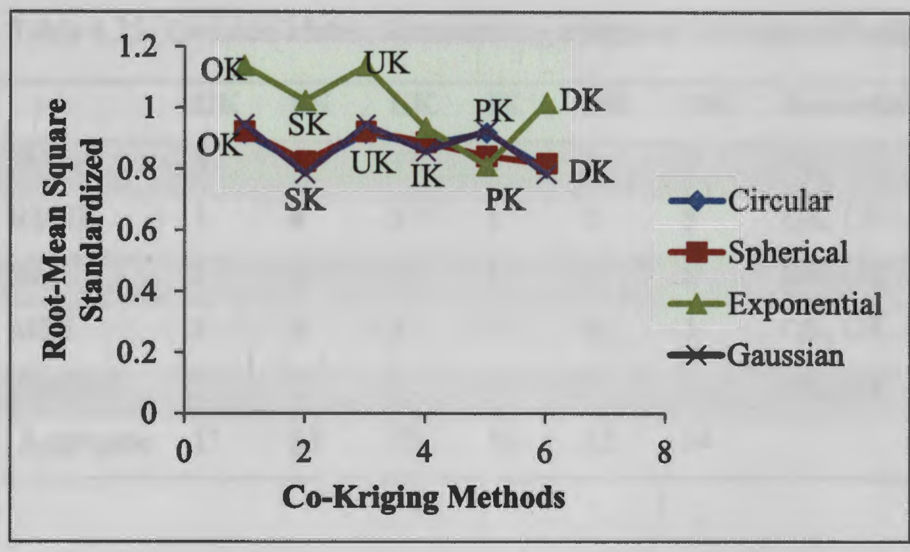

Figure 6.15. Root-mean-square error standardized of co-kriged datasets.

In co-kriging analysis, the decision matrix used for kriging the temperature and precipitation datasets was adopted. The decision matrix summary for co-kriging is given in Tables 6.24 to 6.27.

Table 6.24. Decision Matrix Summarizing Circular Variogram Predictions.

	OK	SK	UK	IK	PK	DK	Remarks
Mean	3	**1**	3	4	3	2	OK, UK, PK - same value
RMSE	2	**3**	2	1	2	4	Ditto
ASE	2	**3**	2	1	2	4	Ditto
MSE	3	**2**	3	6	4	1	OK, UK - same value
RMSES	4	**2**	5	3	4	1	OK, PK- same value
Aggregate	14	**11**	15	15	15	12	

Table 6.25. Decision Matrix Summarizing Spherical Variogram Predictions.

	OK	SK	UK	IK	PK	DK	Remarks
Mean	3	1	3	5	4	2	OK, UK – same value
RMSE	3	4	3	1	2	5	OK, UK – same value
ASE	3	4	3	1	2	5	OK, UK – same value
MSE	3	2	3	5	4	1	OK, UK – same value
RMSES	5	2	5	4	3	1	OK, UK – same value
Aggregate	17	13	17	16	15	14	

Table 6.26. Decision Matrix Summarizing Exponential Variogram Predictions.

	OK	SK	UK	IK	PK	DK	Remarks
Mean	2	4	2	1	3	5	OK, UK – same value
RMSE	3	4	3	1	2	5	OK, UK – same value
ASE	3	4	3	1	2	5	OK, UK – same value
MSE	2	4	2	1	5	3	OK, UK – same value
RMSES	5	4	5	2	1	3	OK, UK – same value
Aggregate	15	20	15	6	13	21	

Table 6.27. Decision Matrix Summarizing Gaussian Variogram Predictions.

	OK	SK	UK	IK	PK	DK	Remarks
Mean	5	4	5	2	1	3	OK, UK- same value
RMSE	3	4	3	1	2	5	OK, UK- same value
ASE	3	4	3	2	1	5	OK, UK- same value
MSE	4	2	4	5	3	1	OK, UK- same value
RMSES	5	2	5	3	4	1	OK, UK- same value
Aggregate	20	16	20	13	11	15	

Apart from the decision matrix, the RMSE and ASE results of the different variogram models for temperature, precipitation, and co-kriging were considered. The model with the RMSE close to ASE is usually the best model. Thus, the relationship between RMSE and ASE should be close to 45 degrees if the model is to be valid. The relationships for the variogram models for temperature, precipitation, and co-kriging of two environmental factors are given in Figures 6.16 to 6.18.

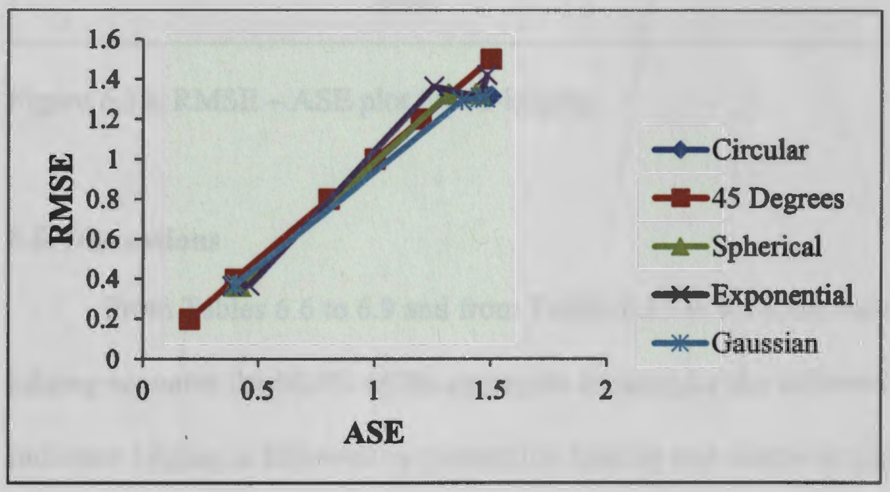

Figure 6.16. RMSE – ASE plot for maximum temperature.

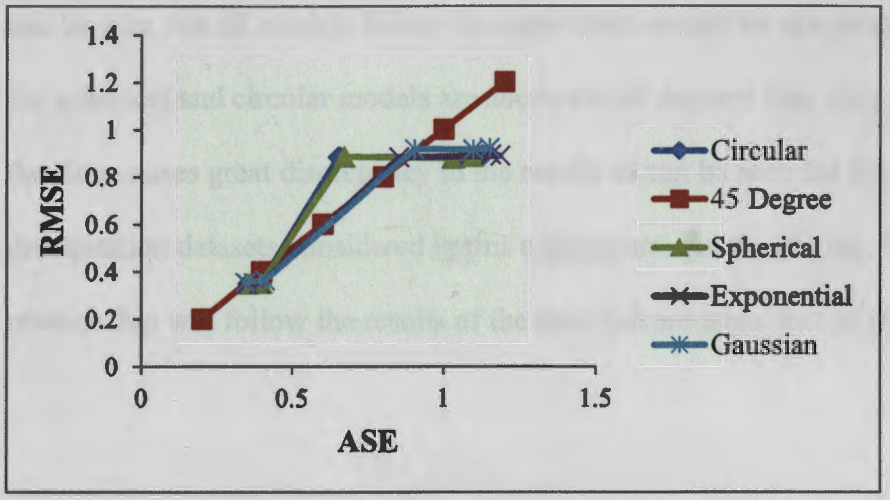

Figure 6.17. RMSE – ASE plot for precipitation.

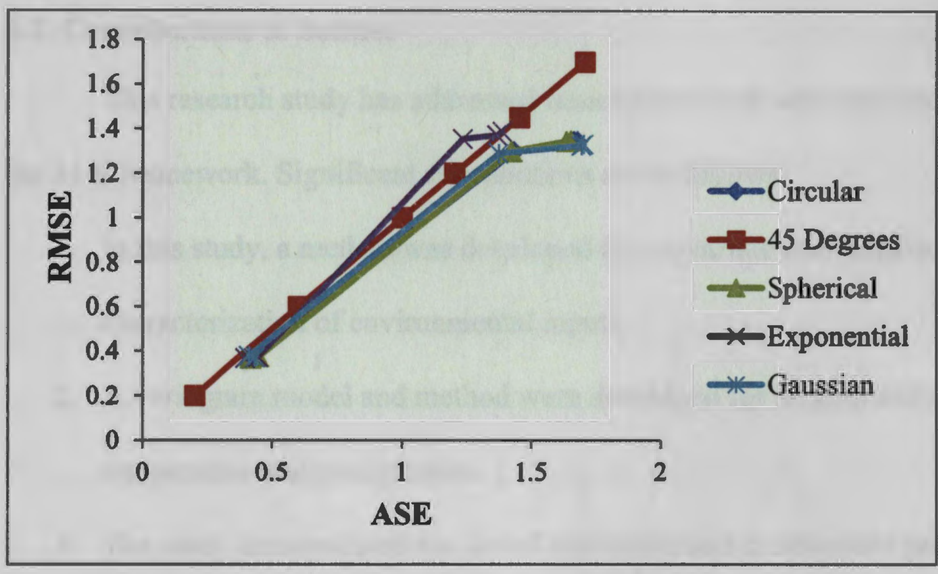

Figure 6.18. RMSE – ASE plot for co-kriging.

6.6. Discussions

From Tables 6.6 to 6.9 and from Tables 6.15 to 6.18, the results show that indicator kriging accounts for 66.6% of the aggregate ranking for the different methods used. Indicator kriging is followed by probability kriging and simple kriging at 16.6% each. Indicator kriging provides better results when used with univariate characterization. For co-kriging, the simple kriging technique is the best. When Figures 16 to 18 are considered, it can be seen that all models follow the same trend except for the precipitation dataset where the spherical and circular models are above the 45 degrees line. Any change in variance for the data causes great discrepancy in the results as can be seen for the temperature and precipitation datasets considered in this experiment. For co-kriging, the results for the relationship will follow the results of the data that are input first in the model.

6.7. Contributions to Science

This research study has addressed issues associated with environmental inputs in the M-E framework. Significant contributions are as follows:

1. In this study, a method was developed for univariate and multivariate characterization of environmental inputs.
2. A variogram model and method were developed for kriging and co-kriging the temperature and precipitation.
3. The study demonstrated the use of univariate and multivariate prediction mapping for locations not sampled.

CHAPTER 7. CONCLUSIONS AND RECOMMENDATIONS

7.1. Conclusions

The design of pavements is a complex process requiring current data for regular updating, calibration, and validation of models to produce durable and resilient road structures. This process requires continuous data collection for new materials and other factors to validate the design processes. Different design tools are available for the engineering community, but the M-E tool is better because it takes into account engineering, traffic, soil, environmental factors, construction, and economics. A number of these input parameters and data used in the design are obtained through studies which have been conducted in different areas of the country. However, the environmental input is based on approximately 800 weather stations maintained in the M-E library.

The current research has extensively covered engineering, traffic, soil, construction, and economics as shown from in the Literature Review. Environmental factors are an issue of concern where the impact has not been adequately addressed. This research developed a method for analyzing univariate and multivariate characterization of temperature and precipitation inputs as well as a variogram model for both kriging and co-kriging. The research also demonstrated the use of univariate and multivariate prediction mapping to obtain data for locations not sampled using Geostatistical Analyst.

When using geostatistical methods to determine the best model to adopt in the analysis, statistical results from the cross-validation, comprised of the mean error, root mean square error, (RMSE), average standard error (ASE), mean standardized error, (MSE), and root mean square error standardized (RMSES), were used. The best kriging method was selected based on the set decision criteria. The results from the analysis show that indicator kriging accounts for 66.6%, and probability kriging and simple kriging have 16.6% each. Where the co-kriging technique is used, the simple kriging gives a higher percentage.

7.2. Recommendations

The research analyzed temperature and precipitation data using different kriging methods (both linear and non-linear) to determine the best kriging method. The indicator kriging method was found to be best based on the decision matrix developed using a circular or spherical variogram.

7.3. Summary and Further Research

This study compared the results of analyzing temperature and precipitation from 118 weather stations in North Dakota using different kriging techniques to determine the best kriging model. The results showed a significant difference among the various kriging models used. However, no differences existed between the results of ordinary kriging and universal kriging. A decision matrix was used to determine the best kriging model. Further research is needed to incorporate real time and viability of the environmental factors.

REFERENCES

AASHO (1962), AASHO Road Test, Special Report 52; Report 5, "Flexible Pavement Research," American Association of State Highway Officials, Washington, DC.

AASHTO (1972), *AASHTO Interim Guide for Design of Pavement Structures*, American Association of State Highway and Transportation Officials, Washington, DC.

AASHTO (1986), *AASHTO Guide for Design of Pavement Structures*, American Association of State Highway and Transportation Officials, Washington, DC.

AASHTO (1993), *AASHTO Guide for Design of Pavement Structures*, American Association of State Highway and Transportation Officials, Washington, DC.

ASCE (2009), Infrastructure Reporting and Asset Management: Best Practices and Opportunities, Reston, VA.

Baladi, G. Y., and A. Thomas (1994), "Mechanistic Evaluation of AASHTO Flexible Pavement Design Equations," *Transportation Research Record 1449*, Washington, DC. pp. 72-78

Basma, A. A., and T. I. Al-Suleiman (1991), "Climatic Considerations in New AASHTO Flexible Pavement Design," *Journal of Transportation Engineering*, Vol. 117, No. 2. pp. 210-223

Bohling. B. (2005), "Estimating the Risk for Erosion of Surface Sediments in the Mecklenburg Bight (South-Western Baltic Sea)," *Baltica*, Vol. 18, No. 1, pp. 3–12.

Brian, M., and D. G. Zollinger (1995), "Sensitivity Analysis of Input Parameters for Pavement Design and Reliability," *Transportation Research Record 1482*, Washington, DC, pp. 111-122.

Chilès, J.P., and P. Delfiner (1999), "Geostatistics: Modeling Spatial Uncertainty," *Wiley Series in Probability and Statistics*. John Wiley & Sons, New York, NY, pp. 687.

Clarke, K. C. (2003), *Getting Started with Geographic Information Systems*, 4th ed., Prentice Hall, Upper Saddle River, NJ.

Deutsch, C.V., and A.G. Journel (1998), "GSLIB" *Geostatistical Software Library and User's Guide*, Oxford University Press, New York: NY, pp. 369.

Estrada-Peña, A. (1999), "Geostatistics and Remote Sensing Using NOAA-AVHRR Satellite Imagery as Predictive Tools in Tick Distribution and Habitat Suitability Estimations for *Boophilus Microplus* (Acari: Ixodidae) in South America," Elsevier B.V., pp.73-82.

FHWA (2001a), "Guide to LTPP Traffic Data Collection and Processing," Federal Highway Administration, Washington: DC.

FHWA (2001b), "Traffic Monitoring Guide," U.S Department of Transportation, Federal Highway Administration, Office of the Highway Policy Information, Washington: DC.

FHWA (2003), "Design Guide Implementation Survey 2003," U.S Department of Transportation, Federal Highway Administration, Office of the Highway Policy Information, Washington, DC.

Garber, N. J., and L. A. Hoel (2009), *Traffic & Highway Engineering*, 4th ed., Cengage Learning, Toronto, ON .

Goldberger, A.S. (1968), "*Topics in Regression Analysis*". Macmillan, NewYork.

Goovaerts, P. (1997), *Geostatistics for Natural Resources Evaluation,* Oxford University Press, New York, N.Y.

Haider, S. W., and R.S. Harichandran (2007), "Relating Axle Load Spectra to Truck Gross Vehicle Weights and Volumes" *Journal of Transportation Engineering,* Vol. 133 No. 12, pp. 696-705.

HRB (1961), "The AASHO Road Test. Special Report 61A - The History and Description of the Project," Highway Research Board, National Academy of Sciences - National Research Council, Washington: DC.

Huang, Y. H. (2004), *Pavement Analysis and Design*, Prentice-Hall, Upper Saddle River, NJ.

Journel, A. G. (1989), *Fundamentals of Geostatistics in Five Lessons*, American Geophysical Union, Washington: D. C.

Journel, A., and C. Huijbregts (2003), *Mining Geostatistics*, The Blackburn Press, Caldwell, NJ.

Khanum, T., M. Hossain, S. A. Romanoschi, and R. Barezinsky (2005), Concrete Pavement Design in Kansas Following the Mechanistic-Empirical Pavement Design Guide, Mid-Continent Transportation Research Symposium, Ames, IA.

Krige, D. G. (1951), "A Statistical Approach to Some Basic Mine Valuation Problems on the Witwatersrand," *Journal of the Chemical, Metallurgical and Mining Society of South Africa*, Vol. 52, pp 119-139.

Kyriakidis, C. K., and A.G. Journel (2001), "Stochastic Modeling of Atmospheric Pollution: A Spatial Time-series Framework. Part I: Methodology," Elsevier, B.V., pp. 2331-2337.

Malabar, F.L., and J. J. Hajek (1995)."General Axle Load Equivalency Factors," *Transportation Research Record 1482*, Washington, DC, pp. 67-78.

Matheron, G. (1962), *Traité de Géostatistique appliqué*, ed. Technip., Paris: France, Vol. 1.

Matheron, G. (1971), *The Theory of Regionalized Variables and its Applications*, Ecole Nationale Superieure des mines de Paris, Fountainebleau: France.

McClave, J. T., and T. Sincich (2009), *Statistics*, 11th ed., Prentice Hall, Upper Saddle River, NJ.

NCHRP (2002), *Guide for Mechanistic-Empirical Design of New and Rehabilitated Pavement Structures: Final Report for Project 1-37 A*, National Cooperative Highway Research Program, Transportation Research Board, National Research Council. Washington, DC.

NCHRP (2004), *Mechanistic-Empirical Design of New and Rehabilitated Pavement Structures*, National Cooperative Highway Research Program, NCHRP Project 1-37A, National Research Council, Washington, DC.

NDDOT (2008), Presentation to Interim Taxation Committee on Extraordinary Road and Bridge Impacts, July 2008.

Nalder, A. I., and R. W. Wein (1998), "Spatial Interpolation of Climatic Normals: Test of a New Method in the Canadian Boreal Forest," Elsevier Science B.V., pp. 211-225.

NOAA (2009) http://cdo.ncdc.noaa.gov/cgi-bin/climatenormals/climatenormals.pl accessed on Mar. 2009.

Olidis, C., and D. Hein (2004), "Guide for the Mechanistic-Empirical Design of New and Rehabilitated Pavement Structures, Material Characterization, Is Your Agency Ready?" ERES Consultants Division, Toronto, Canada, pp. 1-14.

Papagiannakis, A. T., M. Bracher, and N.C. Jackson (2006), "Utilizing Clustering Techniques in Estimating Traffic Data Input for Pavement Design." *Journal of Transportation Engineering*, Vol. 132, No. 11 pp. 872-879.

Papagiannakis, A. T., and E.A. Masad (2008), *Pavement Design and Materials*, Wiley & Sons, Inc., Hoboken, NJ.

Pardo-Iguzquiza, E. (1998), "Comparison of Geostatistical Methods for Estimating the Areal Average Climatological Rainfall Mean Using Data on Precipitation and Topography," International Journal of Climatology, Vol. 18: pp. 1031-1047.

Prudhomme, C., and D.W. Reed, (1999), "Mapping Extreme Rainfall in a Mountain Region Using Geostatistical Techniques: A Case Study in Scotland," *International Journal Climatology,* Vol.19, pp. 1337–1356.

Schwartz, C. W., and R.L. Carvalho (2006), "Implementation of the NCHRP 1-37A Design Guide Volume 2: Evaluation of Mechanistic-Empirical Design Procedure," College Park, MD.

Tonias, E. D., and J. J. Zhao (2007), *Bridge Engineering: Design, Rehabilitation and Maintenance of Modern Highway Bridges*, 2nd ed., McGraw - Hill, New York, NY.

T.R.IP. (2009), "Moving into North Dakota's Future: Meeting the State's Need for Safe and Efficient Mobility," Washington: D.C.

Wikipedia (2010a), "Concrete," Available at http:en.wikipedia.org/wiki/Concrete accessed on Apr. 2, 2010.

Wikipedia (2010b), "History of Road Transport." Available at http://en.wikipedia.org/wiki/History_of_road_transport accessed on Jan. 10, 2010

Zhang, Z., J. P. Leidy, I. Kawa, and W. R. Hudson (2000), "Impact of Changing Traffic Characteristics and Environmental Conditions on Flexible Pavements," *Transportation Research Record 1730*, Washington, DC, pp. 125-131.

Zhou, F., H.C. Guo, Y.S. Ho, and C.Z. Wu (2007), "Scientometric Analysis of Geostatistics Using Multivariate Methods," *Scientometrics,* Vol. 73: pp. 265-279

APPENDIX A. TEMPERATURE DATASET

NORTH DAKOTA
TEMPERATURE NORMALS (Degrees Fahrenheit)

NO	STATION NAME	ELEMENT	JAN	FEB	MA	APR	MAY	JUN	JUL	AUG	SEP	OCT	NOV	DEC	ANN
004	ALEXANDER 18 SW	MAX	22	29.5	41.4	56.5	68.1	77.6	84.4	84.5	71.6	57.9	38.2	26.3	54.8
		MEAN	10.6	18.8	29.8	43.4	54.3	63.8	69.9	69.1	57.1	44.2	27.7	15.2	42
		MIN	-0.8	8	18.1	30.3	40.4	49.9	55.3	53.6	42.6	30.5	17.2	4	29.1
005	ALMONT	MAX	23.1	30.5	41.8	58.3	70.9	78.4	84.5	84	73.4	60.1	39.2	27	55.9
		MEAN	11.4	19.2	29.8	43.8	56.4	64.8	70	68.9	58.1	45.4	28.1	15.7	42.6
		MIN	-0.3	7.8	17.8	29.3	41.8	51.1	55.4	53.8	42.7	30.7	16.9	4.4	29.3
007	AMIDON	MAX	26.5	33.6	43.7	57.1	69.2	78.7	85.8	85.7	73	59.3	40.9	30.3	57
		MEAN	15.5	22.5	31.7	43.9	55.5	64.7	70.9	70.1	58.4	45.9	30	19.3	44
		MIN	4.5	11.3	19.6	30.6	41.7	50.7	56	54.4	43.8	32.4	19	8.3	31
008	ASHLEY	MAX	20.5	27.5	39	55.6	68.8	77.4	84	82.8	71.9	58.3	37.7	24.8	54
		MEAN	9.6	16.8	28.5	43.4	56.5	65.5	71.2	69.3	58.3	45.2	27.4	14.6	42.2
		MIN	-1.3	6	18	31.2	44.1	53.5	58.3	55.7	44.7	32.1	17	4.3	30.3
009	BEACH	MAX	25	31.7	42.5	56.6	68.4	78	84.7	84.6	72.8	58.1	39.5	28.9	55.9
		MEAN	15.2	22	31.5	43.5	54.9	64.1	69.8	69	58.1	45.1	29.4	19.1	43.5
		MIN	5.3	12.3	20.4	30.4	41.4	50.2	54.8	53.3	43.3	32.1	19.3	9.2	31
010	BELCOURT KEYA RADIO	MAX	13.9	21.2	32	49.9	64	72.3	77.7	77.1	65.5	52.8	32.3	18.5	48.1
		MEAN	1.9	9.3	20.6	36.9	50.9	59.8	65	63	52	39.5	21.9	7.4	35.7
		MIN	-10	-2.7	9.1	23.8	37.8	47.2	52.2	48.9	38.4	26.2	11.5	-3.7	23.2
012	BEULAH 1 W	MAX	21.7	29.4	41.2	57.5	70.8	78.7	84.8	84.7	72.9	59.6	38.7	26.2	55.5
		MEAN	11	18.9	30	43.7	56.1	64.5	69.8	69.3	57.8	45.8	28.2	15.8	42.6
		MIN	0.2	8.4	18.8	29.8	41.3	50.3	54.8	53.8	42.6	31.9	17.6	5.4	29.6
013	BISMARCK MUNICIPAL AP	MAX	21.1	28.5	40.2	55.9	69.1	77.8	84.5	83.3	71.6	58.2	38.2	25.7	54.5
		MEAN	10.2	18.1	29.7	43.3	56	64.7	70.4	69	57.7	45.2	28	15.2	42.3
		MIN	-0.6	7.8	19.1	30.6	42.8	51.6	56.4	54.7	43.7	32.1	17.8	4.8	30.1

015	BOTTINEAU	MAX	13.8	21.1	32.9	51.7	66.9	74.8	79.4	78.9	67.3	53.7	32.8	18.7	49.3
		MEAN	3	10.5	22.9	39.7	53.8	62.4	66.7	65.5	54.4	41.4	23.2	8.5	37.7
		MIN	-7.8	-0.1	12.8	27.6	40.6	49.9	54	52	41.5	29.1	13.6	-1.7	26
016	BOWBELLS	MAX	16.1	23.1	34.3	52.6	67.1	75.5	80.4	80.2	67.7	54.7	33.8	21.1	50.6
		MEAN	6.2	13.3	24.4	40.2	53.4	62.3	66.9	65.6	54.2	42	24.4	11.4	38.7
		MIN	-3.8	3.5	14.4	27.7	39.7	49	53.4	50.9	40.6	29.2	15	1.7	26.8
017	BOWMAN	MAX	25.4	31.8	41.3	54.4	66.3	76.1	83.8	83.7	71.6	58	39.8	29.3	55.1
		MEAN	14.6	20.9	29.9	41.9	53.6	63.1	69.4	68.3	56.6	44.2	28.5	18.1	42.4
		MIN	3.7	9.9	18.4	29.3	40.9	50.1	55	52.9	41.6	30.4	17.2	6.9	29.7
018	BREIEN	MAX	23.5	30.6	42.5	58.8	71.2	79.7	86	85.7	74.7	60.7	40.2	28	56.8
		MEAN	11	18.8	30.3	44.2	56.5	65.3	70.7	69.6	58.5	45.4	28.3	15.8	42.9
		MIN	-1.6	6.9	18.1	29.5	41.8	50.8	55.4	53.5	42.2	30.1	16.3	3.6	28.9
019	BUTTE 5 SE	MAX	17	24.1	36.6	54.7	69.4	77.7	83.2	82.5	70.9	56.6	34.6	21.7	52.4
		MEAN	7	14.2	26.5	42.2	56.1	65	70.1	68.9	58	44.7	25.6	12.2	40.9
		MIN	-3.1	4.2	16.4	29.6	42.7	52.2	56.9	55.2	45.1	32.8	16.6	2.6	29.3
021	CARRINGTON	MAX	16.4	23.1	34.4	51.9	67	74.9	79.9	79.3	68.3	55.1	34.2	20.9	50.5
		MEAN	7	13.9	25.3	40.7	55	63.8	68.6	66.8	55.9	43.5	25.5	12.1	39.8
		MIN	-2.5	4.7	16.1	29.4	42.9	52.6	57.2	54.2	43.4	31.8	16.7	3.3	29.2
022	CARRINGTON 4 N	MAX	16.7	24.2	36.3	54.8	70.6	78.1	82.7	82.1	71.5	57.2	34.9	21.8	52.6
		MEAN	6.5	13.8	26	41.8	56.1	64.6	68.9	67.5	57.4	44.4	25.6	12.1	40.4
		MIN	-3.7	3.3	15.6	28.8	41.6	51.1	55.1	52.8	43.3	31.6	16.2	2.3	28.2
023	CARSON	MAX	20.9	27.7	38	53	66.4	74.4	81	80.7	69.5	57	37.7	25.6	52.7
		MEAN	10.8	17.8	27.7	41	54	62.7	68.5	67.3	56.1	44.2	27.7	15.5	41.1
		MIN	0.6	7.8	17.3	28.9	41.6	51	56	53.9	42.7	31.4	17.6	5.4	29.5
024	CASSELTON AGRONOMY FRM	MAX	16.3	23.7	35.8	54.6	70.2	77.8	82.9	82	72	57.8	36.2	21.9	52.6
		MEAN	5.7	12.7	26.2	42.2	56.5	65.2	70.2	68.5	58.3	45.2	26.7	12.4	40.8

		MIN	-4.9	1.7	16.6	29.8	42.8	52.6	57.4	55	44.6	32.6	17.1	2.9	29
025	CAVALIER 7 NW	MAX	12.2	19.8	31.5	51	67.6	74.9	78.7	78.2	67.4	53.5	32.7	17.8	48.8
		MEAN	2.5	9.9	22.5	39.8	54.4	63.1	67.1	65.4	55	42.4	24.1	8.9	37.9
		MIN	-7.3	0	13.5	28.5	41.2	51.3	55.5	52.6	42.6	31.2	15.4	-0.1	27
026	CENTER 4 SE	MAX	22.4	28.2	39.4	54.6	67.9	76.5	82.4	82.1	71	58.2	38.7	26.7	54
		MEAN	10.5	17	27.7	41.1	54	63	68.3	67	56.1	44.3	27.1	15.4	41
		MIN	-1.4	5.8	16	27.5	40.1	49.5	54.1	51.8	41.2	30.3	15.5	4	27.9
028	COLGATE	MAX	13.9	21.4	33.7	53.4	69.2	77.1	82.3	81.8	70.4	55.8	33.7	19.1	51
		MEAN	3.6	10.8	24.1	41.3	55.9	64.4	69.1	68	57	43.3	24.1	9.7	39.3
		MIN	-6.8	0.1	14.4	29.1	42.5	51.7	55.9	54.1	43.5	30.8	14.4	0.2	27.5
029	COOPERSTOWN	MAX	14.3	22.1	34.6	53	68.3	76.4	81.2	80.4	69.4	55.6	33.3	19.5	50.7
		MEAN	5	12.8	25.5	41.5	55.6	64.3	68.9	67.2	56.7	43.9	24.9	10.8	39.8
		MIN	-4.3	3.4	16.3	30	42.8	52.2	56.5	54	43.9	32.2	16.5	2.1	28.8
031	CROSBY	MAX	17.8	25.7	38.2	56.1	69.7	77.9	83	82.3	69.9	56.2	34.9	22.2	52.8
		MEAN	8.1	16.2	28.1	43.3	56.1	64.6	69.2	67.8	56.5	44.2	25.8	12.9	41.1
		MIN	-1.7	6.6	18	30.5	42.4	51.3	55.3	53.2	43.1	32.1	16.7	3.5	29.3
032	DEVILS LAKE KDLR	MAX	14.7	22.3	33.6	52.1	67.5	75.3	80.1	79.1	67.7	53.9	33.1	19.4	49.9
		MEAN	6.1	13.8	25.5	42.1	56.2	64.8	69.4	67.7	57.1	44.3	25.8	11.5	40.4
		MIN	-2.5	5.2	17.3	32	44.9	54.3	58.6	56.2	46.5	34.6	18.4	3.6	30.8
033	DICKINSON AP	MAX	23.7	30.7	40.9	54.9	67.1	76	83.2	82.8	70.6	57.6	38.7	27.9	54.5
		MEAN	14.2	21.2	30.4	42.8	54.5	63.4	69.4	68.7	57.2	45.3	29	18.2	42.9
		MIN	4.6	11.6	19.9	30.6	41.9	50.8	55.6	54.5	43.8	33	19.3	8.4	31.2
034	DICKINSON EXP STN	MAX	23.9	30.9	40.8	54.6	67.1	76	82.6	82.9	71	57.9	39.3	28.2	54.6
		MEAN	12	18.9	28.7	41.3	53.4	62.4	68.1	67.3	55.4	43.3	27.3	16.2	41.2
		MIN	0	6.9	16.5	28	39.7	48.8	53.5	51.6	39.8	28.7	15.2	4.1	27.7
035	DICKINSON RANCH HQ	MAX	22	29	39.5	54.4	66.9	76.1	82.7	82.7	70.4	57.5	37.9	26.1	53.8

		MEAN	11.8	19	29	42.1	54.4	63.7	69.4	68.6	57	44.7	27.7	16.1	42
		MIN	1.5	8.9	18.5	29.8	41.8	51.3	56	54.4	43.6	31.8	17.4	6	30.1
036	DRAKE 9 NE	MAX	15.8	23	34.6	52.8	67.6	75.9	80.9	80.1	69.1	55.3	33.9	20.7	50.8
		MEAN	5	12.5	24.5	41	55.4	64.1	68.6	67	56.3	43	24.4	10.6	39.4
		MIN	-5.8	2	14.4	29.2	43.2	52.3	56.3	53.9	43.4	30.7	14.8	0.4	27.9
038	DUNN CENTER 2 SW	MAX	23.7	30.7	41.3	56.7	69.5	77.8	84.7	85.3	72.9	58.8	39.1	27.8	55.7
		MEAN	12.8	20.2	30.3	44	56.2	64.6	70.2	70.1	58.4	45.9	28.8	17.1	43.2
		MIN	1.9	9.7	19.2	31.2	42.8	51.3	55.7	54.8	43.8	32.9	18.4	6.4	30.7
039	EDGELEY 3 WNW	MAX	18.5	25.1	36.8	53.5	68.2	76.4	82.8	81.8	71.1	57.7	36.5	23.6	52.7
		MEAN	8.9	15.7	27.4	42	55.7	64.3	69.8	68.3	57.7	45.2	27.2	14.2	41.4
		MIN	-0.7	6.2	17.9	30.5	43.2	52.1	56.8	54.8	44.3	32.6	17.8	4.8	30
040	EDMORE 1 NW	MAX	10.8	18.3	31	50.8	66.7	74.4	79	78.8	67.3	53	31.1	16.2	48.1
		MEAN	0.7	8.1	21.6	39.3	53.7	62.2	66.5	65.2	54.5	41.3	21.9	6.9	36.8
		MIN	-9.5	-2.1	12.2	27.7	40.6	49.9	53.9	51.6	41.7	29.5	12.7	-2.5	25.5
041	EDMUNDS ARROWWOOD R.	MAX	18.4	25.8	38.1	55.2	70.6	78.1	83.8	82.4	72.7	59	37	23.8	53.7
		MEAN	8.2	15.8	27.8	42.5	56.6	64.8	69.8	68	58.1	45.8	27.3	14.1	41.6
		MIN	-2.1	5.8	17.4	29.7	42.5	51.5	55.8	53.5	43.5	32.6	17.5	4.4	29.3
043	ELLENDALE	MAX	20.5	27.4	39.3	57.3	71.3	79.6	85.1	84	73.7	59.3	37.6	24.8	55
		MEAN	10.5	17.7	30	45.1	58.2	67	72.2	70.7	60.2	47	28.5	15.5	43.6
		MIN	0.5	8	20.6	32.9	45	54.3	59.3	57.3	46.6	34.6	19.4	6.1	32.1
044	ENDERLIN 2 W	MAX	18	25.5	37.4	55.8	71.1	79.2	84.5	83.1	72.1	58.1	36.8	23.4	53.8
		MEAN	7.9	15.2	27.7	43.5	57.4	66.1	70.9	68.8	58.2	45.3	27.3	13.7	41.8
		MIN	-2.2	4.8	17.9	31.2	43.6	52.9	57.3	54.4	44.3	32.4	17.8	4	29.9
046	FAIRFIELD	MAX	20.4	27.8	38.3	53.2	65.5	74.4	81.2	80.9	68.9	55.6	36.3	24.8	52.3
		MEAN	10.3	17.4	27.6	41.2	53.3	62.3	68.2	67.2	56.1	43.4	26.4	14.8	40.7
		MIN	0.1	6.9	16.8	29.1	41.1	50.2	55.2	53.4	43.2	31.1	16.4	4.7	29

047	FARGO HECTOR AP	MAX	15.9	22.8	35.3	54.5	69.5	77.4	82.2	81	69.9	56.1	35.2	20.8	51.7
		MEAN	6.8	14.1	27.2	43.5	57.4	66	70.6	69	58	45.3	27	12.5	41.5
		MIN	-2.3	5.4	19	32.4	45.3	54.5	59	57	46.1	34.4	18.7	4.2	31.1
048	FESSENDEN	MAX	15.5	22.8	35.2	53.7	69.1	76.5	81.6	80.9	70.6	56	34.2	20.4	51.4
		MEAN	4.9	12.4	25.1	41.5	56.1	64.6	69.3	67.6	57.4	43.5	24.5	10.4	39.8
		MIN	-5.7	1.9	15	29.2	43.1	52.6	56.9	54.3	44.2	30.9	14.7	0.4	28.1
050	FORMAN 5 SSE	MAX	17.5	24.7	36.8	54.5	68.9	77.4	83.2	82.2	71.2	57.4	36.9	23	52.8
		MEAN	7.8	15.1	27.7	43.5	57	65.8	71	69.3	58.3	45.4	27.9	13.9	41.9
		MIN	-2	5.4	18.6	32.4	45.1	54.2	58.8	56.4	45.3	33.3	18.8	4.8	30.9
051	FORTUNA 1 W	MAX	15.5	23.4	35.1	52.4	65.9	74.8	80.5	79.9	67	53.7	32.9	20.6	50.1
		MEAN	5.6	13.6	25	40.2	53.1	62.2	67.1	65.8	53.8	41.3	23.7	11.1	38.5
		MIN	-4.3	3.7	14.8	28	40.2	49.5	53.6	51.6	40.5	28.8	14.5	1.5	26.9
052	FORT YATES 4 SW	MAX	23.5	30.3	40.8	56.3	69.1	78.3	84.8	83.8	73.1	60	39.4	27.3	55.6
		MEAN	13.4	20.6	30.7	44.6	57.4	66.7	72.5	71.1	60	47.6	30.1	17.9	44.4
		MIN	3.2	10.9	20.6	32.8	45.7	55.1	60.2	58.3	46.9	35.2	20.8	8.5	33.2
053	FOXHOLM 7 N	MAX	16.5	23.8	36.3	53.4	67.6	76.1	82	81.5	69.8	56	35	21.8	51.7
		MEAN	6.3	14.1	25.6	40.9	55	63.8	68.6	66.8	55.9	43.3	25.1	11.9	39.8
		MIN	-4	4.3	14.9	28.3	42.4	51.5	55.2	52.1	41.9	30.6	15.2	2	27.9
054	FULLERTON 1 ESE	MAX	19.8	27.3	39.3	57.4	71.2	79.1	84.8	83.5	73.2	58.9	37.1	24.2	54.7
		MEAN	9.6	17	29.1	44.4	57.5	66	71.2	69.4	59.1	46.2	27.9	14.5	42.7
		MIN	-0.7	6.6	18.8	31.4	43.7	52.9	57.5	55.3	45	33.4	18.7	4.8	30.6
055	GACKLE	MAX	18	24.8	36.4	54.6	68.8	77.3	82.8	81.7	70.9	57.1	35.6	22.5	52.5
		MEAN	8.9	15.9	27.4	43	56.5	65.4	70.7	69.2	58.4	45.6	27.1	13.8	41.8
		MIN	-0.3	6.9	18.3	31.4	44.1	53.5	58.5	56.6	45.9	34.1	18.5	5.1	31.1
056	GARRISON 1 NNW	MAX	18.1	25.4	36.9	53.5	67.3	75.4	81.2	81	69.4	56.1	36.3	23.5	52
		MEAN	7.5	14.8	26.6	41.5	54.6	63.2	68.2	67.4	56.2	43.4	26.5	13.6	40.3

		MIN	-3.1	4.1	16.2	29.4	41.9	50.9	55.2	53.7	42.9	30.7	16.6	3.7	28.5
058	GRAFTON	MAX	13	20.9	33.3	53	69.7	77.7	81.7	81.1	69.7	55	32.9	18.3	50.5
		MEAN	5.1	12.9	25.7	43	58.2	67	71.1	69.6	58.9	45.6	26.3	11	41.2
		MIN	-2.8	4.9	18	32.9	46.6	56.2	60.4	58.1	48.1	36.1	19.7	3.7	31.8
059	GRAND FORKS INTL AP	MAX	14.9	22.4	34.3	53.6	70	77.6	81.9	81	69.7	55.6	34.1	20.1	51.3
		MEAN	5.3	13.1	25.7	42.3	56.8	65.2	69.4	67.8	57	44.3	25.8	11.3	40.3
		MIN	-4.3	3.7	17.1	31	43.5	52.8	56.8	54.5	44.3	33	17.4	2.5	29.4
060	GRAND FORKS UNIV NWS	MAX	14.5	22.3	34.3	53.4	69.1	76.9	80.7	80	68.8	54.7	33.2	19.3	50.6
		MEAN	5.3	12.9	25.6	42.2	56.5	65.3	69.2	67.8	57	44.3	25.6	11	40.2
		MIN	-4	3.5	16.9	31	43.8	53.6	57.7	55.5	45.2	33.8	17.9	2.7	29.8
061	GRANVILLE	MAX	18.6	26.1	37.3	55.4	69.6	78.1	82.9	83.2	70.7	57.3	37.3	23.6	53.3
		MEAN	8.6	16.5	27.7	42.9	56.2	64.9	69.3	68.5	57.5	45.1	27.6	13.9	41.6
		MIN	-1.5	6.8	18	30.4	42.7	51.7	55.7	53.7	44.2	32.8	17.8	4.2	29.7
062	GRASSY BUTTE 2 ENE	MAX	22	29.2	40.5	55.7	68.3	76.1	82.7	82.8	70.4	56.4	36.8	25	53.8
		MEAN	12.4	19.7	29.8	42.8	54.6	62.7	68.4	67.9	56.7	44.5	27.5	16	41.9
		MIN	2.8	10.2	19	29.9	40.9	49.3	54.1	52.9	43	32.5	18.2	6.9	30
063	GRENORA	MAX	17.6	26	39.1	55.2	68.5	77.1	83	82.2	69.9	56.8	34.9	22.1	52.7
		MEAN	6.9	16	28.2	42.1	55.1	63.7	68.8	67.3	55.9	43.7	25.2	11.7	40.4
		MIN	-3.8	5.9	17.2	29	41.6	50.3	54.5	52.3	41.8	30.5	15.4	1.2	28
065	HANKINSON	MAX	18.9	25.6	36.7	54.6	69.5	78.3	83.7	82.2	71.6	58.5	38.1	24.5	53.5
		MEAN	8.3	15.1	27.3	43.6	57.3	66.4	71.4	69.3	58.6	46.2	28.6	14.6	42.2
		MIN	-2.3	4.5	17.8	32.5	45	54.4	59	56.3	45.6	33.8	19	4.6	30.9
066	HANNAH	MAX	13.1	20.1	32.2	51.8	68.8	75.8	79.3	79.4	68.6	55.1	32.9	18	49.6
		MEAN	2.6	9.7	22	39.5	54.6	62.6	66.2	65	55	43	23.5	8	37.6
		MIN	-7.9	-0.8	11.7	27.2	40.4	49.4	53	50.6	41.4	30.9	14.1	-2	25.7
067	HANSBORO 4 NNE	MAX	11.9	19.4	31	50.1	66.2	74	78.6	78.6	67.4	53.2	31.1	17.1	48.2

		MEAN	0.8	8.8	21.3	38.7	53	61.2	65.5	64.2	53.5	40.5	20.9	6.7	36.3
		MIN	-10.4	-1.8	11.6	27.3	39.8	48.4	52.3	49.8	39.6	27.8	10.7	-3.8	24.3
068	HARVEY	MAX	19.5	27.2	38.8	57.5	72.4	79.3	84.5	84.3	73.5	59.7	37.6	24.3	54.9
		MEAN	9.3	17.1	28.7	44.4	58	66	70.8	69.7	59.3	46.7	27.7	14.8	42.7
		MIN	-1	7	18.5	31.3	43.6	52.6	57	55	45.1	33.7	17.8	5.3	30.5
069	HEART BUTTE DAM	MAX	22.4	29.6	39.9	55.2	67.8	76.6	83.1	82.6	71.6	58.5	39	27.3	54.5
		MEAN	11.2	18.4	28.5	42.4	55.1	64.4	70	68.7	57.5	45	28.2	16.4	42.2
		MIN	0	7.1	17.1	29.6	42.4	52.1	56.9	54.8	43.3	31.5	17.4	5.4	29.8
070	HEBRON	MAX	20.9	28.1	38.9	53.9	66.7	75.2	81.8	81.1	69.5	56.1	36.9	25.5	52.9
		MEAN	10.7	17.9	28.2	41.7	54.2	63	68.5	67.2	55.9	43.3	27.1	15.6	41.1
		MIN	0.5	7.7	17.5	29.5	41.6	50.8	55.1	53.2	42.2	30.4	17.2	5.7	29.3
071	HETTINGER	MAX	24.4	30.5	40.3	54	66.2	75.8	83	82.7	71.1	57.9	39.3	28.3	54.5
		MEAN	13.7	20.1	29.3	41.8	53.6	63.1	69	67.9	56.6	44.3	28.2	17.4	42.1
		MIN	3	9.7	18.3	29.6	41	50.4	55	53.1	42	30.6	17	6.4	29.7
072	HILLSBORO 3 N	MAX	15.8	23	35	54	69.9	77.6	82.5	81.5	70.1	56.2	35.2	21.3	51.8
		MEAN	5.7	12.8	25.5	42.3	56.9	65.4	70.1	68.5	57.4	44.6	26.3	12.2	40.6
		MIN	-4.4	2.5	16	30.6	43.8	53.2	57.7	55.5	44.6	33	17.3	3.1	29.4
073	HURDSFIELD 8 SW	MAX	16	22.7	34.4	51.7	66.1	74.5	80.4	80.1	68.7	55	34.1	21.1	50.4
		MEAN	5.6	12.5	23.8	38.9	52.9	61.8	67.1	65.5	54.5	41.6	24.2	11	38.3
		MIN	-4.8	2.2	13.2	26	39.6	49	53.7	50.9	40.2	28.2	14.3	0.8	26.1
074	JAMESTOWN MUNICIPAL	AP MAX	17.9	24.9	36.7	54.2	69.1	77.2	83	81.9	70.3	56.4	35.6	22.4	52.5
		MEAN	8.7	15.9	27.9	42.9	56.7	65.4	70.7	69	57.9	45.2	27.1	13.8	41.8
		MIN	-0.5	6.9	19.1	31.5	44.2	53.5	58.3	56.1	45.4	33.9	18.6	5.2	31
075	JAMESTOWN ST HOSPITAL	MAX	16.2	23.5	35.6	53.8	69.2	77.7	83.2	82	70.7	56.3	34.8	21.1	52
		MEAN	6.2	13.4	25.5	40.8	55.3	64.7	70.2	67.9	56.8	43.9	25.6	11.9	40.2

		MIN	-3.8	3.3	15.3	27.8	41.3	51.7	57.1	53.8	42.9	31.5	16.4	2.7	28.3
076	KEENE 3 S	MAX	21	28.9	40.8	57	69.6	77.8	83.9	84.3	72.1	58.6	37.2	25.3	54.7
		MEAN	10.8	18.6	29.6	43.5	55.5	64.1	69.4	69.2	57.9	45.6	27.6	15.4	42.3
		MIN	0.5	8.3	18.3	30	41.4	50.4	54.8	54	43.7	32.6	18	5.5	29.8
077	KENMARE 1 WSW	MAX	17.1	24.2	35.5	52.5	66.1	74.7	80.2	79.7	67.9	54.6	34.9	21.9	50.8
		MEAN	6.7	14.2	25.2	40.4	53.4	62.4	67	65.4	54.3	42.1	25.1	12.2	39
		MIN	-3.7	4.1	14.9	28.2	40.7	50	53.8	51.1	40.7	29.6	15.2	2.5	27.3
080	LA MOURE	MAX	18	25.7	37.6	54.8	69.2	77.3	83.1	81.8	71.2	57.8	37	23.6	53.1
		MEAN	7.1	14.6	27.1	42.4	55.8	64.8	69.9	67.6	56.8	44.1	26.6	13.2	40.8
		MIN	-3.8	3.4	16.5	30	42.3	52.2	56.6	53.4	42.3	30.3	16.1	2.7	28.5
081	LANGDON EXP FARM	MAX	9.9	17.3	29.4	48.3	64.8	72.9	76.7	76.6	65.6	51.3	30.1	15.3	46.5
		MEAN	0.4	7.6	20.2	37.8	52.6	61.5	65.4	64.2	53.5	40.2	21.5	6.6	36
		MIN	-9.1	-2.1	11	27.2	40.3	50	54	51.8	41.3	29.1	12.9	-2.2	25.4
082	LARIMORE	MAX	13.9	21.3	33	51.6	67.7	75.7	80.1	79.1	68.5	54.7	33.9	19.7	49.9
		MEAN	4.9	11.9	23.6	39.8	55	64	68.3	66.3	55.4	43.1	25.3	10.5	39
		MIN	-4.1	2.4	14.2	27.9	42.3	52.2	56.5	53.5	42.3	31.5	16.7	1.3	28.1
083	LEEDS	MAX	14.3	21.5	32.9	51.4	67.2	75.5	80.1	80	68.2	54.7	33.6	19.6	49.9
		MEAN	4.1	11.2	22.4	38.8	53.5	62.7	67	65.1	54.2	42.1	24.3	10	38
		MIN	-6.2	0.8	11.9	26.1	39.7	49.8	53.8	50.1	40.2	29.4	14.9	0.3	25.9
084	LINTON	MAX	20.3	27.8	39.7	55.9	69.1	78	84.5	83.5	72.1	58.5	37.4	24.8	54.3
		MEAN	9.5	17.5	29.4	43.6	56.1	65.1	71.1	69.7	58	45	27.2	14.7	42.2
		MIN	-1.4	7.2	19	31.2	43.1	52.2	57.6	55.8	43.8	31.4	16.9	4.5	30.1
085	LISBON	MAX	17	23.9	36.1	54.7	69.1	78.2	83.6	82.5	71.3	57.7	36.7	22.9	52.8
		MEAN	6.9	13.8	26.4	42.1	55.9	65.3	70.5	68.6	57.1	44.4	27.1	13.3	41
		MIN	-3.3	3.7	16.6	29.4	42.7	52.4	57.4	54.7	42.8	31.1	17.5	3.6	29.1
088	MANDAN EXPERIMENT STN	MAX	20.4	27.2	38.6	54.4	67.9	76.5	82.8	81.9	70.5	57.3	37.8	25	53.4

		MEAN	10	17.2	28.5	42.7	55.7	64.6	70.2	68.7	57.3	44.7	27.9	15.1	41.9
		MIN	-0.5	7.2	18.4	31	43.4	52.6	57.5	55.4	44.1	32	18	5.2	30.4
090	MAX	MAX	16.5	23.9	35.5	52.1	66.4	74.9	80.7	80.2	68	54.4	34.1	21.3	50.7
		MEAN	7.2	14.5	25.7	40.6	54.3	63.2	68.3	66.6	55.1	42.5	25.3	12.3	39.6
		MIN	-2.2	5	15.9	29	42.2	51.5	55.9	53	42.2	30.6	16.5	3.2	28.6
091	MAYVILLE	MAX	16.4	24.6	36.5	56.2	71.3	78.8	83.3	82.3	71.2	57.2	35.6	21.5	52.9
		MEAN	6.3	14	26.5	43.3	57.5	65.8	70.1	68.6	58.2	45.6	26.7	12	41.2
		MIN	-3.9	3.3	16.5	30.4	43.6	52.8	56.9	54.9	45.1	33.9	17.8	2.4	29.5
092	MC CLUSKY	MAX	18.3	25.5	37.5	55.4	69.9	78.1	83.5	82.9	71.3	57.2	35.8	22.7	53.2
		MEAN	9.2	16.5	28.1	43.3	56.9	65.6	70.6	69.5	58.5	45.5	27.2	14	42.1
		MIN	0	7.5	18.7	31.2	43.9	53.1	57.6	56	45.6	33.7	18.6	5.3	30.9
093	MC HENRY 3 W	MAX	14.3	22.1	33.7	52.4	68.4	75.8	81.1	80.3	68.7	54.8	33.2	19.1	50.3
		MEAN	4.8	12.6	24.9	41.2	55.7	64	69	67.5	56.5	43.7	24.9	10.5	39.6
		MIN	-4.8	3	16	29.9	42.9	52.2	56.9	54.6	44.2	32.5	16.6	1.8	28.8
094	MC LEOD 3 E	MAX	16	23.3	35.9	54.7	69.7	78.1	83	82	71	57.4	36	21.5	52.4
		MEAN	5.3	12.6	26	42.7	57.2	66.1	70.9	69.3	58.3	45	26.3	11.7	41
		MIN	-5.5	1.9	16	30.7	44.6	54	58.7	56.5	45.6	32.6	16.6	1.9	29.5
095	MC VILLE	MAX	14.6	22.6	34.5	53.8	69.8	77.5	82.6	81.2	70	55.6	33.3	19.3	51.2
		MEAN	4.8	12.6	25	41.5	56.1	64.7	69.5	67.6	56.9	43.5	24.5	10.2	39.7
		MIN	-5	2.5	15.4	29.2	42.3	51.8	56.3	53.9	43.8	31.4	15.6	1.1	28.2
097	MEDORA	MAX	27.3	35.1	44.8	58.1	69.9	78.7	86.2	86.1	74.4	61.3	42.3	30.9	57.9
		MEAN	15.6	23.2	32.4	44.3	55.8	64.7	70.9	70	58.3	46.6	30.5	19.4	44.3
		MIN	3.9	11.3	20	30.5	41.7	50.6	55.6	53.8	42.2	31.8	18.7	7.8	30.7
098	MINOT AP	MAX	18.2	25.2	36.6	53.7	67.2	75.6	81.2	80.6	68.4	55.2	35	23	51.7
		MEAN	9.8	17.2	28	42.8	55.6	64.4	69.6	68.2	57	44.7	27.2	14.9	41.6
		MIN	1.4	9.1	19.4	31.8	44	53.1	57.9	55.7	45.5	34.2	19.4	6.7	31.5

099	MINOT EXPERIMENT STN	MAX	16.8	23.6	35.2	52.5	67.2	75.5	80.4	80	67.7	54.4	34.4	21.8	50.8
		MEAN	7.5	14.6	25.9	41.1	55	63.9	68.4	67	55.6	43.2	25.9	12.8	40.1
		MIN	-1.8	5.6	16.6	29.7	42.7	52.3	56.3	53.9	43.5	31.9	17.3	3.8	29.3
100	MOFFIT 3 SE	MAX	20.9	27.8	39.9	57.3	71	79.2	85.3	85	74.2	60.1	38.5	25	55.4
		MEAN	10.1	17.4	29	44.1	57.2	65.9	71.3	70.1	59.3	46.4	28.2	14.9	42.8
		MIN	-0.7	6.9	18	30.8	43.3	52.6	57.2	55.1	44.3	32.7	17.9	4.8	30.2
101	MOHALL	MAX	16	23.2	34.8	52.8	67.3	75.6	80.4	80.8	68.7	54.9	34.6	21.4	50.9
		MEAN	5.9	13	24.3	39.4	53	61.9	66.3	65.2	53.8	41.7	24.9	11.5	38.4
		MIN	-4.3	2.7	13.8	26	38.6	48.2	52.2	49.5	38.9	28.5	15.2	1.6	25.9
103	MOTT	MAX	23.6	30.8	40.8	55	67.5	76.6	83.5	83.4	72	58.5	39	28	54.9
		MEAN	12.1	19.4	28.9	41.5	54.2	63.5	69.4	67.9	56.4	43.9	27.6	16.4	41.8
		MIN	0.5	7.9	17	28	40.9	50.3	55.2	52.3	40.8	29.3	16.1	4.8	28.6
104	NAPOLEON	MAX	18	24.9	36.5	53	67	75.8	82.3	81.4	70.2	56.8	36.6	22.9	52.1
		MEAN	8.3	15.1	27	41.9	54.8	63.9	69.5	68.2	57	44.3	26.7	13.5	40.9
		MIN	-1.5	5.2	17.5	30.7	42.6	52	56.6	54.9	43.8	31.7	16.8	4	29.5
105	NEW ENGLAND	MAX	24.7	31.6	41.6	55.4	67.9	77	83.5	82.8	71.1	58.1	39.3	28.7	55.1
		MEAN	14.2	21.2	30.4	42.8	54.9	64	69.5	68.5	57.1	44.9	28.5	18	42.8
		MIN	3.7	10.8	19.1	30.2	41.9	51	55.5	54.1	43	31.6	17.7	7.2	30.5
106	NEW SALEM 5 NW	MAX	19.4	26.6	38.3	54.2	67.7	76.3	82.7	81.9	71.1	56.9	36.2	23.6	52.9
		MEAN	8.8	15.9	27.3	41.6	54.8	63.5	69.1	67.8	57.2	43.7	26	13.4	40.8
		MIN	-1.9	5.1	16.2	29	41.8	50.7	55.5	53.6	43.3	30.5	15.8	3.1	28.6
107	OAKES 2 S	MAX	17.7	25	37	55	70.3	79	84.4	83.3	72.2	57.9	36.9	23.6	53.5
		MEAN	7.4	14.8	27.3	43	56.7	65.8	70.8	69.1	58.2	44.9	27.1	13.7	41.6
		MIN	-2.9	4.6	17.6	30.9	43.1	52.5	57.2	54.9	44.1	31.8	17.2	3.8	29.6
108	PARK RIVER	MAX	14.7	22.5	34.4	53.5	69.4	77.5	81.5	80.3	69.6	55.6	33.6	19.6	51
		MEAN	5.9	13.5	25.5	42	56.4	65.2	69.4	67.5	57.3	44.7	25.8	11.5	40.4

		MIN	-3	4.5	16.5	30.4	43.3	52.8	57.2	54.6	45	33.7	18	3.3	29.7
109	PEMBINA	MAX	11.5	19.3	31.7	51.5	67.9	75.6	79.7	79.1	67.9	53.5	32.5	17.5	49
		MEAN	1.2	8.6	21.9	39.5	54.5	63	66.9	65.1	54.4	41.6	23.5	7.9	37.3
		MIN	-9.2	-2.1	12.1	27.5	41.1	50.4	54.1	51.1	40.8	29.7	14.4	-1.7	25.7
110	PETERSBURG 2 N	MAX	12.6	19.9	31.5	50.3	66.5	74.7	79.1	78.6	67.7	53.5	32.3	17.9	48.7
		MEAN	2.5	9.7	22.2	39.3	53.9	62.8	66.9	65.4	54.7	41.7	23.4	8.5	37.6
		MIN	-7.7	-0.5	12.9	28.3	41.3	50.8	54.6	52.1	41.6	29.8	14.5	-0.9	26.4
111	PETTIBONE	MAX	16.8	24.3	36.4	54.9	69.3	77.3	83	82.5	70.8	56.6	35.5	21.6	52.4
		MEAN	7.3	14.9	26.9	43	56.3	65	70.4	69.3	58	44.9	26.6	12.5	41.3
		MIN	-2.3	5.4	17.4	31.1	43.3	52.7	57.7	56	45.2	33.2	17.7	3.4	30.1
112	POWERS LAKE 1 N	MAX	16	23.4	34.9	52.3	66.6	74.2	79.6	79.4	67.5	54.5	34.3	21.4	50.3
		MEAN	5.3	13.3	24.9	40.1	53.2	61.7	66.5	65.5	54	41.6	24.2	10.8	38.4
		MIN	-5.5	3.2	14.9	27.9	39.7	49.1	53.4	51.6	40.5	28.6	14.1	0.2	26.5
113	PRETTY ROCK	MAX	23.3	30.3	40.4	55.6	68.5	77.4	84.6	84	72.7	58.5	38.6	27.7	55.1
		MEAN	13.5	20.6	30	43	55.3	64.4	70.3	69.3	58.2	45.7	28.8	17.8	43.1
		MIN	3.6	10.8	19.6	30.4	42	51.3	55.9	54.5	43.6	32.9	18.9	7.9	31
116	RICHARDTON ABBEY	MAX	22.1	29	39.8	54.5	67.3	75.8	82	81.1	69.5	56.1	37	25.9	53.3
		MEAN	13.5	20.4	30.3	43.4	55.7	64.3	70	68.9	57.9	45.6	28.8	17.4	43
		MIN	4.8	11.7	20.7	32.2	44.1	52.8	57.9	56.6	46.3	35.1	20.5	8.9	32.6
118	ROLLA 3 NW	MAX	13.1	19.9	30.1	47.9	63.5	70.8	75.3	74.7	63.3	50.5	30.6	17.5	46.4
		MEAN	4.1	10.6	21.5	37.6	51.6	60.1	65.1	64	53.1	40.9	22.9	9.2	36.7
		MIN	-4.9	1.3	12.9	27.2	39.7	49.4	54.8	53.2	42.8	31.2	15.2	0.9	27
119	RUGBY	MAX	15.8	23.4	35.3	54.6	69.6	77.6	82	81.4	69.5	56.2	34.2	20.5	51.7
		MEAN	5.6	13.5	25.5	42.2	56	64.5	68.7	67.4	56	43.6	24.8	10.5	39.9
		MIN	-4.7	3.5	15.6	29.8	42.3	51.4	55.3	53.3	42.4	31	15.4	0.5	28
120	SAN HAVEN	MAX	13.4	21.3	32.3	50.9	65.9	73.2	77.8	77.4	65.9	53.1	32.5	18.2	48.5

		MEAN	2.7	10.4	21.6	38.7	52.7	61	65.6	63.9	52.6	40.8	22.8	8.2	36.8
		MIN	-8.1	-0.5	10.9	26.5	39.5	48.7	53.3	50.4	39.3	28.5	13.1	-1.9	25
121	SHARON	MAX	13.1	20.8	33.1	52.2	67.4	74.5	78.9	78.7	68.2	54.2	32.5	18	49.3
		MEAN	4.7	12.4	25	41.5	55.6	63.7	68.1	66.9	56.6	43.8	24.7	10.2	39.4
		MIN	-3.8	3.9	16.8	30.8	43.8	52.8	57.2	55.1	45	33.4	16.9	2.3	29.5
124	STANLEY 3 NNW	MAX	15.6	22.8	35	52	66.1	74.7	80.2	80	67.6	54.2	33.8	20.5	50.2
		MEAN	5.7	13.1	24.5	39.4	52.5	61.6	66.4	65.1	53.6	41.3	24.1	10.8	38.2
		MIN	-4.2	3.4	13.9	26.7	38.9	48.4	52.6	50.2	39.5	28.4	14.4	1.1	26.1
125	STEELE 3 N	MAX	18.1	25.6	37.5	54.7	68.6	76.6	82.8	82.4	71.3	57.7	36.5	22.7	52.9
		MEAN	7.7	15	27.1	42.5	55.8	64.5	69.9	68.5	57.6	44.6	26.3	12.9	41
		MIN	-2.8	4.4	16.7	30.2	42.9	52.4	57	54.5	43.9	31.5	16	3	29.1
126	STREETER 7 NW	MAX	18.3	24.4	36.4	53	66.6	74.4	81.3	80.1	68.9	56.2	36	22.8	51.5
		MEAN	7.5	13.9	25.8	40.6	53.6	62.5	68.2	66.7	55.7	43.3	26.1	12.5	39.7
		MIN	-3.4	3.4	15.1	28.1	40.5	50.5	55	53.3	42.5	30.4	16.1	2.2	27.8
129	TIOGA 1 E	MAX	16.7	24.4	36.4	53.4	66.8	75.3	81.2	80.9	68.2	55	34	21.7	51.2
		MEAN	6.9	15.1	26.3	40.8	53.4	62.4	67.4	66.5	54.5	42.4	24.9	12.1	39.4
		MIN	-2.9	5.7	16.1	28.1	39.9	49.5	53.6	52	40.7	29.7	15.8	2.5	27.6
130	TOWNER 2 NE	MAX	14.8	22.5	34.1	52.9	67.9	76.6	81.7	81.2	69.3	55.8	34.1	20.4	50.9
		MEAN	4	11.5	23.5	40.1	54.1	63.2	67.8	66.5	55.1	42.4	24.1	10	38.5
		MIN	-6.9	0.5	12.8	27.3	40.3	49.7	53.9	51.7	40.8	28.9	14.1	-0.4	26.1
131	TROTTERS 3 SSE	MAX	23	30.1	41.3	55.8	67.4	76.2	83	82.5	69.9	56.5	37.4	26.5	54.1
		MEAN	13.5	20.7	30.7	43.3	54.7	63.5	69.3	68.5	56.9	44.8	28.2	17.2	42.6
		MIN	4	11.3	20.1	30.8	42	50.8	55.6	54.4	43.9	33	19	7.9	31.1
132	TURTLE LAKE	MAX	17.6	24.6	36.7	53.6	67.6	75.9	82	81.4	70.1	56.6	35.8	22.6	52
		MEAN	7.4	14.7	26.9	41.4	54.7	63.5	68.8	67.7	56.7	44	25.9	12.8	40.4
		MIN	-2.8	4.7	17	29.1	41.7	51.1	55.6	53.9	43.2	31.4	15.9	2.9	28.6

133	TUTTLE	MAX	21.2	28	39.5	56.8	71	78.8	84.3	84.5	72.6	59.1	39.1	26.2	55.1
		MEAN	10.5	17.5	28.7	43.6	56.8	65.1	70.1	69.1	57.7	45.6	28.5	15.5	42.4
		MIN	-0.3	7	17.9	30.4	42.5	51.4	55.9	53.7	42.8	32	17.9	4.8	29.7
134	UNDERWOOD	MAX	17	24.3	36.9	53.5	67.6	76	81.9	81.1	70.2	55.9	34.6	21.5	51.7
		MEAN	7.1	14.3	26.5	41.5	55.1	64	69.2	67.6	57.3	43.7	25.5	12.2	40.3
		MIN	-2.8	4.2	16	29.4	42.6	51.9	56.4	54.1	44.3	31.5	16.3	2.9	28.9
135	UPHAM 3 N	MAX	15.1	23.3	35	53.8	68.5	76.4	81.4	81.1	69.5	56.1	34.9	20.5	51.3
		MEAN	3.3	11.4	23.8	40.8	54.8	63.3	67.4	66	54.5	41.4	23.7	9.3	38.3
		MIN	-8.6	-0.6	12.5	27.7	41	50.1	53.4	50.9	39.4	26.6	12.5	-1.9	25.3
136	VALLEY CITY 3 NNW	MAX	16.3	23.5	35.4	53.2	68.1	75.8	80.8	79.9	69.5	56.5	35.6	21.6	51.4
		MEAN	5.7	12.9	25.5	41	55.1	63.8	68.5	66.6	56.1	43.7	26	11.9	39.7
		MIN	-4.9	2.3	15.6	28.8	42.1	51.7	56.2	53.3	42.6	30.9	16.3	2.2	28.1
137	VELVA 3 NE	MAX	18	25.6	37.5	54.8	69.1	77.2	82.3	81.3	70.2	57	35.8	22.8	52.6
		MEAN	7.1	14.6	26.3	41.5	55.5	64.4	69.1	67	56.1	43.6	25.7	12.6	40.3
		MIN	-3.8	3.6	15	28.1	41.9	51.5	55.8	52.6	42	30.2	15.5	2.4	27.9
139	WAHPETON 3 N	MAX	17.8	24.9	37.2	56.7	71.8	79.9	84.3	82.6	72.1	57.9	36.8	23	53.8
		MEAN	8.7	16	28.8	45.3	59.3	67.8	72.2	70.3	60	47.3	28.9	14.6	43.3
		MIN	-0.5	7	20.4	33.9	46.7	55.7	60	57.9	47.9	36.6	20.9	6.2	32.7
141	WASHBURN	MAX	20	27.3	39.5	55.6	69.2	77.6	83.3	82.8	72	58	37	24	53.9
		MEAN	9.7	16.9	28.7	43.2	56.2	64.9	70	68.9	58.4	45.5	27.7	14.8	42.1
		MIN	-0.7	6.5	17.9	30.7	43.2	52.2	56.7	54.9	44.7	32.9	18.4	5.5	30.2
143	WATFORD CITY	MAX	19.1	28.4	39.4	55	67.9	76.9	83.6	83.4	70.5	57	37.2	24.9	53.6
		MEAN	8.2	17	27.6	41.3	53.9	63	68.6	67.5	55.2	43.1	26.1	14	40.5
		MIN	-2.8	5.5	15.7	27.6	39.9	49	53.6	51.6	39.9	29.1	15	3	27.3
144	WATFORD CITY 14 S	MAX	25.1	32.9	44.2	58.7	70.8	79.2	86	86.2	74.1	60.7	40.3	29	57.3
		MEAN	13.6	21.6	32	44.8	56.6	65.2	70.8	70.2	58.6	46.6	29.4	17.9	43.9

		MIN	2.1	10.2	19.8	30.8	42.3	51.2	55.6	54.1	43.1	32.4	18.4	6.7	30.6
145	WESTHOPE	MAX	14.2	22.3	34.6	54.8	69.6	76.9	81	81	69.7	55.7	33.4	19	51
		MEAN	4.7	12.8	25.2	42.2	55.9	64	67.9	66.9	56.2	43.4	24.6	10	39.5
		MIN	-4.9	3.3	15.7	29.6	42.2	51.1	54.7	52.8	42.6	31	15.8	0.9	27.9
146	WILDROSE 3 NW	MAX	15.8	23.3	35.4	52.7	66.1	74.8	80.2	80	67.5	54.2	33.6	20.9	50.4
		MEAN	6.1	13.8	25.5	40.7	53.5	62.4	67.1	65.8	54.3	41.9	24.6	11.6	38.9
		MIN	-3.6	4.2	15.6	28.6	40.8	50	54	51.5	41.1	29.6	15.6	2.3	27.5
147	WILLISTON SLOULIN AP	MAX	19.4	27.6	40.1	56	68.2	77.3	83.4	82.8	70	57	36.2	24	53.5
		MEAN	8	16.8	28.7	42.5	54.6	63.7	69.3	68.3	56.1	43.6	25.6	13	40.9
		MIN	-3.3	5.9	17.2	29.1	40.9	50.1	55.2	53.8	42.2	30.2	14.9	2.1	28.2
148	WILLISTON EXP FARM	MAX	20.9	29.5	42.1	57.9	70.4	78.8	84.9	84.8	72.8	59.6	37.7	25.4	55.4
		MEAN	11.3	19.7	31.1	44.9	57.1	65.7	71.1	70.2	58.8	46.7	28.4	16.1	43.4
		MIN	1.6	9.8	20.1	31.8	43.7	52.6	57.2	55.6	44.8	33.7	19.1	6.7	31.4
149	WILLOW CITY	MAX	12.7	20.6	32.7	52	67.2	75.1	79.8	79.3	67.5	54.3	33.2	18.3	49.4
		MEAN	2.1	9.8	22.3	39.9	54.1	62.7	67	65.3	53.8	41.2	23.2	8.2	37.5
		MIN	-8.6	-1.1	11.9	27.8	40.9	50.3	54.1	51.2	40.1	28.1	13.2	-2	25.5
150	WILTON	MAX	17.1	23.8	36.1	52.4	66.7	74.6	80.4	80.1	69	55.2	34.3	22	51
		MEAN	8.1	15.2	27.3	41.7	54.8	63.2	68.3	67.3	56.7	43.9	25.8	13.2	40.5
		MIN	-1	6.6	18.5	30.9	42.8	51.7	56.1	54.4	44.3	32.5	17.2	4.4	29.9

APPENDIX B. PRECIPITATION DATASET

NORTH DAKOTA
PRECIPITATION NORMALS (Totals in inches)

NO.	STATION NAME	JAN	FEB	MAR	APR	MAY	JUN	JUL	AUG	SEP	OCT	NOV	DEC	ANN
004	ALEXANDER 18 SW	0.36	0.29	0.57	1.03	2.02	2.56	1.87	1.2	1.54	0.79	0.53	0.47	13.2
005	ALMONT	0.37	0.33	0.63	1.49	2.22	3.41	2.48	2.28	1.24	1.17	0.62	0.4	16.6
007	AMIDON	0.37	0.35	0.57	1.15	2.29	3.06	2.24	1.42	1.37	1.17	0.53	0.33	14.9
008	ASHLEY	0.41	0.39	0.94	1.49	2.73	3.48	2.52	2.3	1.57	1.57	0.61	0.29	18.3
009	BEACH	0.43	0.47	0.62	1.56	2.41	2.63	1.93	1.41	1.53	1.2	0.7	0.37	15.3
010	BELCOURT KEYA RADIO	0.39	0.37	0.6	1.11	2.33	3.55	2.84	2.61	1.95	1.15	0.61	0.44	18
012	BEULAH 1 W	0.31	0.42	0.73	1.71	2.21	3.3	2.35	1.53	1.6	1.35	0.7	0.38	16.6
013	BISMARCK MUNIC	0.45	0.51	0.85	1.46	2.22	2.59	2.58	2.15	1.61	1.28	0.7	0.44	16.8
015	BOTTINEAU	0.49	0.46	0.79	1.22	2.16	3.29	3.04	2.62	1.94	1.27	0.66	0.51	18.5
016	BOWBELLS	0.46	0.44	0.69	1.25	2.21	2.94	2.96	1.94	2.02	1.11	0.46	0.29	16.8
017	BOWMAN	0.49	0.48	0.73	1.32	2.53	3.07	2.03	1.2	1.31	1.33	0.59	0.42	15.5
018	BREIEN	0.35	0.38	0.66	1.6	2.49	2.92	2.69	1.77	1.48	1.32	0.52	0.35	16.5
019	BUTTE 5 SE	0.46	0.44	0.72	1.42	2.37	2.89	2.65	1.67	1.56	1.39	0.7	0.38	16.7
021	CARRINGTON	0.68	0.56	0.91	1.36	2.11	3.32	3.15	2.19	1.6	1.45	0.89	0.51	18.7
022	CARRINGTON 4 N	0.52	0.4	0.75	1.44	2.49	3.79	3.11	2.48	1.84	1.82	0.84	0.41	19.9
023	CARSON	0.31	0.42	0.9	1.7	2.36	3.06	2.46	1.74	1.4	1.39	0.6	0.36	16.7
024	CASSELTON AGRONOMY	0.75	0.51	1.23	1.43	2.67	3.6	3.24	2.68	2.13	1.89	1.03	0.37	21.5
025	CAVALIER 7 NW	0.39	0.41	0.66	1.1	2.19	3.17	3.31	2.63	1.78	1.54	0.68	0.39	18.3
026	CENTER 4 SE	0.4	0.45	0.71	1.63	2.3	3	2.7	1.85	1.85	1.55	0.62	0.42	17.5
028	COLGATE	0.47	0.39	0.81	1.17	2.49	3.08	2.65	2.42	2.06	1.69	0.76	0.38	18.4
029	COOPERSTOWN	0.67	0.53	1.01	1.31	2.56	3.3	3.33	2.78	1.96	1.65	0.9	0.5	20.5
031	CROSBY	0.48	0.33	0.59	1.02	2.01	2.69	2.75	1.54	1.62	0.93	0.53	0.45	14.9
032	DEVILS LAKE KDLR	0.58	0.51	0.8	0.9	2.14	3.83	3.29	2.21	1.8	1.47	0.83	0.57	18.9

033	DICKINSON AP	0.37	0.43	0.69	1.76	2.28	3.31	2.11	1.51	1.62	1.34	0.59	0.34	16.4
034	DICKINSON EXP STN	0.35	0.37	0.67	1.63	2.24	3.57	2.2	1.65	1.62	1.31	0.63	0.37	16.6
035	DICKINSON RANCH HQ	0.37	0.35	0.61	1.5	2.03	3.18	2.3	1.79	1.4	1.06	0.58	0.33	15.5
036	DRAKE 9 NE	0.36	0.39	0.6	1.25	2.26	3.04	2.75	1.97	1.48	1.24	0.68	0.34	16.4
038	DUNN CENTER 2 SW	0.4	0.41	0.68	1.52	2.3	3.26	2.13	1.72	1.57	1.3	0.68	0.39	16.4
039	EDGELEY 3 WNW	0.61	0.41	1.16	1.63	2.9	3.26	2.18	2.87	1.8	1.45	0.67	0.38	19.3
040	EDMORE 1 NW	0.5	0.4	0.65	1.02	2.15	3.21	3.32	2.59	1.71	1.39	0.74	0.48	18.2
041	EDMUNDS ARROWWOOD	0.57	0.58	0.82	1.29	2.2	3.32	3.13	2.51	1.98	1.39	0.63	0.42	18.8
043	ELLENDALE	0.49	0.5	1.11	1.95	2.99	3.61	2.94	2.53	2.2	1.95	0.83	0.33	21.4
044	ENDERLIN 2 W	0.58	0.38	0.85	1.42	2.62	3.4	3.42	2.2	2.02	1.77	0.56	0.38	19.6
046	FAIRFIELD	0.31	0.33	0.56	1.41	2.04	2.95	2.1	1.62	1.5	1.16	0.5	0.31	14.8
047	FARGO HECTOR AP	0.76	0.59	1.17	1.37	2.61	3.51	2.88	2.52	2.18	1.97	1.06	0.57	21.2
048	FESSENDEN	0.53	0.43	0.67	1.12	2.13	3.47	2.77	1.93	1.57	1.32	0.67	0.46	17.1
050	FORMAN 5 SSE	0.65	0.53	1.24	1.68	2.6	3.54	3.02	2.25	1.93	1.68	1.02	0.44	20.6
051	FORTUNA 1 W	0.34	0.36	0.76	0.99	1.98	2.87	2.71	1.62	1.33	0.85	0.33	0.39	14.5
052	FORT YATES 4 SW	0.24	0.3	0.66	1.34	2.16	2.64	2.06	1.62	1.28	1.26	0.35	0.23	14.1
053	FOXHOLM 7 N	0.51	0.44	0.8	1.25	1.96	2.97	2.6	1.84	1.67	1.39	0.68	0.46	16.6
054	FULLERTON 1 ESE	0.75	0.66	1.44	1.91	2.84	3.16	2.88	2.22	2.02	1.8	1.03	0.41	21.1
055	GACKLE	0.44	0.38	0.94	1.49	2.61	3.37	3.06	2.03	1.89	1.48	0.77	0.35	18.8
056	GARRISON 1 NNW	0.39	0.36	0.63	1.27	2.1	3.12	2.62	1.91	1.44	1.22	0.57	0.39	16
058	GRAFTON	0.52	0.5	0.85	1.13	2.31	3.3	2.77	2.39	1.76	1.46	0.9	0.43	18.3
059	GRAND FORKS INTL AP	0.68	0.58	0.89	1.23	2.21	3.03	3.06	2.72	1.96	1.7	0.99	0.55	19.6
060	GRAND FORKS UNIV NW	0.78	0.62	0.89	1.17	2.11	2.98	2.89	2.92	1.95	1.59	0.86	0.59	19.4
061	GRANVILLE	0.37	0.49	0.83	1.39	2.37	3.47	2.83	1.91	1.67	1.32	0.64	0.41	17.7
062	GRASSY BUTTE 2 ENE	0.32	0.37	0.67	1.34	2.38	2.99	1.97	1.49	1.47	1.22	0.68	0.37	15.3

063	GRENORA	0.32	0.28	0.55	1.12	2.02	2.4	2.29	1.35	1.5	0.82	0.45	0.46	13.6
065	HANKINSON	0.81	0.74	1.24	1.76	2.76	3.47	3.35	2.7	2.16	1.8	1.08	0.44	22.3
066	HANNAH	0.34	0.24	0.38	0.99	2.04	3.05	2.75	3.12	2.24	1.31	0.57	0.34	17.4
067	HANSBORO 4 NNE	0.64	0.63	0.85	1.12	2.39	3.19	2.87	2.59	1.62	1.22	0.81	0.57	18.5
068	HARVEY	0.42	0.28	0.62	0.78	1.97	2.8	2.29	2.29	1.45	1.48	0.45	0.28	15.1
069	HEART BUTTE DAM	0.51	0.32	0.87	1.7	2.34	2.91	2.31	1.45	1.16	0.99	0.77	0.42	15.8
070	HEBRON	0.26	0.31	0.56	1.66	2.53	3.23	2.7	1.64	1.69	1.28	0.58	0.29	16.7
071	HETTINGER	0.3	0.32	0.6	1.59	2.54	2.95	2.16	1.46	1.4	1.35	0.53	0.31	15.5
072	HILLSBORO 3 N	0.5	0.55	0.93	1.56	2.35	3.46	3.23	2.78	2.05	1.92	0.89	0.48	20.7
073	HURDSFIELD 8 SW	0.49	0.45	0.64	1.26	2.22	3.35	2.57	1.96	1.45	1.35	0.69	0.39	16.8
074	JAMESTOWN MUNICIPAL	0.62	0.52	0.89	1.36	2.21	3.05	3.22	2.33	1.74	1.4	0.71	0.44	18.5
075	JAMESTOWN ST HOSPIT	0.5	0.35	0.73	1.27	2.27	3.24	3.28	2.43	2.01	1.49	0.63	0.33	18.5
076	KEENE 3 S	0.39	0.37	0.59	1.26	2.32	3.19	2.47	1.51	1.68	1.16	0.66	0.4	16
077	KENMARE 1 WSW	0.83	0.63	0.9	1.26	2.07	2.66	2.67	1.8	1.92	1.19	0.69	0.53	17.2
080	LA MOURE	0.78	0.64	1.36	1.85	2.67	3.69	3.42	2.3	1.9	1.78	0.91	0.45	21.8
081	LANGDON EXP FARM	0.42	0.39	0.61	1	2.36	3.33	3.18	2.73	1.66	1.38	0.66	0.39	18.1
082	LARIMORE	0.53	0.53	0.97	1.25	2.24	3.57	3.45	2.91	2.05	1.55	0.91	0.45	20.4
083	LEEDS	0.55	0.51	0.83	1.28	2.08	2.98	3.17	2.07	1.61	1.53	0.84	0.48	17.9
084	LINTON	0.34	0.37	0.77	1.36	2.32	2.95	2.57	1.8	1.3	1.44	0.51	0.39	16.1
085	LISBON	0.63	0.48	1.09	1.47	2.59	3.45	2.87	2.27	2.2	1.82	0.86	0.45	20.2
088	MANDAN EXPERIMENT S	0.38	0.37	0.58	1.52	2.41	2.91	2.9	2.02	1.56	1.41	0.62	0.36	17
090	MAX	0.55	0.43	0.74	1.48	2.16	3.21	2.69	1.84	1.72	1.41	0.63	0.44	17.3
091	MAYVILLE	0.72	0.62	1.08	1.38	2.29	3.5	2.73	2.85	1.98	1.77	0.86	0.6	20.4
092	MC CLUSKY	0.58	0.49	0.71	1.49	2.13	3.41	2.61	2.06	1.61	1.39	0.71	0.49	17.7
093	MC HENRY 3 W	0.6	0.48	0.87	1.32	2.28	3.63	3.09	2.76	1.99	1.47	1.03	0.57	20.1

094	MC LEOD 3 E	0.65	0.51	1.01	1.3	2.63	3.39	3.54	2.32	2.05	1.78	0.94	0.42	20.5
095	MC VILLE	0.58	0.36	0.88	1.09	2.26	3.39	3.23	2.54	2.16	1.38	0.83	0.46	19.2
097	MEDORA	0.35	0.36	0.64	1.35	2.26	2.89	2.16	1.38	1.45	1.12	0.58	0.37	14.9
098	MINOT AP	0.65	0.53	1.05	1.55	2.31	3.15	2.7	1.95	1.74	1.32	0.86	0.63	18.4
099	MINOT EXPERIMENT ST	0.77	0.6	1.03	1.56	2.28	3.01	2.52	2.01	1.78	1.4	1.05	0.64	18.7
100	MOFFIT 3 SE	0.29	0.33	0.66	1.31	2.16	3	2.84	2.08	1.73	1.36	0.5	0.27	16.5
101	MOHALL	0.52	0.42	0.73	1.24	2.17	2.98	2.86	2.17	1.89	1.46	0.63	0.39	17.5
103	MOTT	0.41	0.5	0.8	1.83	2.59	3.17	2.13	1.69	1.26	1.24	0.55	0.38	16.6
104	NAPOLEON	0.58	0.51	0.98	1.64	2.48	3.2	2.88	2.19	1.77	1.55	0.8	0.44	19
105	NEW ENGLAND	0.38	0.39	0.69	1.62	2.46	3.38	1.93	1.73	1.44	1.37	0.47	0.38	16.2
106	NEW SALEM 5 NW	0.47	0.49	0.81	1.88	2.42	3.17	2.76	2.11	1.53	1.38	0.76	0.5	18.3
107	OAKES 2 S	0.6	0.44	1.04	1.71	2.45	3.25	2.76	2.04	2.26	1.77	0.82	0.41	19.6
108	PARK RIVER	0.66	0.56	0.92	1.25	2.41	3.42	3.19	2.61	1.8	1.64	0.88	0.55	19.9
109	PEMBINA	0.44	0.4	0.72	0.99	2.09	3.41	2.95	2.68	2.12	1.48	0.85	0.45	18.6
110	PETERSBURG 2 N	0.66	0.43	0.94	1.17	2.27	3.62	3.25	2.71	2.06	1.54	0.9	0.51	20.1
111	PETTIBONE	0.53	0.38	0.69	1.34	2.14	3.32	2.81	1.86	1.8	1.44	0.71	0.43	17.5
112	POWERS LAKE 1 N	0.38	0.37	0.72	1.27	2.12	2.74	2.9	1.94	1.71	1.07	0.55	0.33	16.1
113	PRETTY ROCK	0.33	0.41	0.86	1.89	2.64	3.02	2.34	1.76	1.4	1.34	0.62	0.31	16.9
116	RICHARDTON ABBEY	0.45	0.48	0.86	1.75	2.49	3.39	2.27	1.88	1.6	1.41	0.75	0.45	17.8
118	ROLLA 3 NW	0.51	0.52	0.76	1.13	2.3	3.41	2.87	2.55	1.95	1.25	0.8	0.53	18.6
119	RUGBY	0.51	0.45	0.8	1.28	2.25	3.05	3.21	2.28	1.92	1.32	0.7	0.5	18.3
120	SAN HAVEN	0.43	0.58	0.61	0.93	1.9	2.69	2.68	2.59	1.8	1.26	0.43	0.4	16.3
121	SHARON	0.68	0.54	1.12	1.33	2.65	3.55	3.45	2.67	2.05	1.67	0.97	0.55	21.2
124	STANLEY 3 NNW	0.57	0.49	0.87	1.59	2.58	3.88	2.94	2.13	2.15	1.23	0.76	0.54	19.7
125	STEELE 3 N	0.48	0.44	0.98	1.51	2.53	3.24	2.95	2.01	1.9	1.55	0.74	0.44	18.8

126	STREETER 7 NW	0.31	0.34	0.68	1.26	1.96	3.04	3.09	2.38	1.97	1.1	0.69	0.27	17.1
129	TIOGA 1 E	0.48	0.36	0.58	1.17	2	2.6	2.2	1.8	1.58	0.94	0.59	0.4	14.7
130	TOWNER 2 NE	0.55	0.55	0.72	1.21	1.93	2.67	2.69	2.06	1.83	1.3	0.64	0.53	16.7
131	TROTTERS 3 SSE	0.35	0.39	0.58	1.23	2.09	2.9	1.89	1.5	1.61	1.16	0.61	0.4	14.7
132	TURTLE LAKE	0.63	0.49	0.85	1.44	2.19	3.32	2.67	1.96	1.5	1.32	0.73	0.52	17.6
133	TUTTLE	0.44	0.39	0.62	1.38	2.29	3.14	2.81	1.77	1.76	1.28	0.59	0.36	16.8
134	UNDERWOOD	0.54	0.46	0.78	1.64	2.25	3.52	2.48	1.77	1.59	1.44	0.77	0.53	17.8
135	UPHAM 3 N	0.57	0.47	0.76	1.33	2.07	3.32	2.71	2	1.8	1.28	0.85	0.56	17.7
136	VALLEY CITY 3 NNW	0.54	0.46	0.8	1.22	2.6	3.27	2.75	2.43	2.1	1.53	0.8	0.39	18.9
137	VELVA 3 NE	0.68	0.5	0.78	1.34	2.3	3.22	2.8	1.83	1.62	1.61	0.92	0.5	18.1
139	WAHPETON 3 N	0.62	0.39	1.02	1.76	2.96	3.33	3.53	2.69	2.43	2.03	0.74	0.37	21.9
141	WASHBURN	0.45	0.48	0.75	1.64	2.26	3.28	2.75	1.99	1.67	1.44	0.68	0.41	17.8
143	WATFORD CITY	0.45	0.39	0.56	1.04	2.13	3.05	2.11	1.55	1.3	0.77	0.65	0.41	14.4
144	WATFORD CITY 14 S	0.36	0.37	0.62	1.3	2.15	2.89	2.17	1.7	1.66	1.35	0.55	0.37	15.5
145	WESTHOPE	0.47	0.46	0.71	1.16	2.06	3.03	2.9	2.04	1.87	1.21	0.62	0.49	17
146	WILDROSE 3 NW	0.42	0.35	0.6	1	2.04	2.56	2.83	1.56	1.48	0.83	0.53	0.45	14.7
147	WILLISTON SLOULIN A	0.54	0.39	0.74	1.05	1.88	2.36	2.28	1.48	1.35	0.87	0.65	0.57	14.2
148	WILLISTON EXP FARM	0.48	0.34	0.62	1.13	2.09	2.72	2.45	1.63	1.56	0.94	0.58	0.45	15
149	WILLOW CITY	0.52	0.42	0.78	1.18	1.99	3.1	2.85	2.34	1.72	1.2	0.63	0.44	17.2
150	WILTON	0.47	0.36	0.58	1.44	2.32	3.65	3.06	2.15	1.72	1.43	0.67	0.43	18.3

APPENDIX C. UNIVARIATE STOCHASTIC CHARACTERIZATION DIAGRAMS

Linear Kriging Temperature dataset

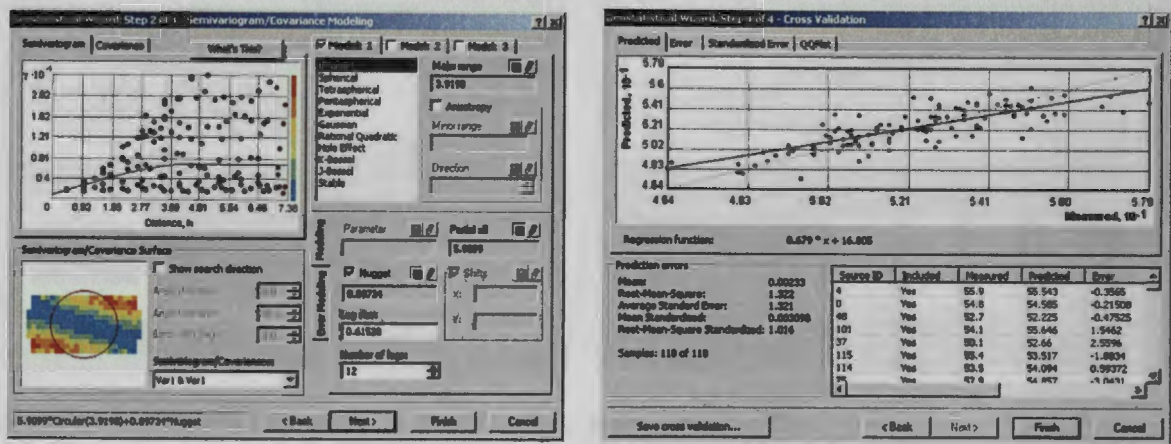

Semivariogram and cross-validation results – ordinary kriging

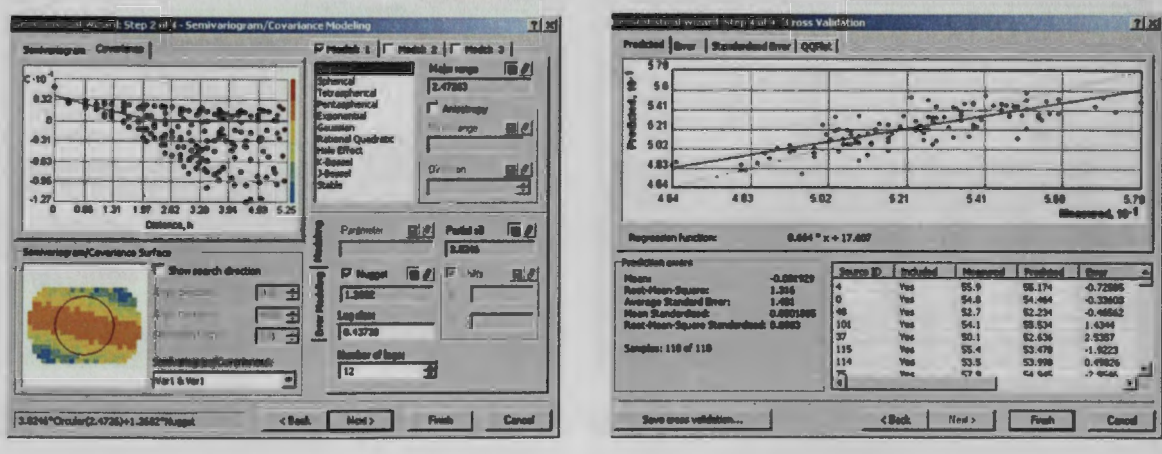

Semivariogram and cross-validation results – simple kriging

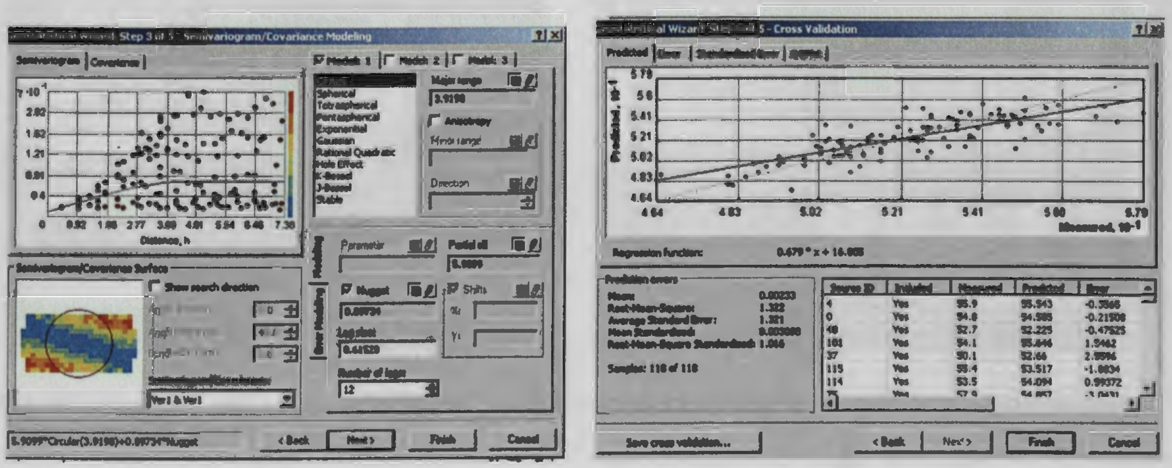

Semivariogram and cross-validation results – universal kriging

Figure C.1. Linear kriging results for temperature dataset using circular model.

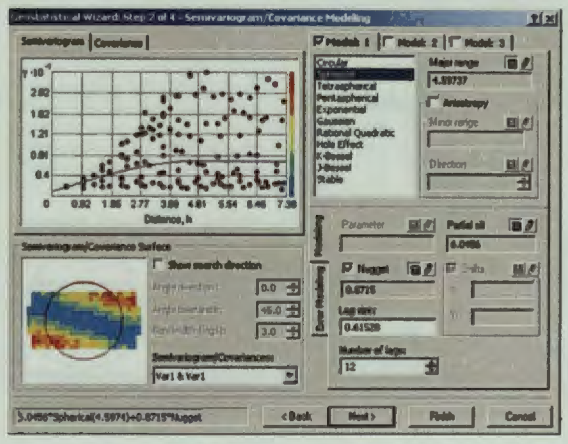

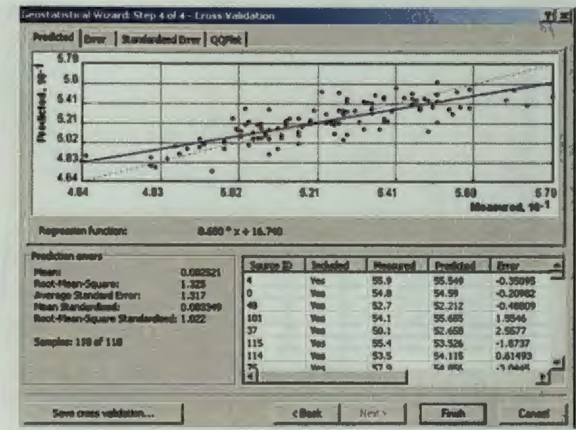

Semivariogram and cross-validation results – ordinary kriging

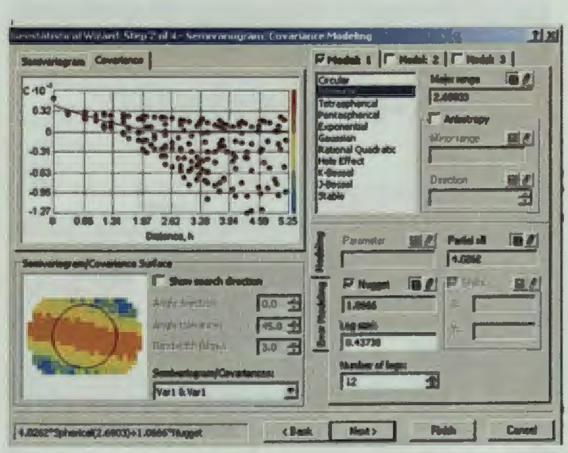

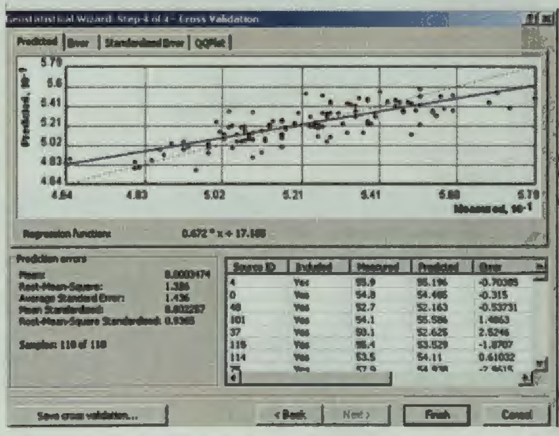

Semivariogram and cross-validation results – simple kriging

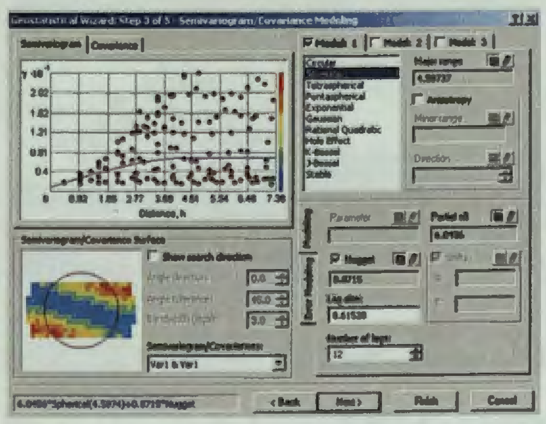

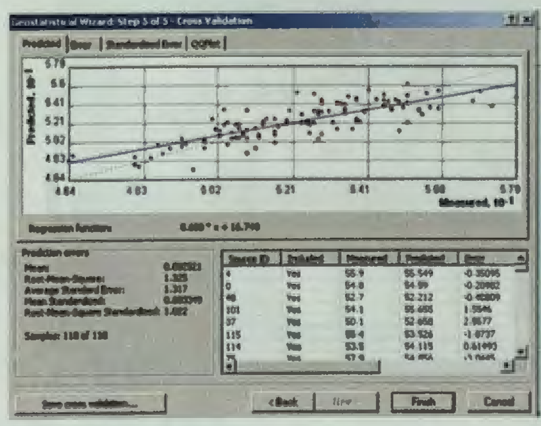

Semivariogram and cross-validation results – universal kriging

Figure C.2. Linear kriging results for temperature dataset using spherical model.

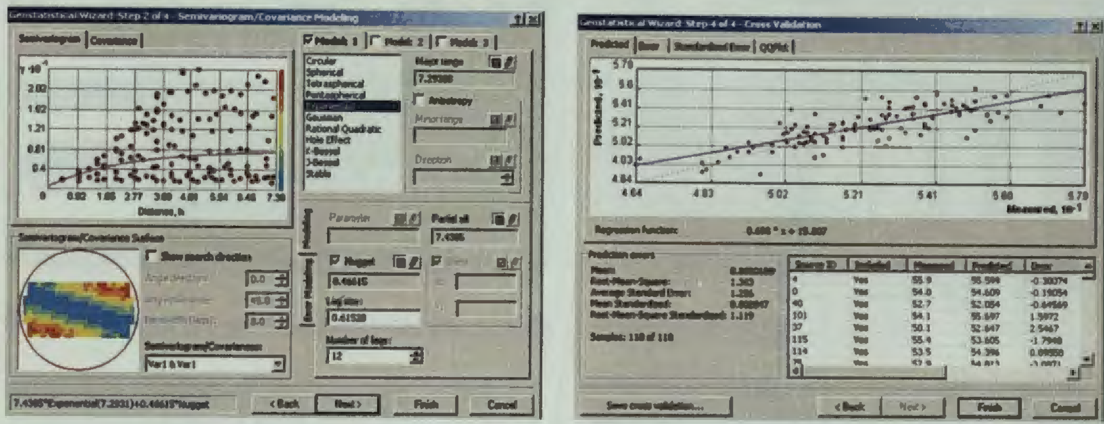

Semivariogram and cross-validation results – ordinary kriging

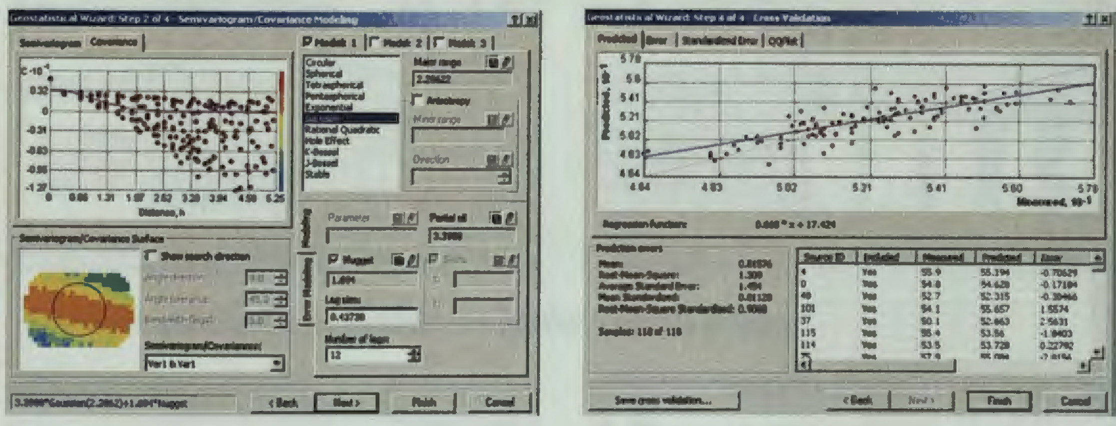

Semivariogram and cross-validation results – simple kriging

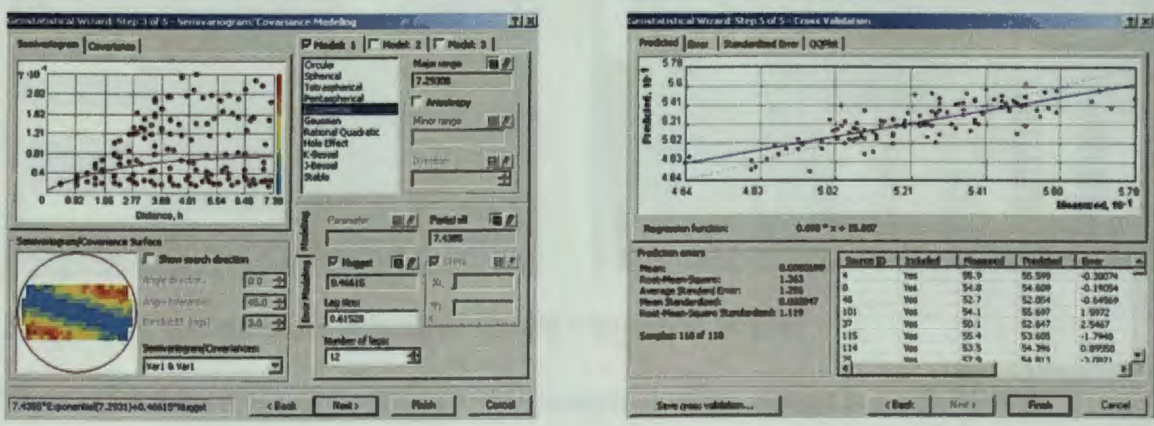

Semivariogram and cross-validation results – universal kriging

Figure C.3. Linear kriging results for temperature dataset using exponential model.

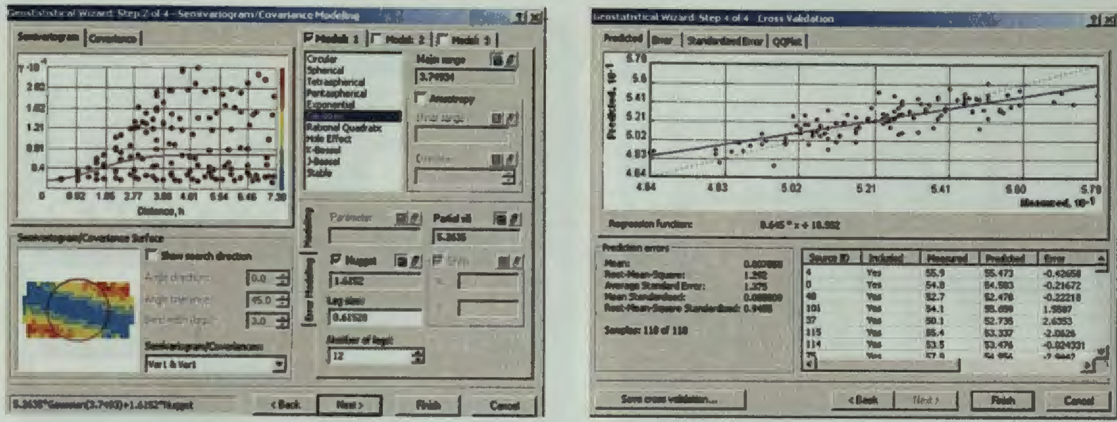

Semivariogram and cross-validation results – ordinary kriging

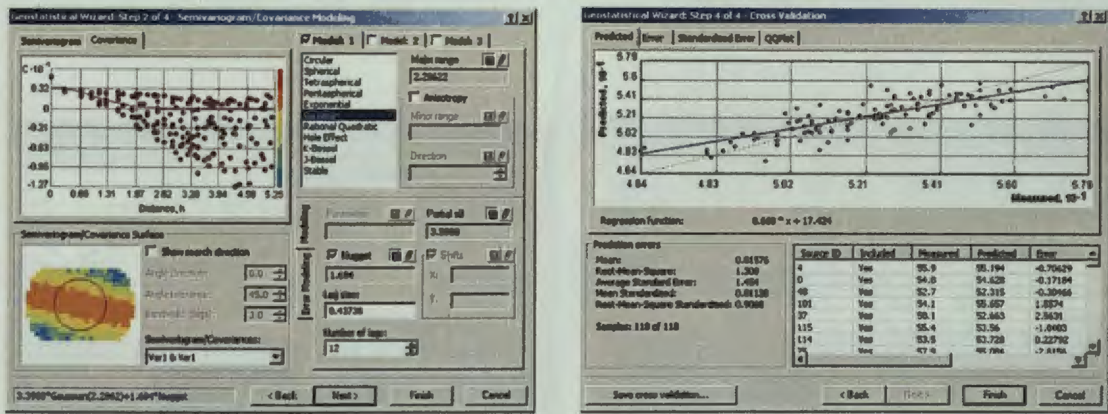

Semivariogram and cross-validation results – simple kriging

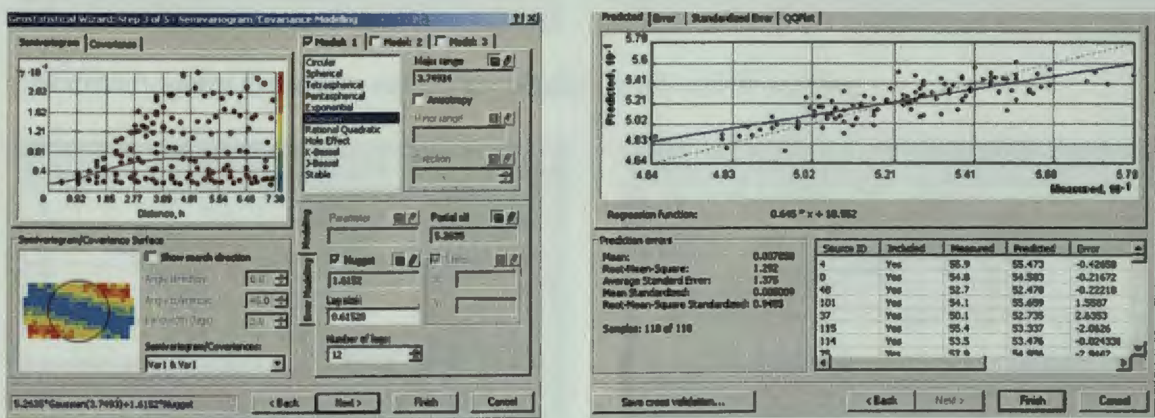

Semivariogram and cross-validation results – universal kriging

Figure C.4. Linear kriging results for temperature datasets using Gaussian Model.

Non-Linear Kriging Temperature Dataset

Results using non-linear kriging methods for temperature dataset are presented.

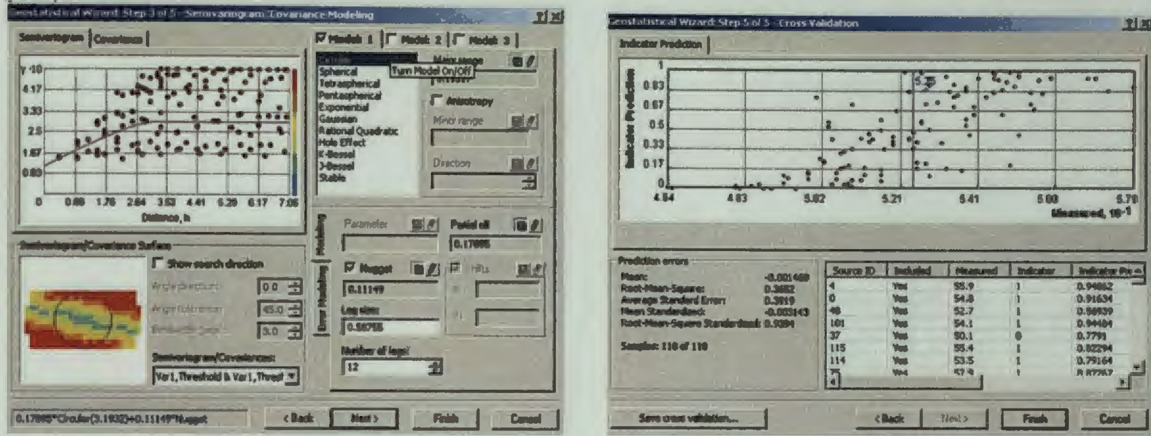

Semivariogram and cross-validation results – indicator kriging

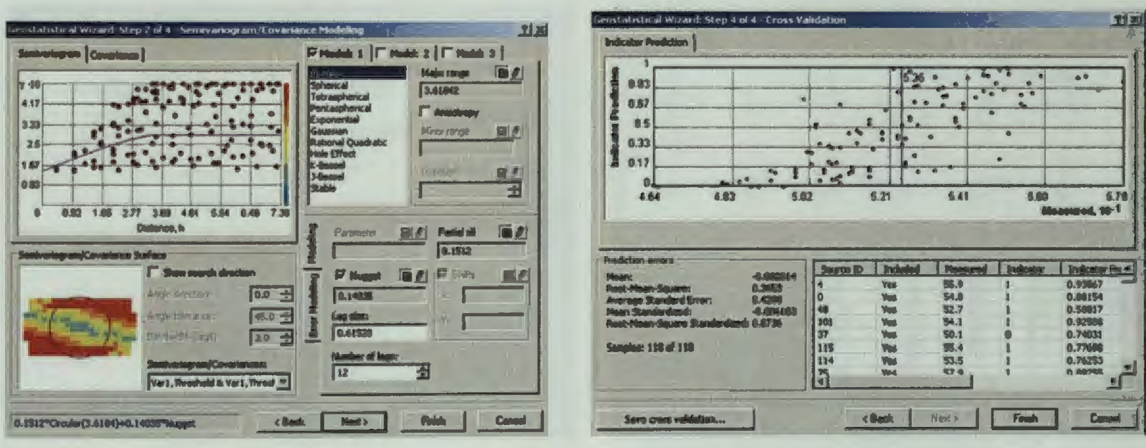

Semivariogram and cross-validation results – probability kriging

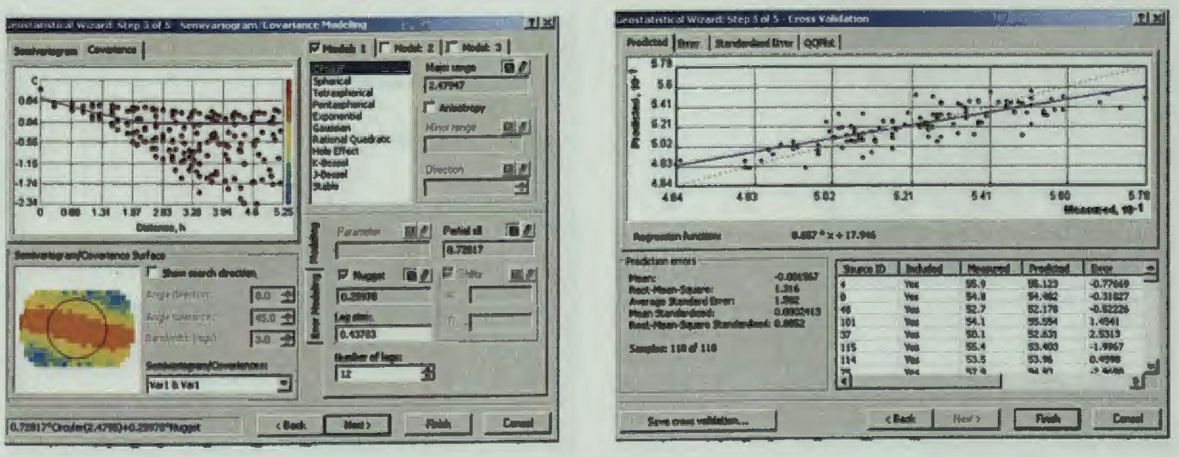

Semivariogram and cross-validation results – disjunctive kriging

Figure C.5. Non-linear kriging results for temperature datasets using Circular Model.

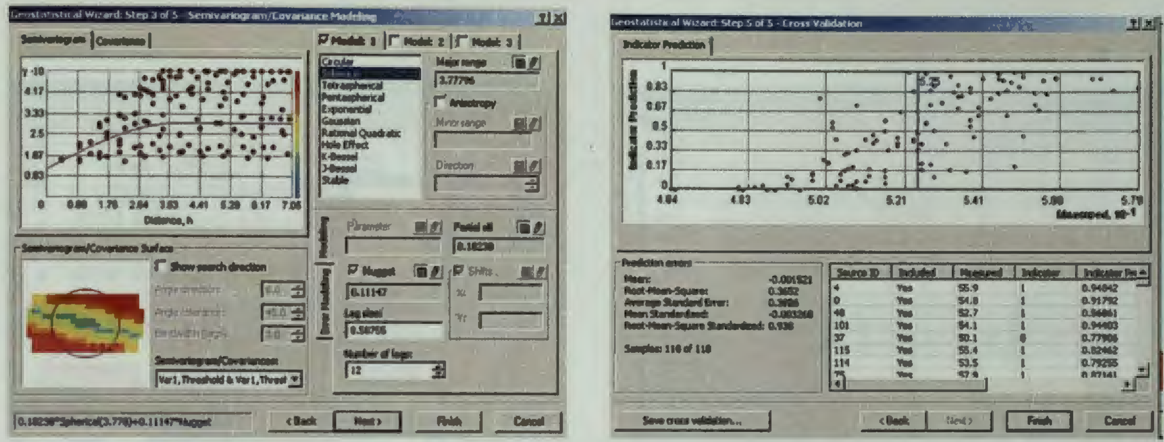

Semivariogram and cross-validation results – indicator kriging

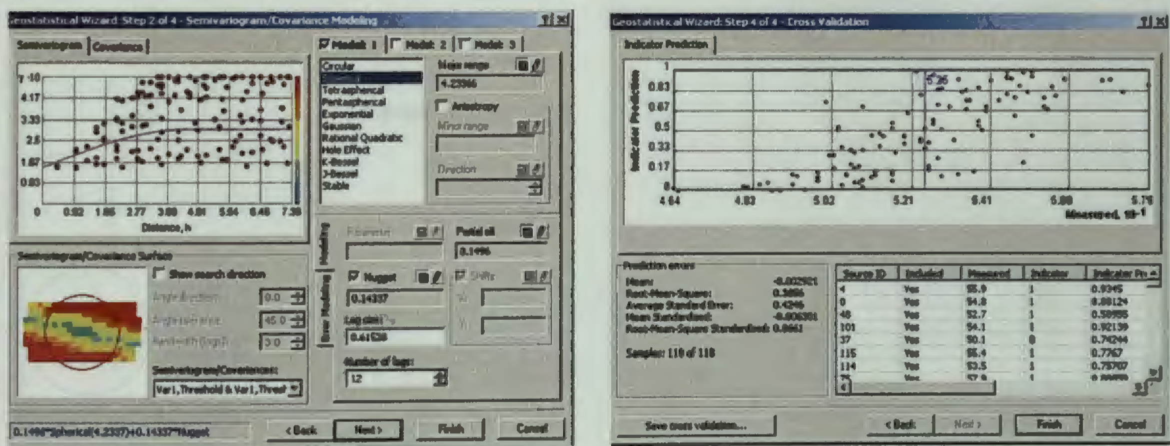

Semivariogram and cross-validation results probability kriging

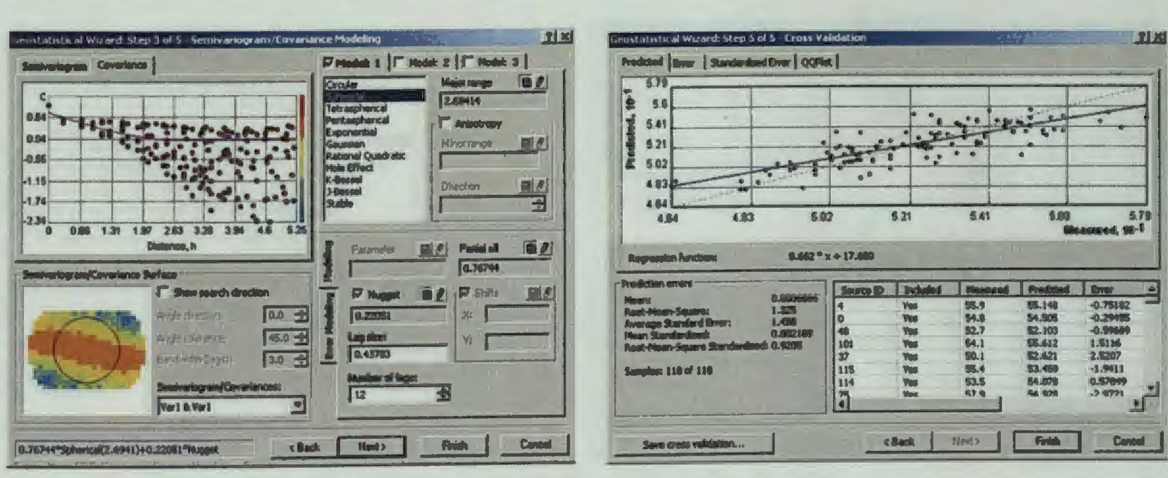

Semivariogram and cross-validation results disjunctive kriging

Figure C.6. Non-linear kriging results for temperature datasets using spherical model.

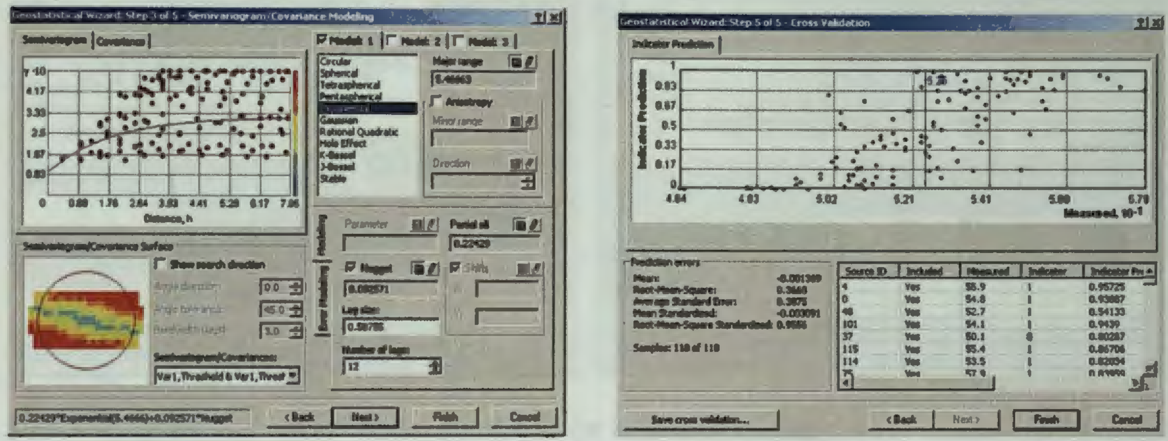

Semivariogram and cross-validation results for indicator kriging

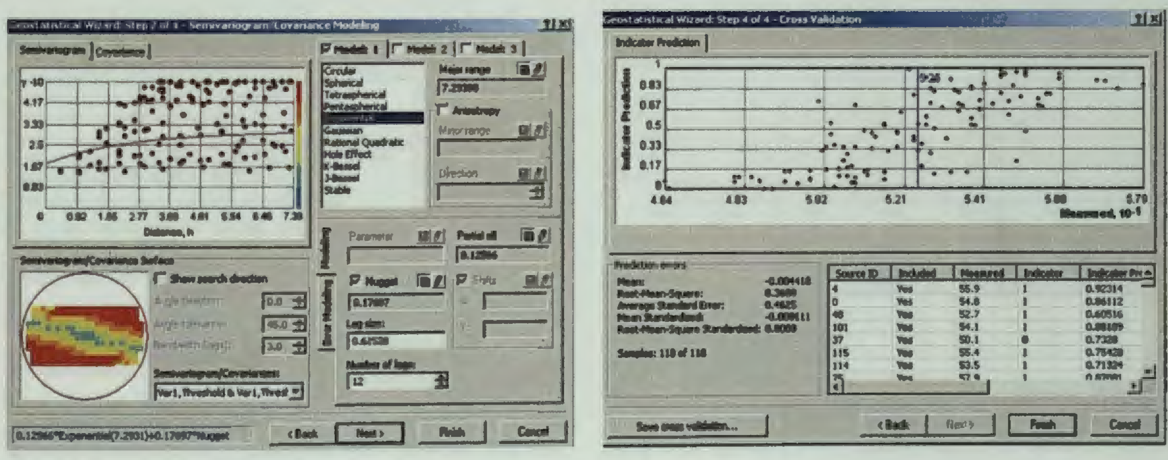

Semivariogram and cross-validation results for probability kriging

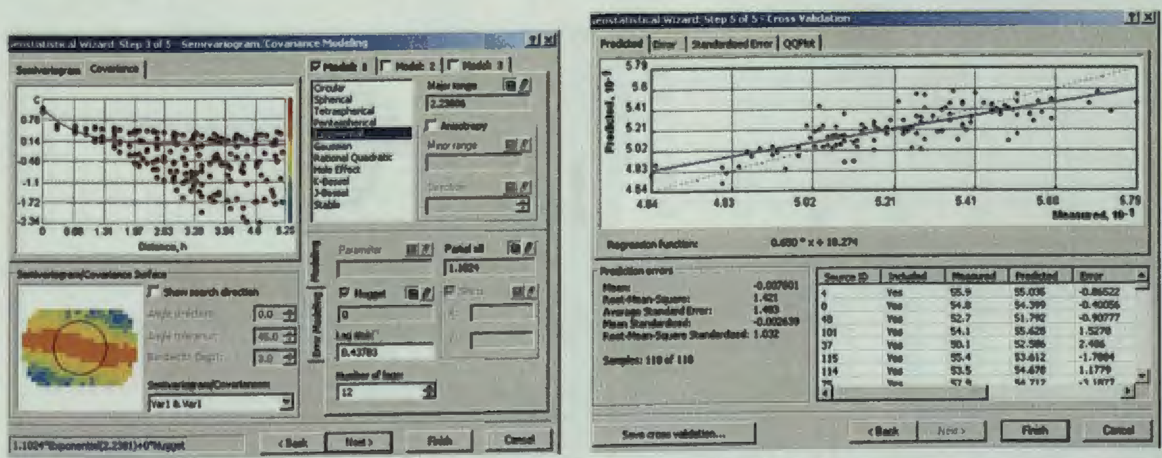

Semivariogram and cross-validation results for disjunctive kriging

Figure C.7. Non-linear kriging results for temperature datasets using exponential model.

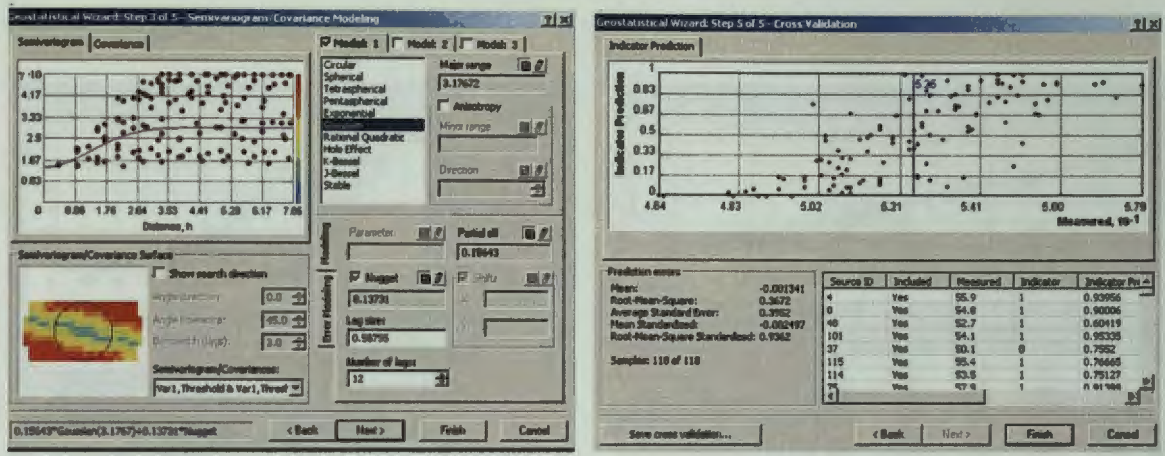

Semivariogram and cross-validation results for indicator kriging

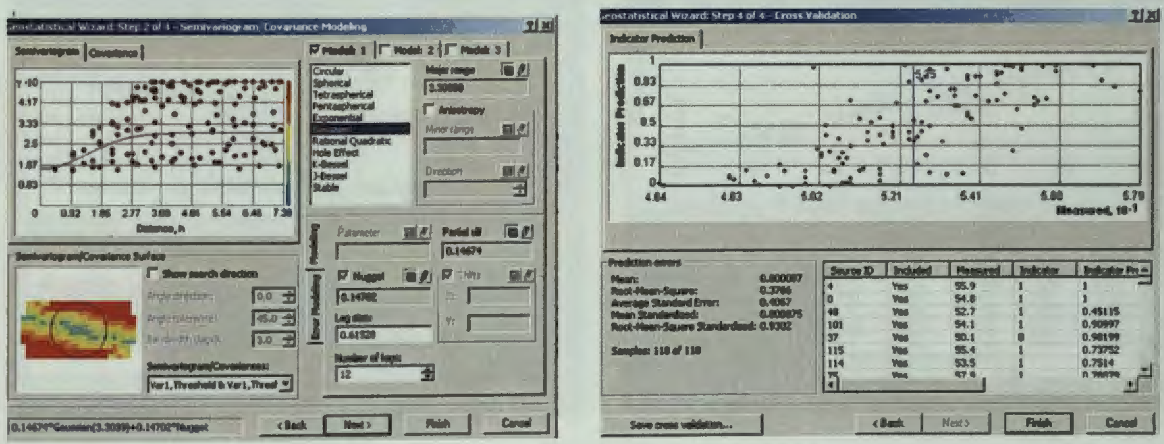

Semivariogram and cross-validation results for probability kriging

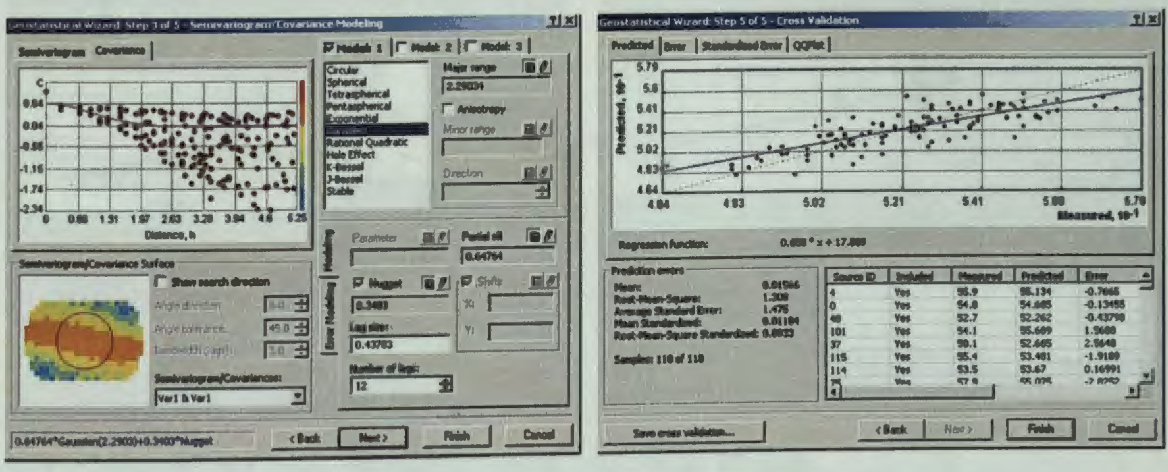

Semivariogram and cross-validation results disjunctive kriging

Figure C.8. Non-linear kriging results for temperature datasets using Gaussian model.

Linear Kriging Precipitation data

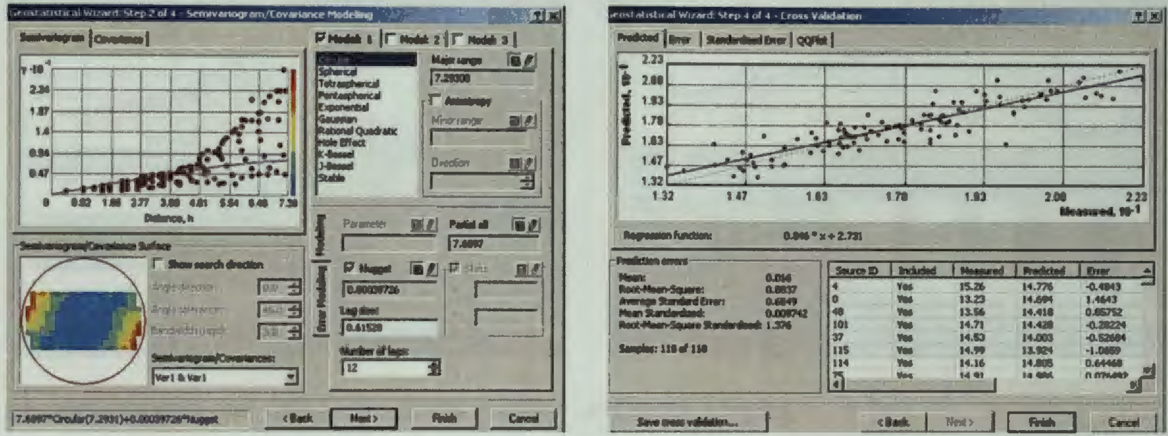

Semivariogram and cross-validation results – ordinary kriging

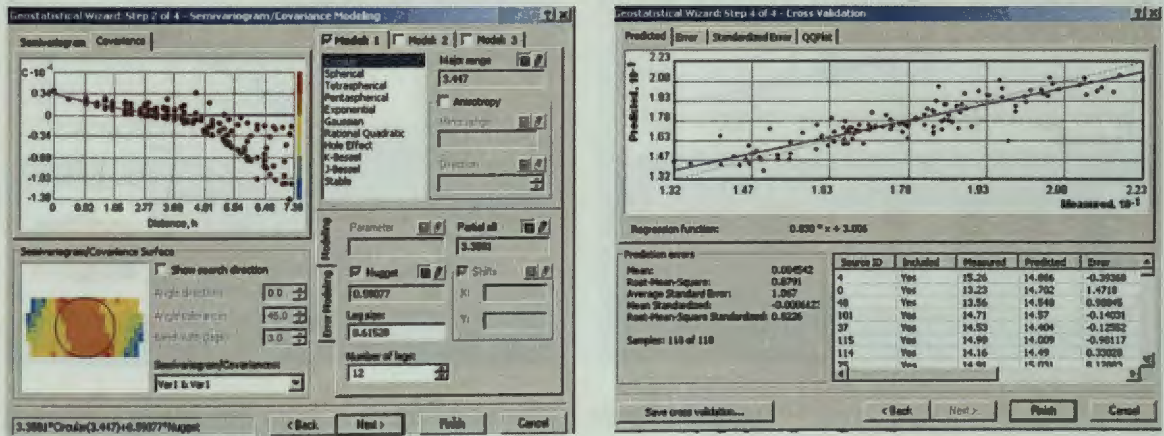

Semivariogram and cross-validation results – simple kriging

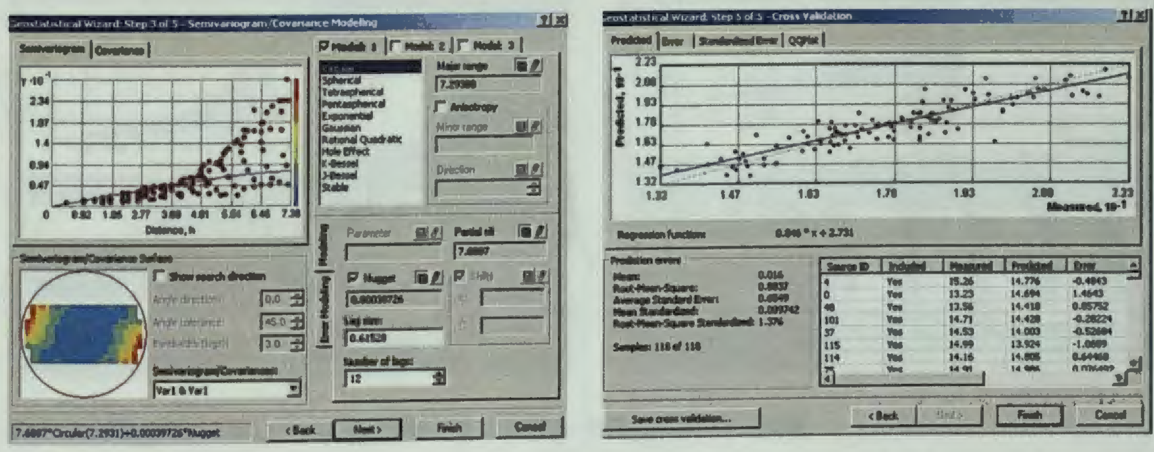

Semivariogram and cross-validation results – universal kriging

Figure C.9. Linear kriging results for temperature datasets using circular model.

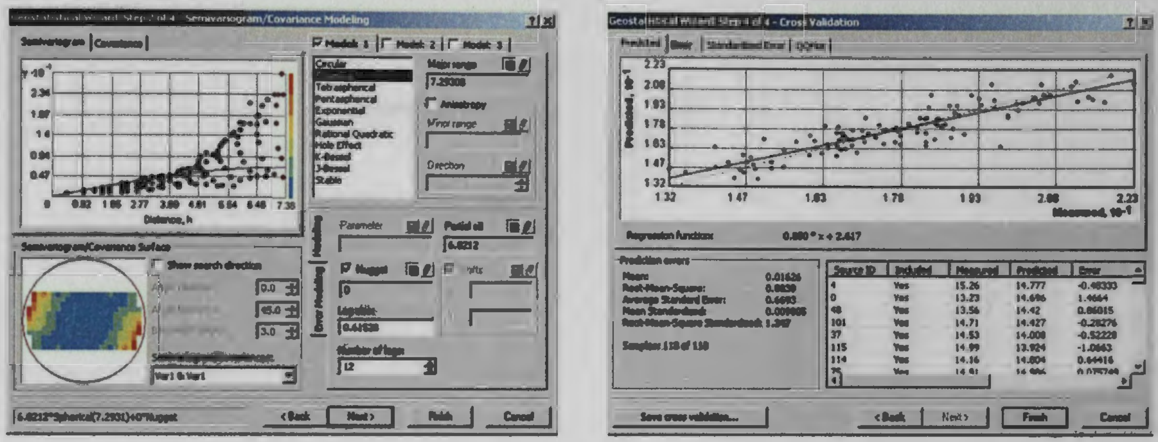

Semivariogram and cross-validation results – ordinary kriging

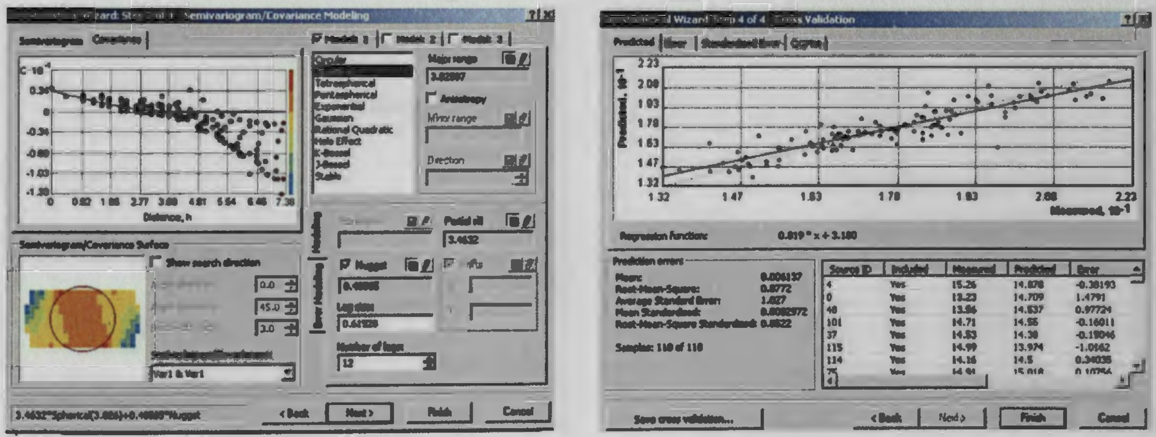

Semivariogram and cross-validation results – simple kriging

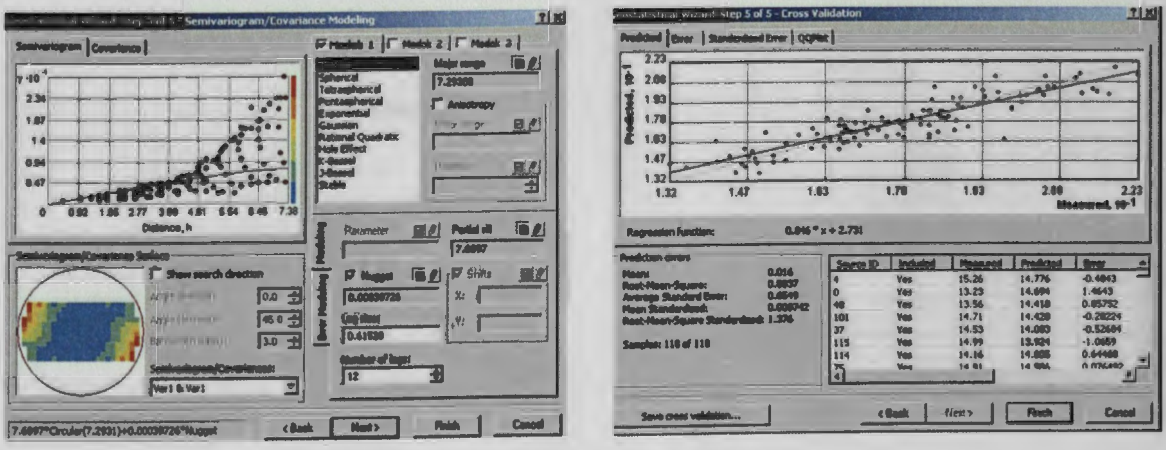

Semivariogram and cross-validation results – universal kriging

Figure C.10. Linear kriging results for temperature datasets using spherical model.

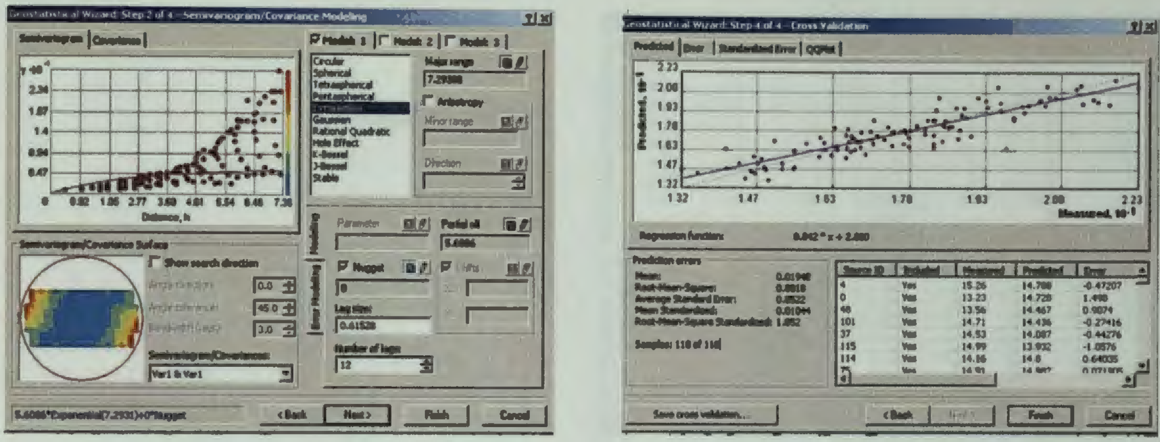

Semivariogram and cross-validation results – ordinary kriging

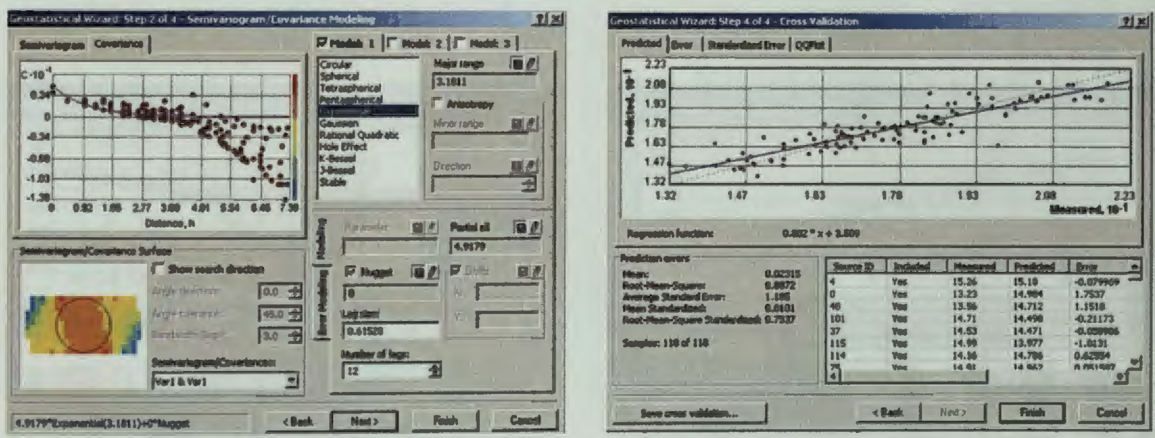

Semivariogram and cross-validation results – simple kriging

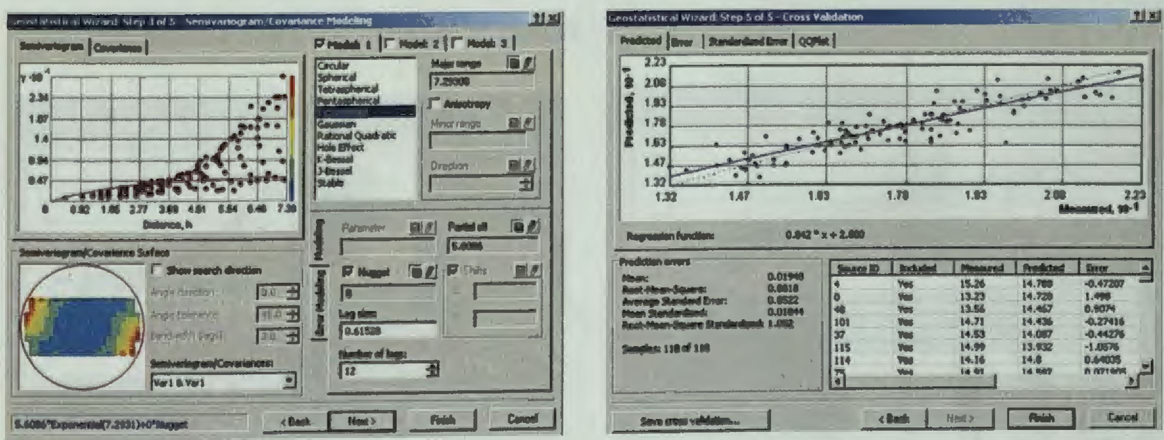

Semivariogram and cross-validation results – universal kriging

Figure C.11. Linear kriging results for temperature datasets using exponential model.

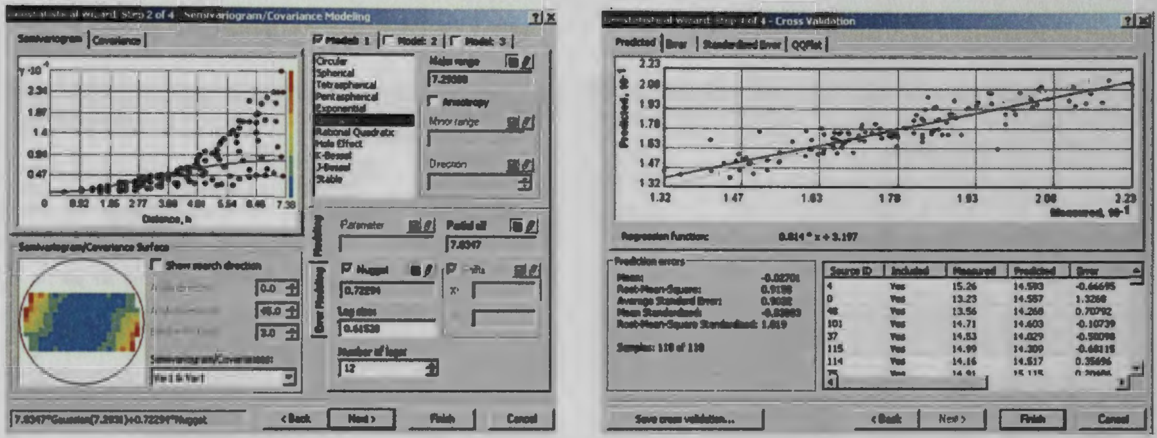

Semivariogram and cross-validation results – ordinary kriging

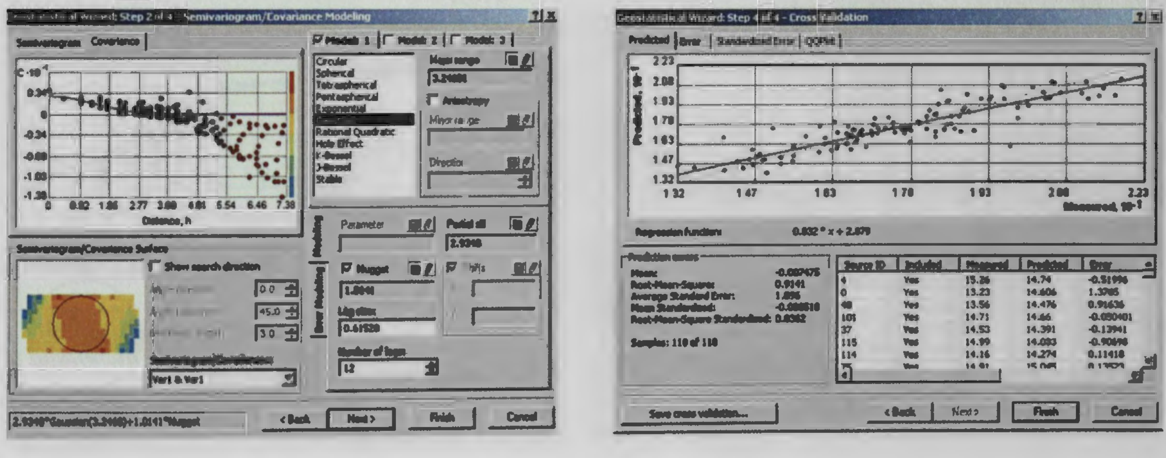

Semivariogram and cross-validation results – simple kriging

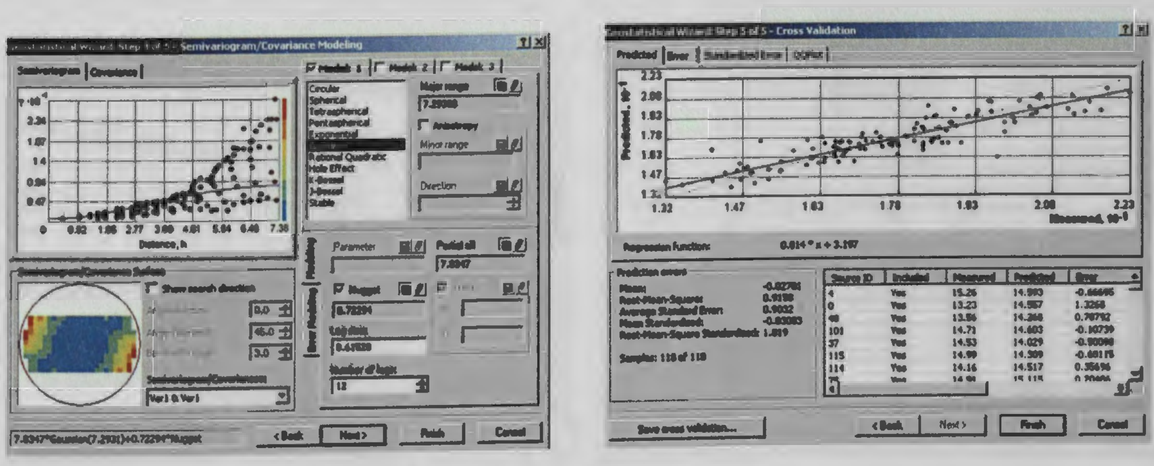

Semivariogram and cross-validation results – universal kriging

Figure C.12. Linear kriging results for temperature datasets using Gaussian model.

Non-Linear Kriging Precipitation Data

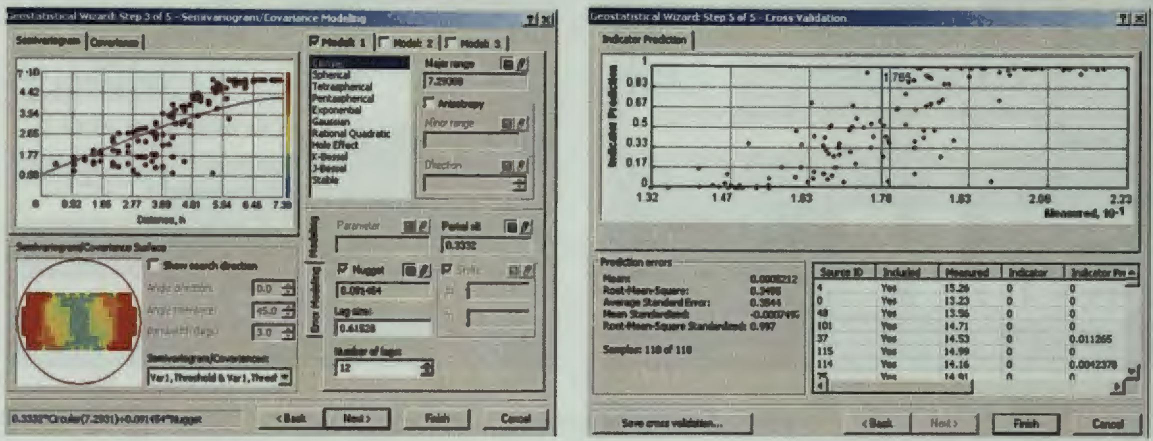

Semivariogram and cross-validation results – indicator kriging

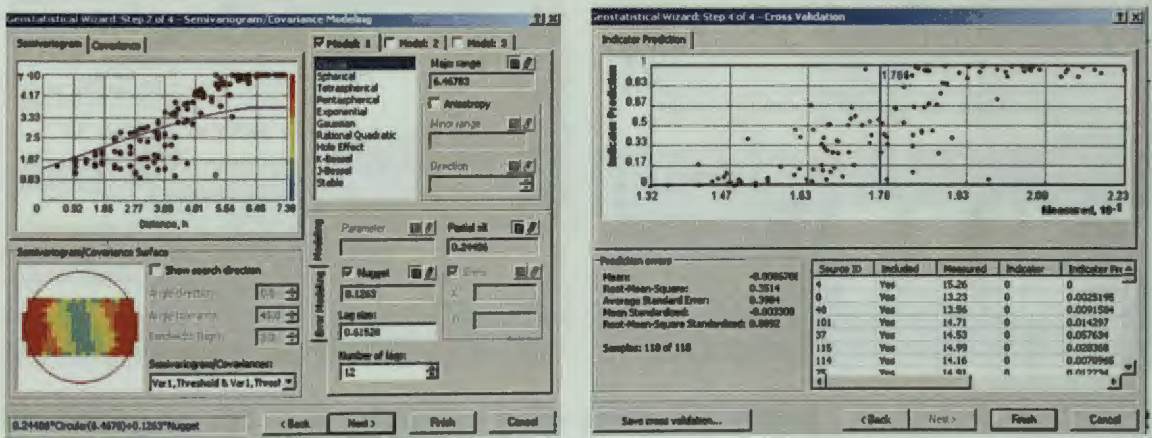

Semivariogram and cross-validation results – probability kriging

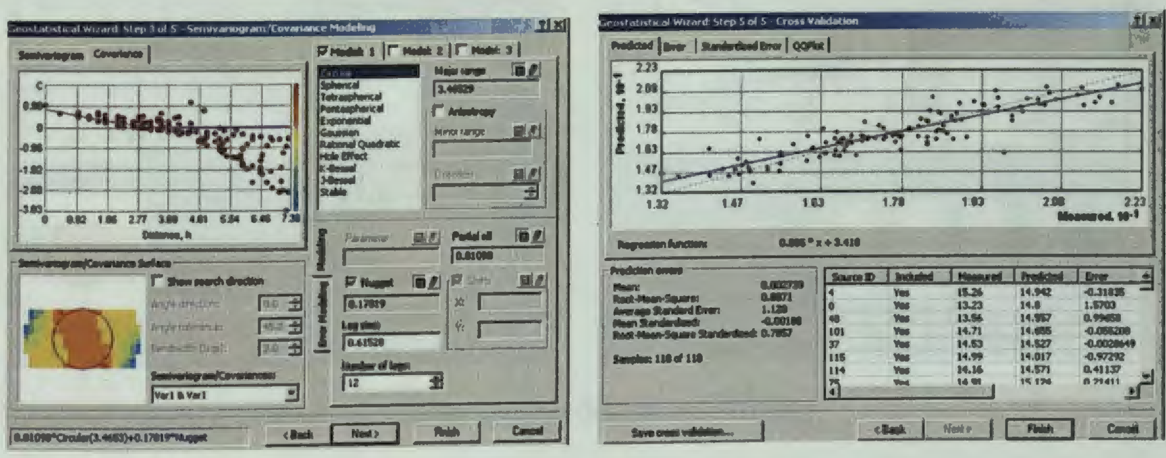

Semivariogram and cross-validation results – disjunctive kriging

Figure C.13. Non-linear kriging results for precipitation datasets using circular model.

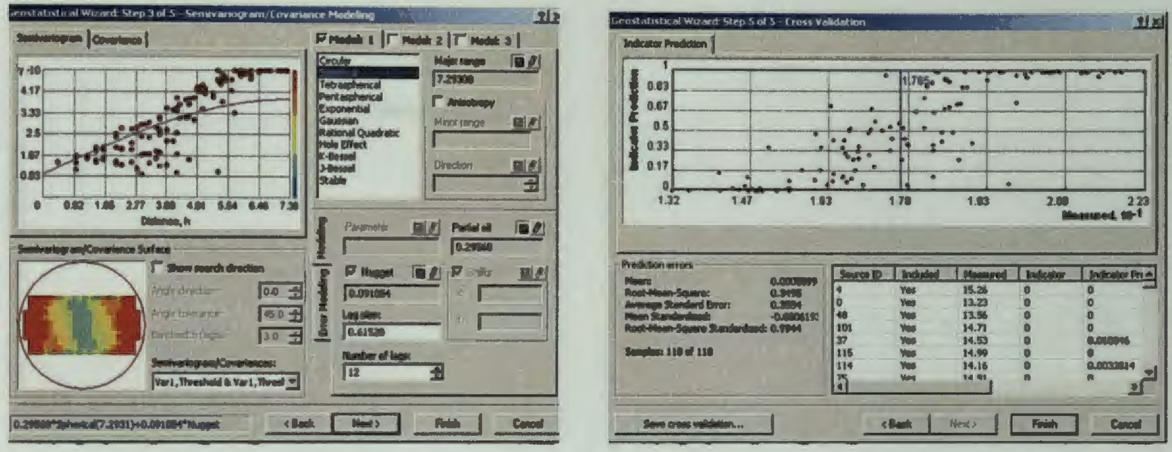

Semivariogram and cross-validation results – indicator kriging

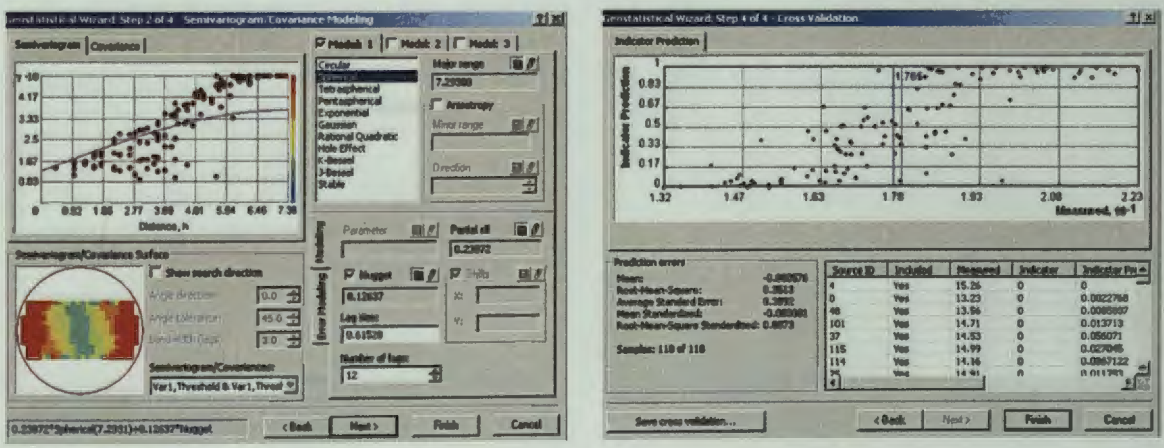

Semivariogram and cross-validation results - probability kriging

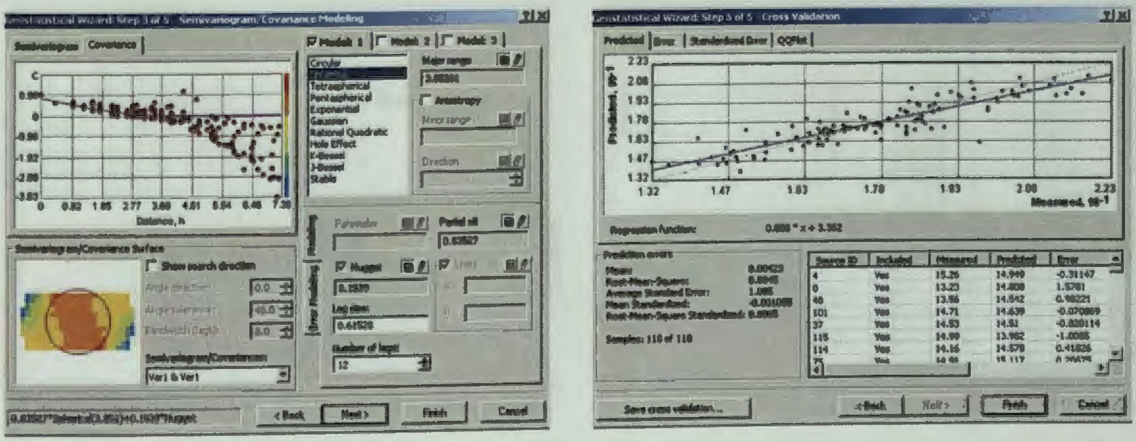

Semivariogram and cross-validation results- disjunctive kriging

Figure C.14. Non-linear kriging results for precipitation datasets using spherical model.

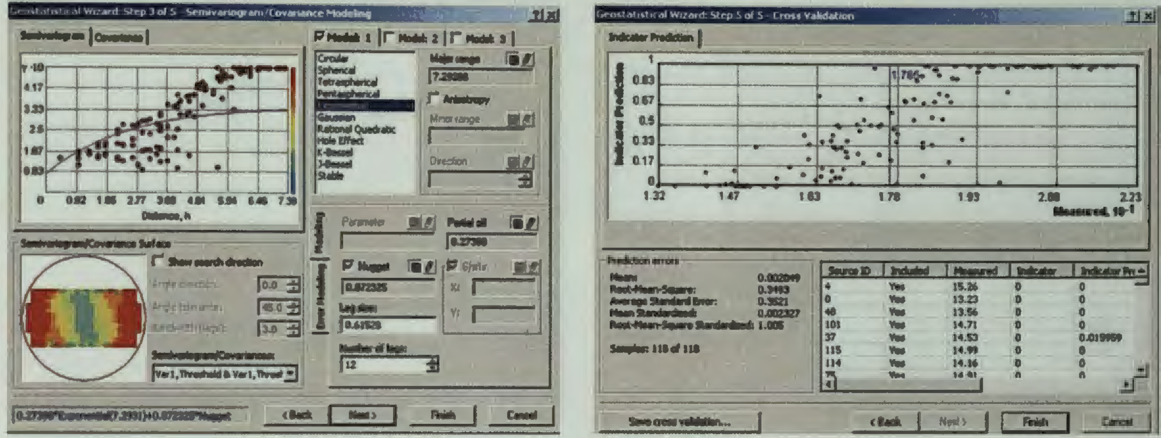

Semivariogram and cross-validation results- indicator kriging

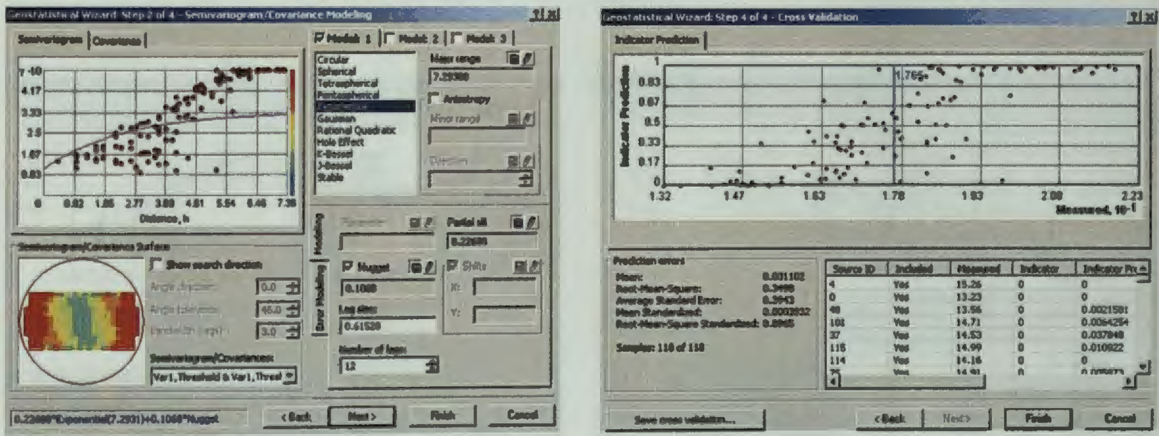

Semivariogram and cross-validation results -probability kriging

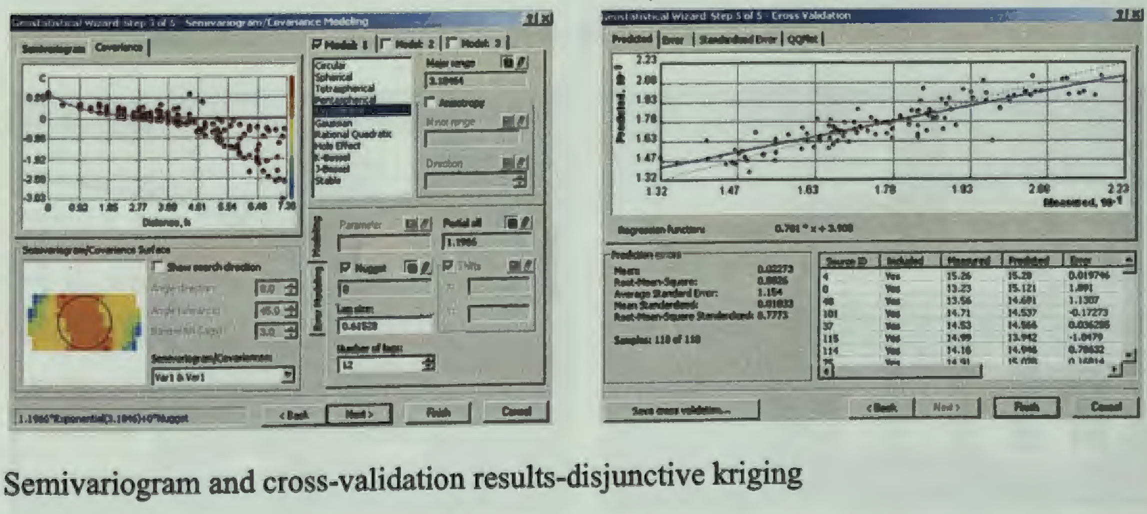

Semivariogram and cross-validation results-disjunctive kriging

Figure C.15. Non-linear kriging results for precipitation datasets using exponential model.

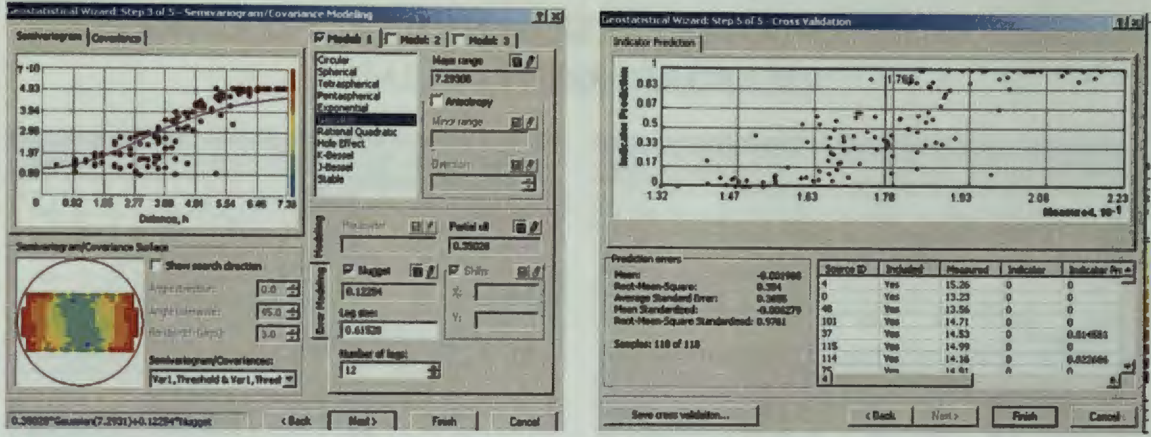

Semivariogram and cross-validation results- indicator kriging

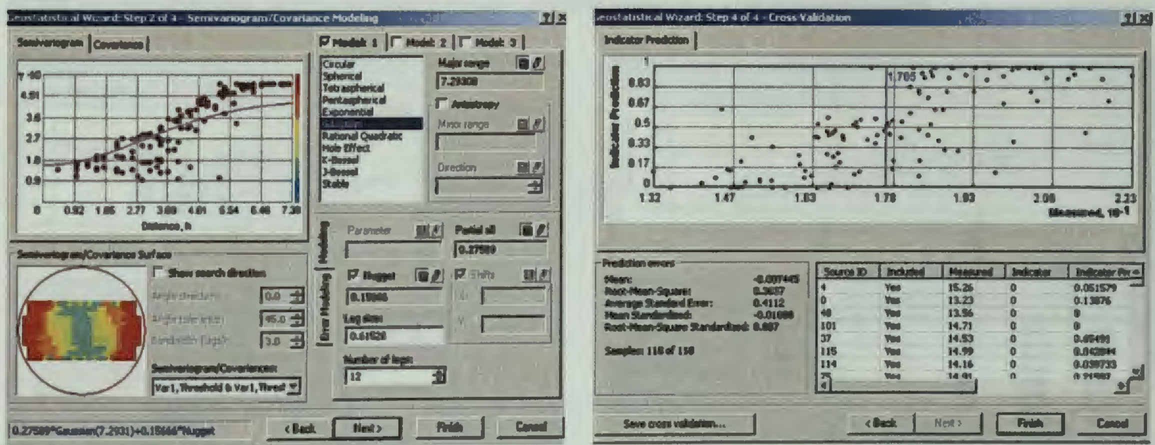

Semivariogram and cross-validation results- probability kriging

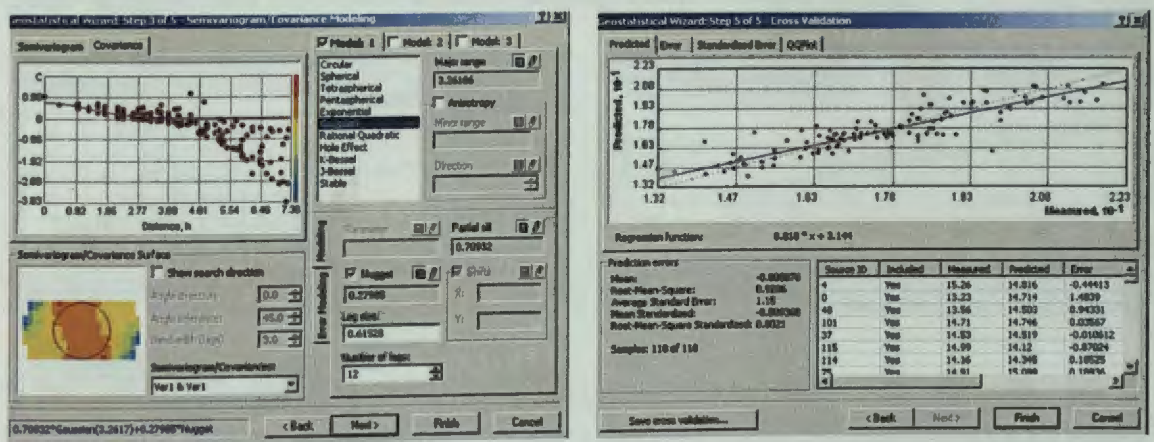

Semivariogram and cross-validation results- disjunctive kriging

Figure C.16. Non-linear kriging results for precipitation datasets using Gaussian model.

APPENDIX D. CO-KRIGING SEMIVARIOGRAM AND CROSS VALIDATIONS DIAGRAMS

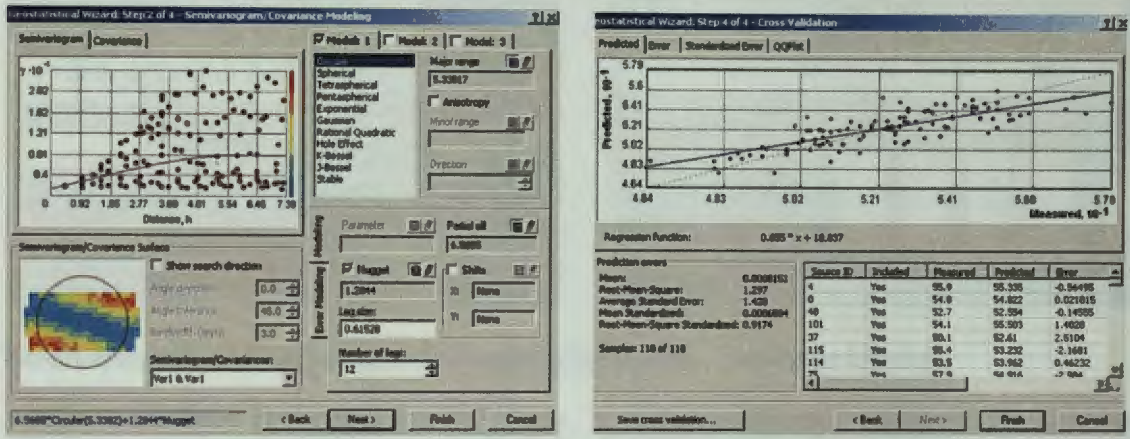

Semivariogram and cross-validation co-kriging results – ordinary kriging

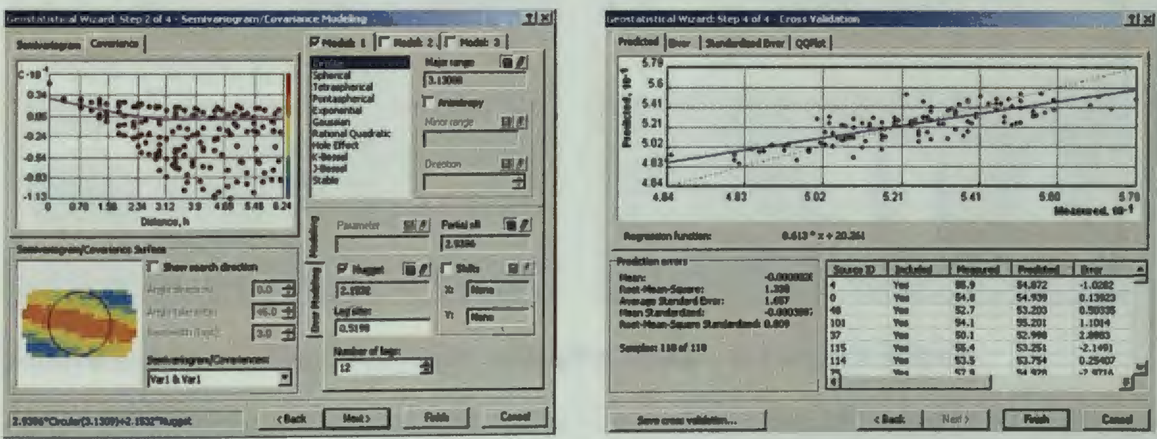

Semivariogram and cross-validation co-kriging results – simple kriging

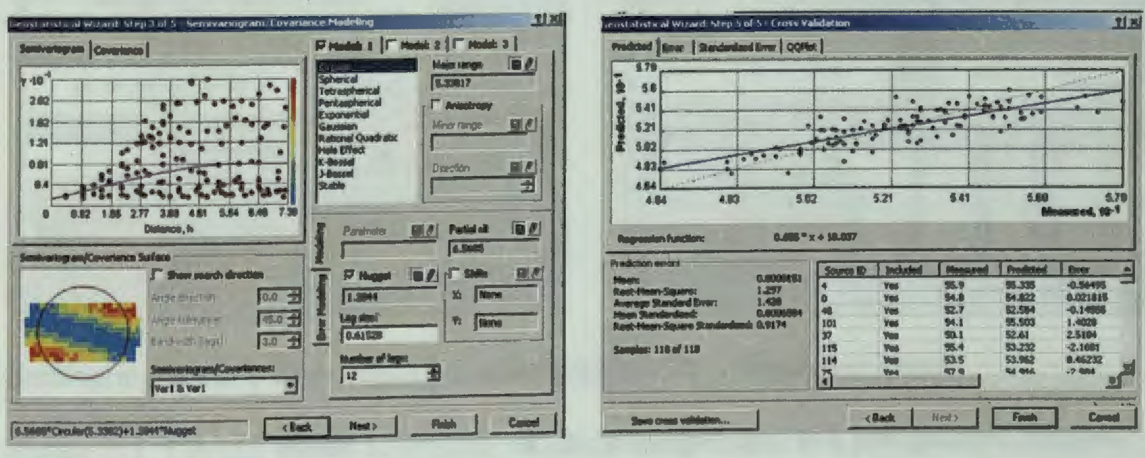

Semivariogram and cross-validation co-kriging results – universal kriging

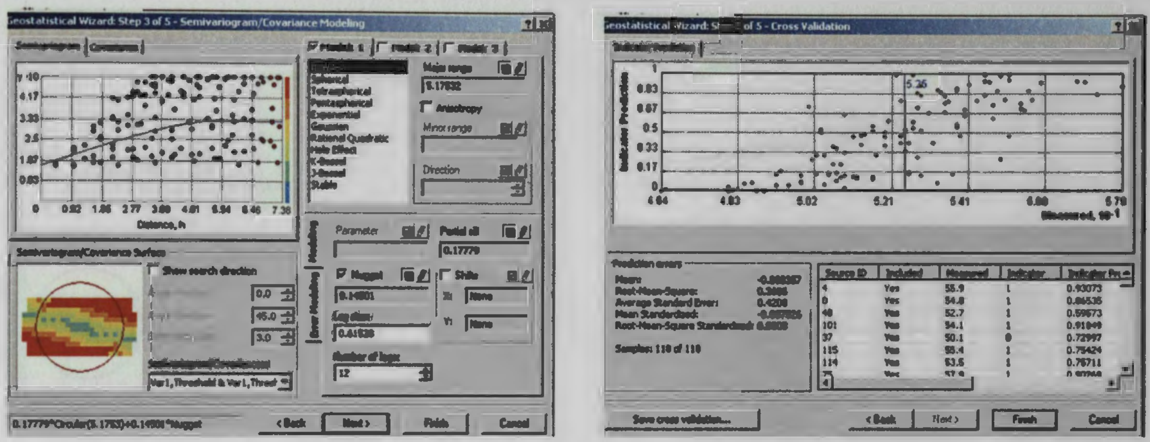

Semivariogram and cross-validation co-kriging results – indicator kriging

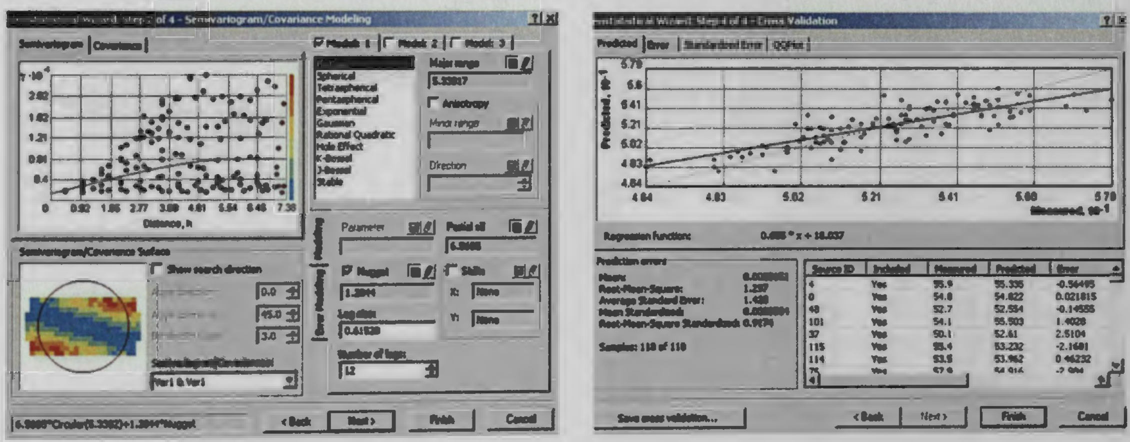

Semivariogram and Cross-validation co-kriging results – probability kriging

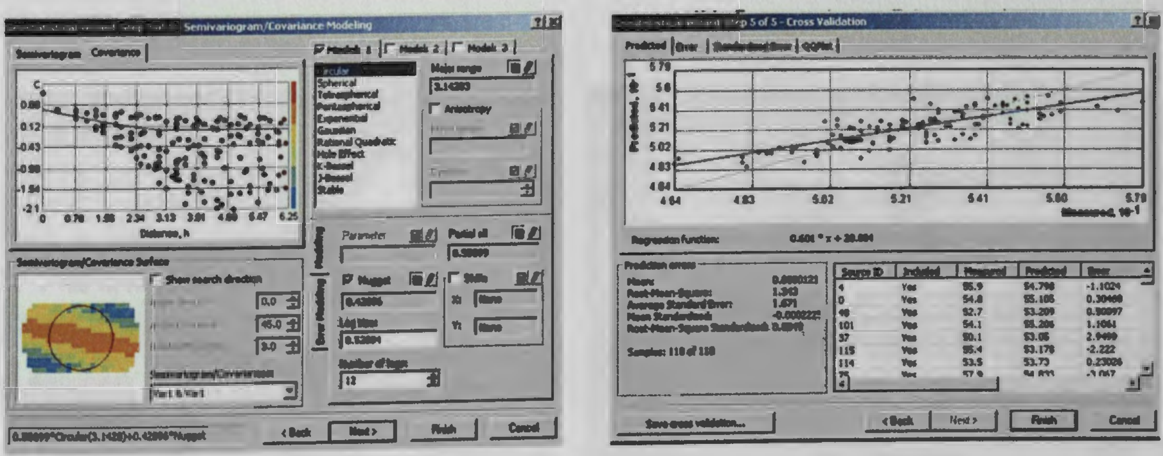

Semivariogram and cross-validation co-kriging results – disjunctive krigin

Figure D.1. Circular model co-kriging results for temperature and precipitation datasets.

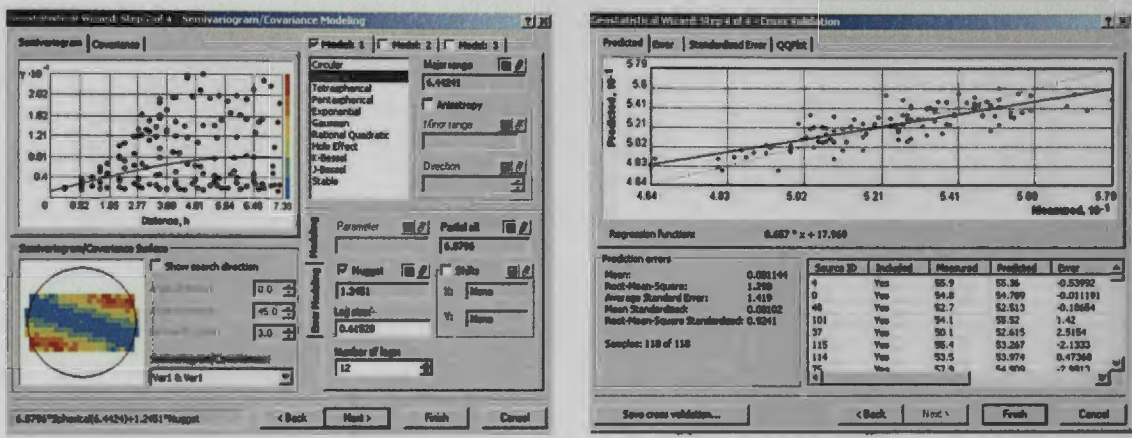

Semivariogram and cross-validation co-kriging results – ordinary kriging

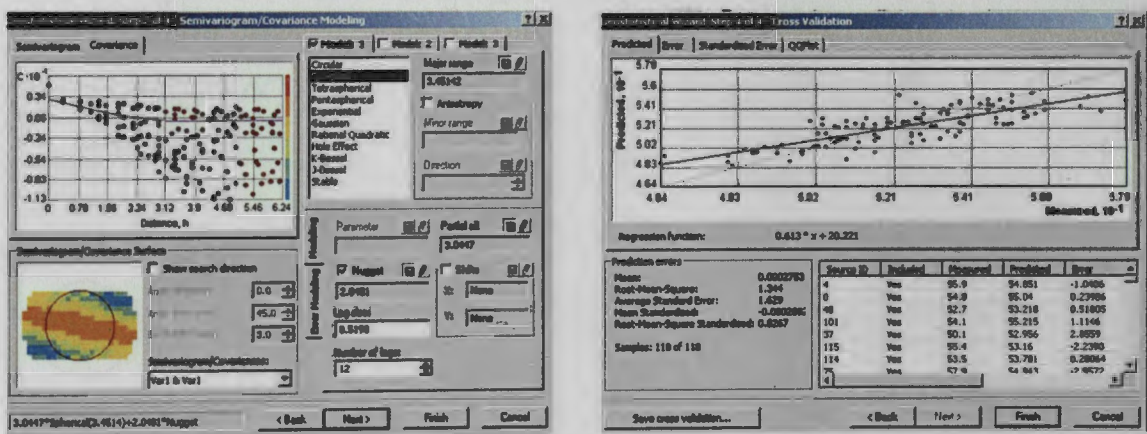

Semivariogram and cross-validation co-kriging results – simple kriging

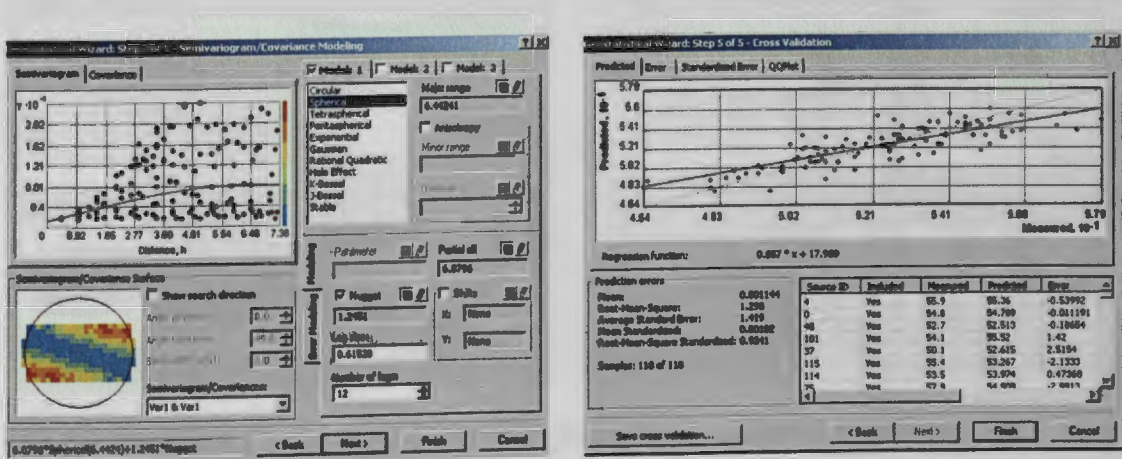

Semivariogram and cross-validation co-kriging results – universal kriging

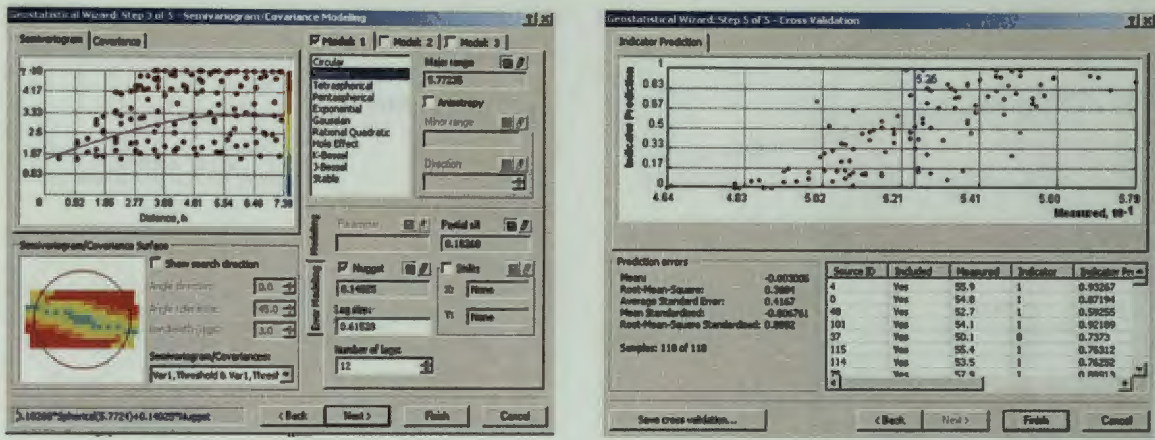

Semivariogram and cross-validation co-kriging results – indicator kriging

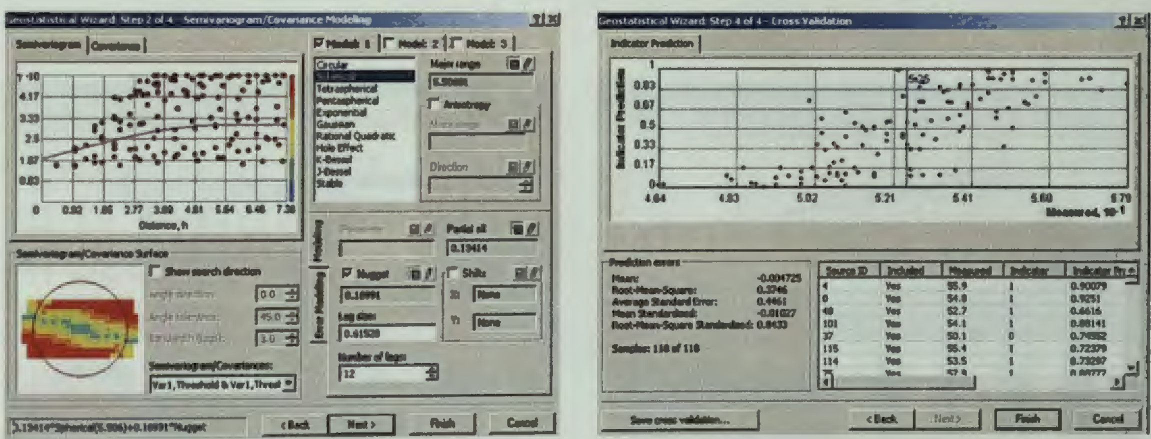

Semivariogram and cross-validation co-kriging results – probability kriging

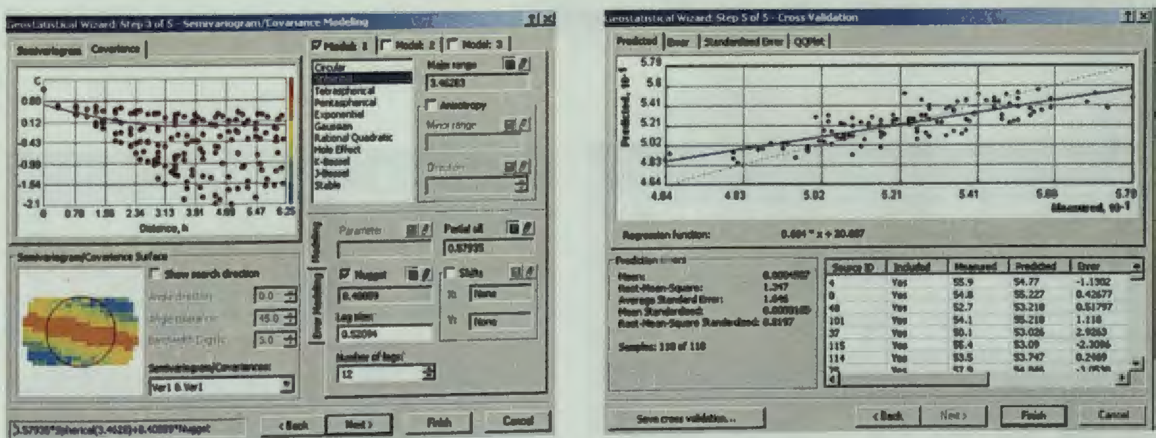

Semivariogram and cross-validation co-kriging results – disjunctive kriging

Figure D.2. Spherical model co-kriging results for temperature and precipitation datasets.

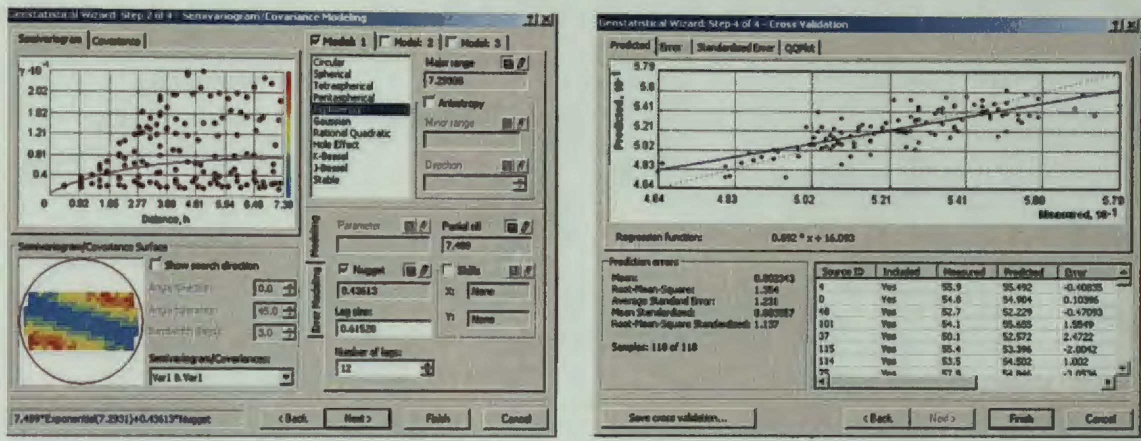

Semivariogram and cross-validation co-kriging results – ordinary kriging

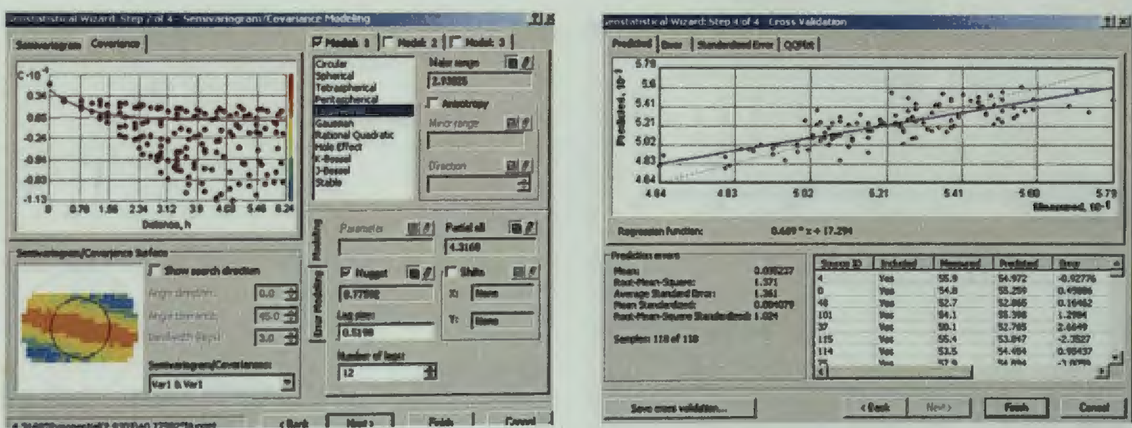

Semivariogram and cross-validation co-kriging results – simple kriging

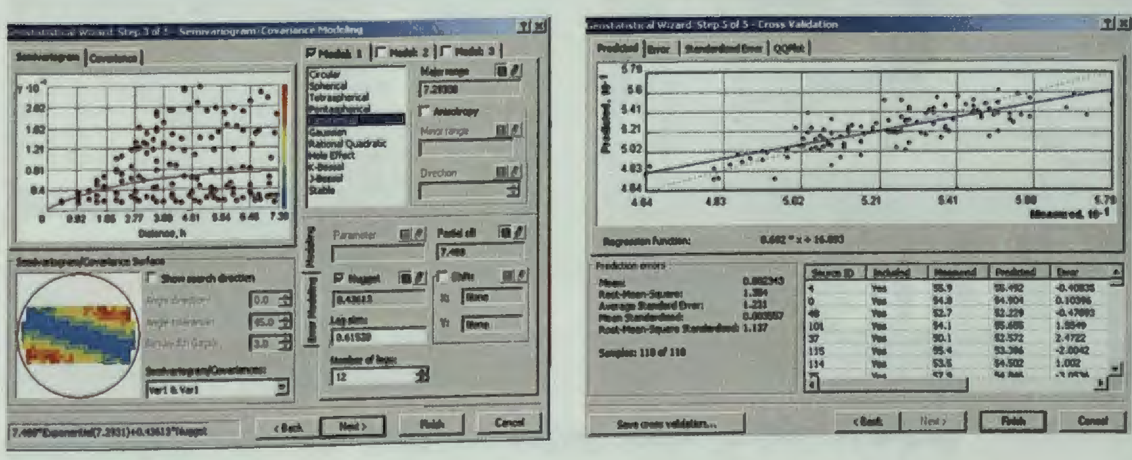

Semivariogram and cross-validation co-kriging results – universal kriging

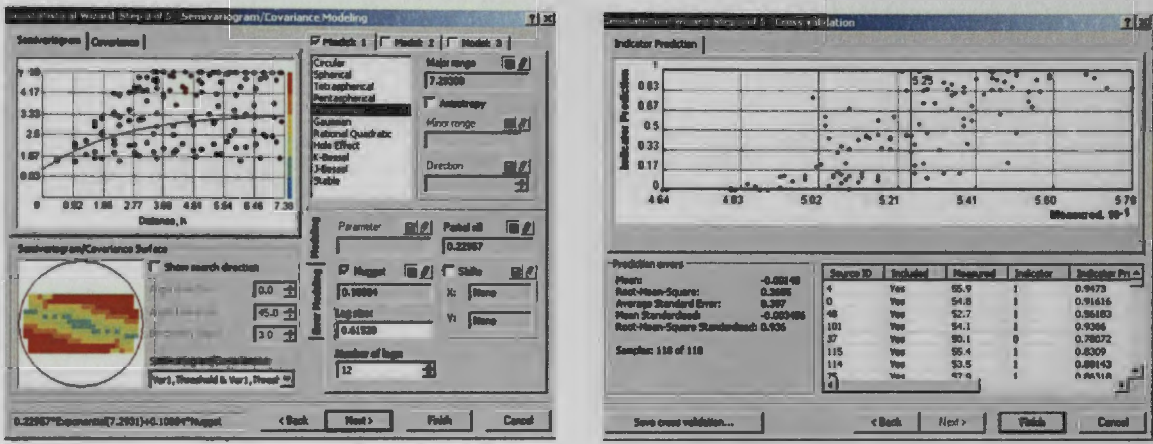

Semivariogram and cross-validation co-kriging results – indicator kriging

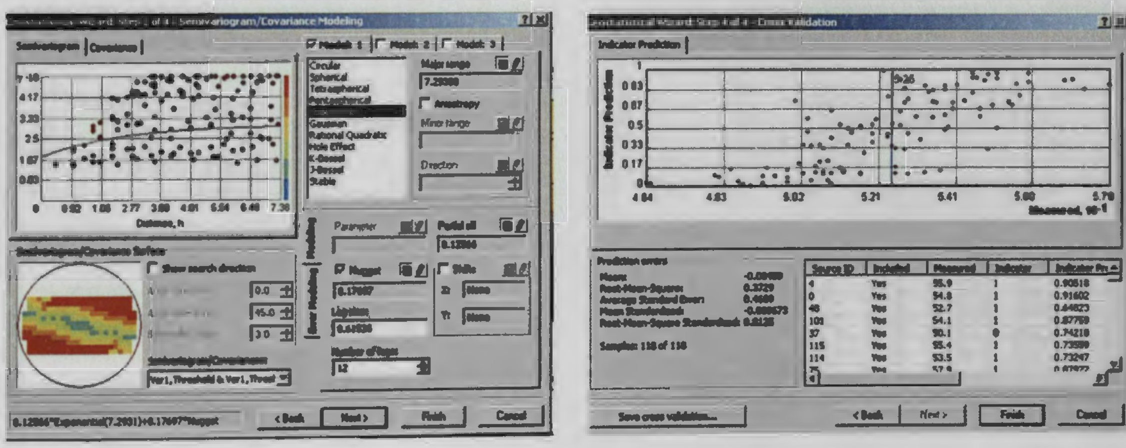

Semivariogram and cross-validation co-kriging results – probability kriging

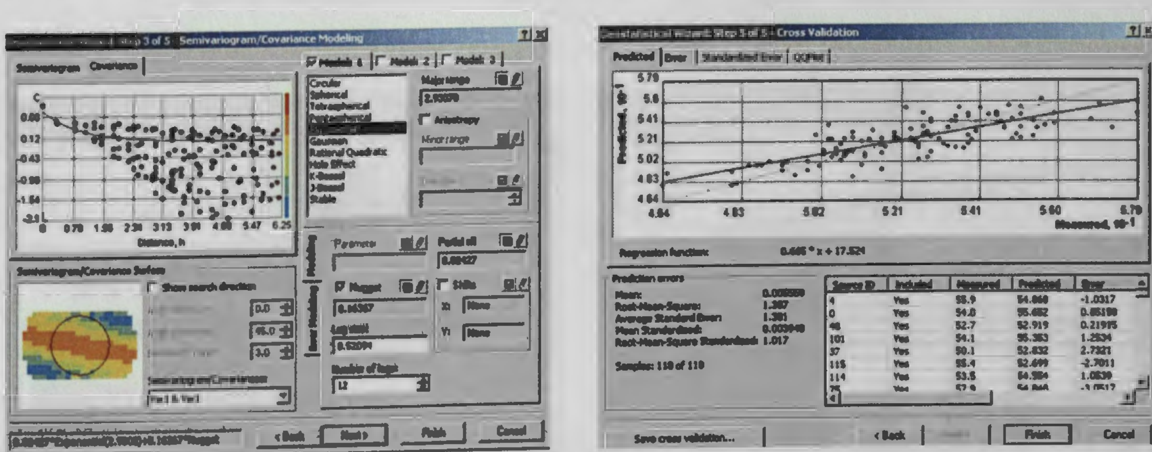

Semivariogram and cross-validation co-kriging results – disjunctive kriging

Figure D.3. Exponential model co-kriging results for temperature and precipitation datasets.

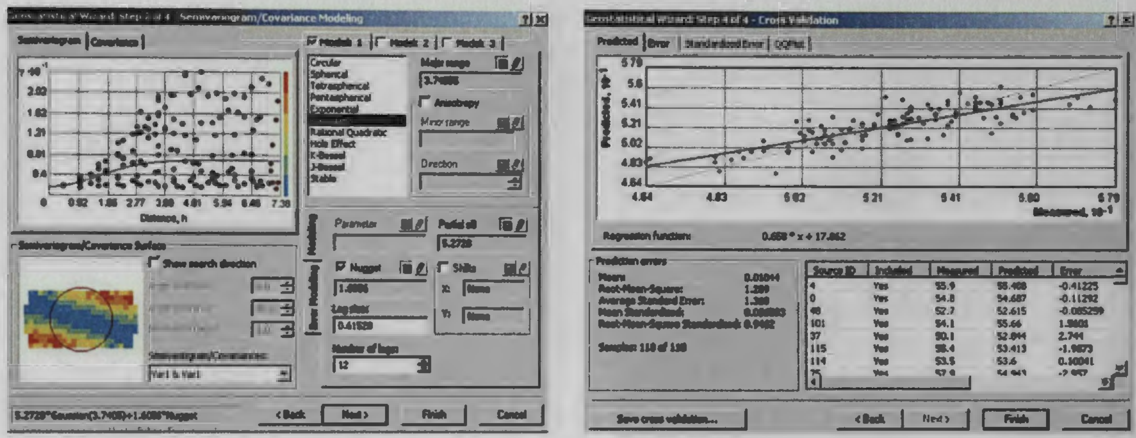

Semivariogram and cross-validation co-kriging results – ordinary kriging

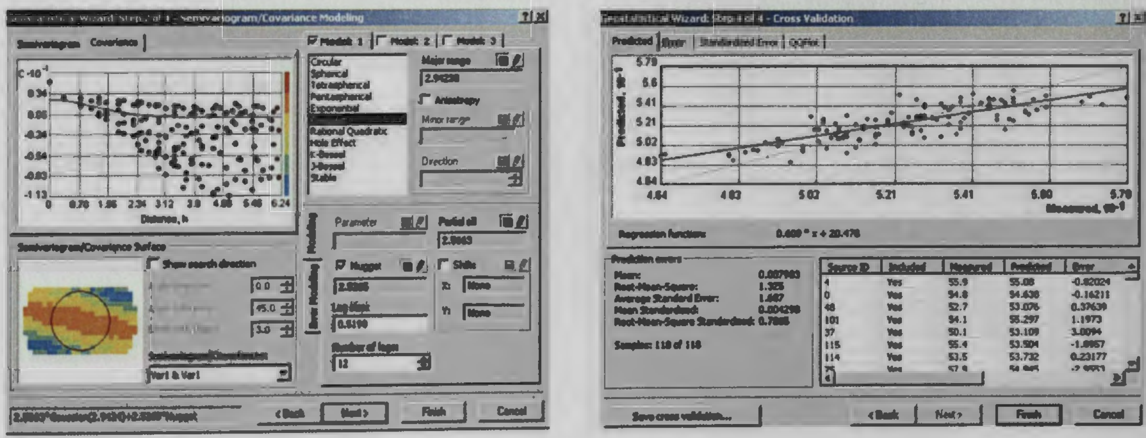

Semivariogram and cross-validation co-kriging results – simple kriging

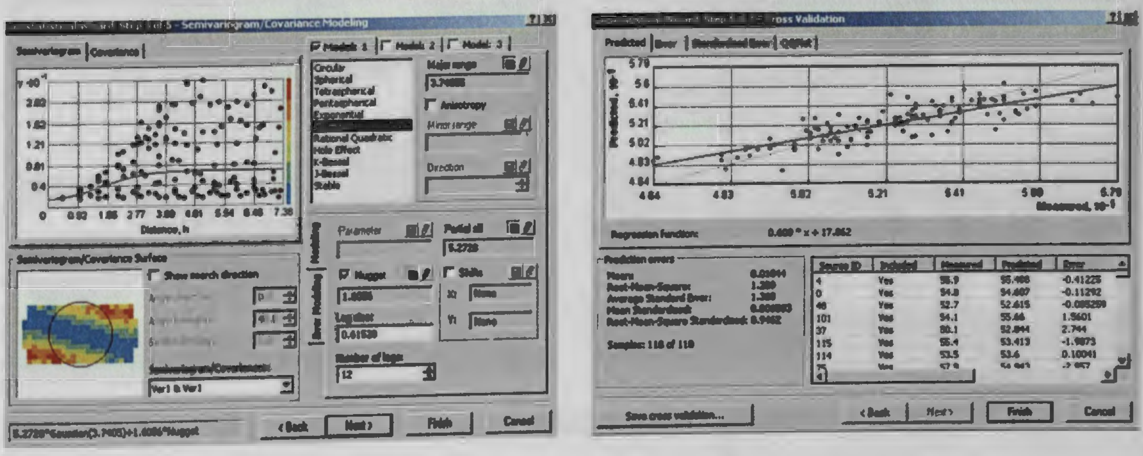

Semivariogram and cross-validation co-kriging results – universal kriging

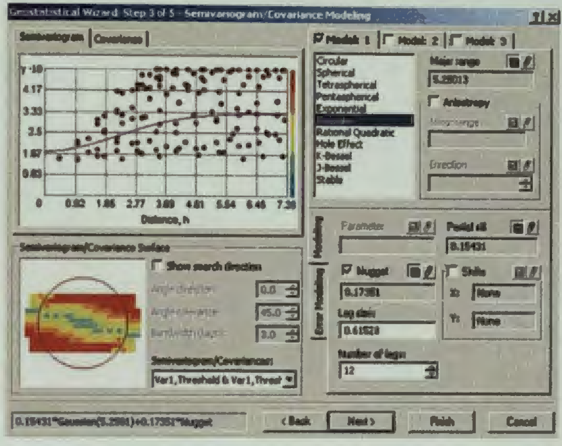

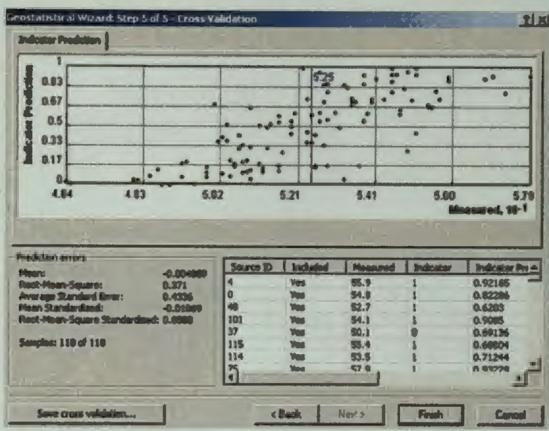

Semivariogram and cross-validation co-kriging results – indicator kriging

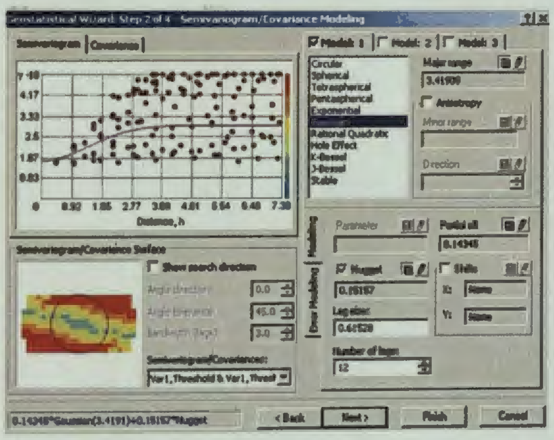

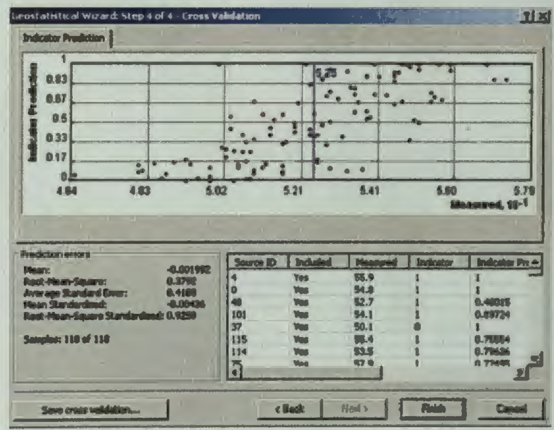

Semivariogram and cross-validation co-kriging results – probability kriging

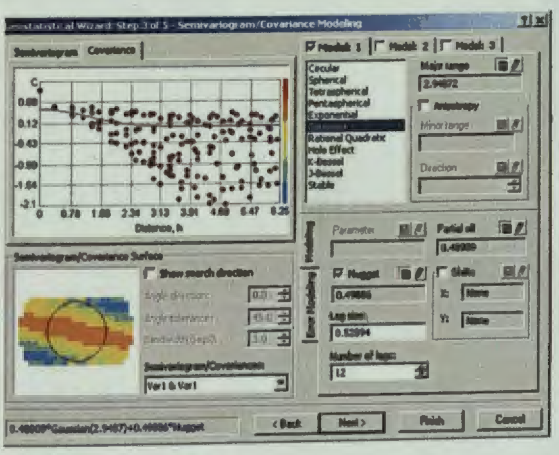

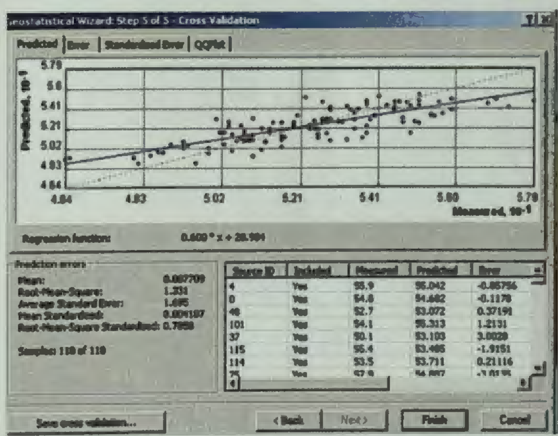

Semivariogram and cross-validation co-kriging results – disjunctive kriging

Figure D.4. Gaussian model co-kriging results for temperature and precipitation datasets.